

**Role of impaired lysosomal trafficking in the
development of lung fibrosis in a murine model of
Hermansky-Pudlak syndrome**

Inaugural - Dissertation
zur Erlangung
des
Doktorgrades der
Naturwissenschaften
-Dr. rer. nat.-

dem
Fachbereich Biologie
der
Justus-Liebig-Universität Gießen
vorlegt von
M.Sc. Poornima Mahavadi
aus
Manthani, Indien

Gießen, February 2009

Dekan

Prof. Dr. Peter R. Schreiner

Gutachter

Prof. Dr. Andreas Guenther

Prof. Dr. Michael U. Martin

Dedicated to my parents...

Erklärung

Hermit erkläre ich, dass ich die vorliegende Arbeit selbstständig verfasst habe und dabei keine anderen als die angegebenen Quellen und Hilfsmittel verwendet habe. Zitate sind als solche gekennzeichnet.

Giessen, den 16.02.2009.

Poornima Mahavadi.

INDEX

Index	I
Abbreviations	IV
1. Introduction	1
1.1. The Pulmonary Surfactant	1
1.1.1. Synthesis, composition and secretion of pulmonary surfactant	1
1.1.2. Surfactant lipids	3
1.1.3. Surfactant proteins	4
1.1.3.1. The hydrophilic surfactant proteins, SP-A & SP-D	4
1.1.3.2. The hydrophobic surfactant proteins, SP-B & SP-C	5
1.2. Disorders of the pulmonary surfactant system	7
1.3. Idiopathic pulmonary fibrosis	8
1.4. Genetically defined disorders that may end up in progressive lung fibrosis.	10
1.5. Hermansky-Pudlak Syndrome	11
1.5.1. The BLOC complex	12
1.5.2. The AP-3 complex	13
1.5.3. Hermansky-Pudlak syndrome associated interstitial pneumonia	15
1.5.4. Types of HPS and corresponding mouse models	17
2. Aim of the study	24
3. Materials	25
3.1. General materials	25
3.2. Materials for animal work	26
3.3. Materials for histology	26
3.4. Kits	27
3.5. List of primers	27
3.6. List of antibodies	28
3.7. Equipment & software	29
4. Methods	30
4.1. Animals	30
4.2. Histology	31
4.2.1. Hematoxylin & Eosin staining	31
4.2.2. Trichrome staining	32

4.3. Western blot analysis.....	33
4.4. Phospholipid analysis	35
4.5. Lipidomics.....	35
4.6. Isolation of RNA from mice lungs	37
4.7. Preparation of cDNA from RNA probes	38
4.8. Semi-quantitative RT-PCR.....	39
4.9. Agarose gel electrophoresis	39
4.10. Immunohistochemistry	40
4.11. In-situ apoptosis assay.....	41
4.12. Microscopy	42
4.13. Isolation of alveolar epithelial cells	42
4.14. Densitometry analysis	44
4.15. Statistics.....	44
5. Results.....	45
5.1. General appearance and phenotype of HPS mice	45
5.2. Lung histology of HPS mice.....	45
5.3. Surfactant alterations in HPS mice.....	48
5.3.1. Altered processing and transport of the hydrophobic surfactant proteins	48
5.3.1.1. Reduction in mature SP-B & mature SP-C in BALF occurs almost exclusively in HPS1/2 mice.....	48
5.3.1.2. Extensive surfactant protein accumulation in HPS1/2 double mutant mice.....	49
5.3.1.3. Surfactant protein alterations in HPS1/6 double mutant mice	51
5.3.1.4. Surfactant protein alterations in HPS mono mutant mice	52
5.3.1.5. Comparative analysis of surfactant protein alterations in HPS mice.....	53
5.3.2. Phospholipidosis in HPS mice	55
5.3.3. Lipidomic profiling of HPS lung tissues.....	57
5.3.3.1. Accumulation of PC and surfactant specific DPPC in HPS1/2 mice	59
5.3.3.2. Glucosylceramides in HPS mice.....	60
5.4. AECII undergo early and extensive apoptosis in HPS1/2 mice	61
5.5. Early lysosomal stress underlies AECII apoptosis in HPS1/2 mice	64
5.5.1. Lysosomal stress is specific in HPS1/2 mice	65
5.5.2. Cathepsin D mediated apoptosis in HPS1/2 mice.....	66
5.6. Induction of ER stress in HPS1/2 mice.....	67

5.7. Alveolar type II cell apoptosis due to lysosomal and ER stress is a prominent finding in human HPSIP	69
6. Discussion.....	71
6.1. Role of HPS gene products in surfactant processing and transport	71
6.2. Altered surfactant processing or transport occurs in other forms of ILDs too	74
6.3. Lysosomal and ER stress reflect epithelial stress in HPS1/2 mice	76
6.3.1. Altered surfactant processing and trafficking as underlying reason for AECII injury	76
6.3.2. Lysosomal stress	77
6.3.3. ER stress.....	79
6.3.4. Other possible pathways, leading to ER or lysosomal stress	81
6.3.5. Integrative concept of AECII apoptosis in HPS1/2 lungs.....	82
6.4. The role of AECII injury in the development of lung fibrosis in general and HPSIP in particular.....	83
6.4.1. AECII injury underlies HPSIP	83
6.4.2. Endogenous regenerative responses to the AECII injury in HPSIP	84
6.4.3. Additional factors that possibly contribute to AECII apoptosis in HPSIP	85
6.5. Murine HPSIP: A model for IPF and other "idiopathic" forms of lung diseases?.....	85
6.6. Therapeutic strategies	86
7. Summary.....	88
8. Zusammenfassung.....	91
9. References.....	94
Acknowledgements.....	110
Anhang.....	111

Abbreviations

AP	Alkaline Phosphatase
APS	Ammonium per Sulphate
ARDS	Adult Respiratory Distress Syndrome
ABCA3	ATP-binding cassette transporter protein A3
AECII	Alveolar epithelial cells type II
AP-3	Adaptor Protein – 3
ANG II	Angiotensin II
ATF6	Activating Transcription Factor 6
ATF4	Activating Transcription Factor 4
bp	Base pairs
BLOC	Biogenesis of Lysosome related Organelle Complex
BSA	Bovine Serum Albumin
cDNA	Complimentary deoxyribonucleic acid
C/EBP	CCAAT / enhancer binding proteins
CHOP	C/EBP Homologous Protein
CNS	Central Nervous System
DMEM	Dulbecco's Modified Eagle Medium
dNTP	Deoxy ribonucleotide triphosphate
DOC	Downstream of CHOP
DPPC	Dipalmitoylated Phosphatidyl Choline
ER	Endoplasmic Reticulum
EDTA	Ethylendinitrilo-N,N,N',N',-tetra-acetate
ECL	Enhanced Chemi Luminiscence
FCS	Fetal Calf Serum
GADD 153	Growth arrest and DNA-damage-inducible protein 153
GC	Gas Chromatography
GlcCer	Glucosyl Ceramides
Hepes	2-(-4-2-hydroxyethyl)-piperaziny-1-ethansulfonate
HPS	Hermansky – Pudlak syndrome
HRP	Horseradish Peroxidase

HPSIP	Hermansky–Pudlak syndrome associated Interstitial Pneumonia
H&E	Hematoxylin & Eosin
IPF	Idiopathic Pulmonary Fibrosis
ILD	Interstitial Lung Disease
IRDS	Infant Respiratory Distress Syndrome
IHC	Immuno histochemistry
kDa	Kilo Dalton
NaOH	Sodium Hydroxide
NaCl	Sodium Chloride
Na ₂ HPO ₄ .2H ₂ O	di-Sodium hydrogen phosphate dihydrate
KH ₂ PO ₄	Potassium dihydrogen phosphate
LB	Lamellar Body
LRO	Lysosome Related Organelle
LAMP	Lysosome Associated Membrane Protein
LSD	Lysosomal Storage Disease
PCR	Polymerase Chain Reaction
PC	Phosphatidyl Choline
RPMI	Cell Culture medium developed by Roswell Park Memorial Institute
RNase	Ribonuclease
RT	Room Temperature
SP	Surfactant Proteins
SDS	Sodium Dodecyl Sulphate
SEM	Standard Error Mean
TEMED	N',N',N',N'-Tetra methyl diamine
TLC	Thin Layer Chromatography
Tris	Tris-(hydroxy methyl)-Amino Methane
WB	Western Blot
XBP	X-box binding protein
UV	Ultra Violet

1. Introduction

1.1. The Pulmonary Surfactant

Pulmonary surfactant, which is also known as the “**surface active agent**”, is a complex mixture of lipids and proteins and primarily serves to reduce the surface tension at the air-water interphase, thereby promoting expansion of the lung during inspiration and preventing lung collapse during end-expiration [1]. It was first studied by a Swedish physiologist, Kurt von Neergard in 1929, who claimed the existence of a surface tension-reducing factor in the alveolar compartment [2]. Later, discovery of the low surface tension in lungs was made in 1955 by Pattle [3] and Clements [4] independently. A correlation between lack of surface active material and Infant Respiratory Distress Syndrome (IRDS) was already established during early years of surfactant discovery [5]. Further studies emerged and isolation of this surface active substance led to the learning of its chemical composition as a phospholipid-rich, membrane-like, lipoprotein complex.

1.1.1. Synthesis, composition and secretion of pulmonary surfactant

Type-II alveolar cells are cuboidal epithelial cells. They coexist with the much thinner type-I cell and can synthesize and secrete pulmonary surfactant. Clara cells in the respiratory bronchioles manufacture at least some components of pulmonary surfactant [6]. Lipids account for about 90% of the surfactant and are, again, composed to roughly 90% by the amphiphilic phospholipids, the working principle of surface-activity. Surfactant proteins (SP–A thorough –D) and a small amount of plasma proteins account for the remaining 10% of pulmonary surfactant (Fig.1) [7-11]. This composition is normally constant in all mammalian species. Bronchoalveolar lavage (BAL) has been the main source to study the surfactant composition. The phospholipid composition in different surfactant subfractions is similar [12-14], with a high variability of protein composition [15, 16], suggesting the prominent influence of surfactant proteins on structure and function of different surfactant fractions.

Some lipid components of surfactant are taken up by alveolar epithelial cells type II (AECII) from the blood stream and some of them are produced at the endoplasmic reticulum of the AECII [17]. Some lipids are produced and fed to the AECII by pulmonary lipofibroblasts. These lipofibroblasts are found next to AECII in the pulmonary interstitium and are characterized by neutral lipid inclusions wrapped in adipocyte differentiation related protein, which mediates the uptake and trafficking of lipid from the lipofibroblast to the AECII for surfactant phospholipid synthesis and protects the alveolar acinus against oxidant injury [18, 19].

AECII uses the lysosomal compartment and secretory pathway to process the lipids and the four apoproteins, all of which undergo substantial post-translational modifications, and to finally assemble the mature surfactant in lamellar bodies [6]. These are about 1 μ m diameter, consisting of concentric rings of proteins and lipids. About 10% of the material present in the lamellar bodies is secreted per hour by a normal lung. Secretion of surfactant occurs by constitutive exocytosis. Freed from the confinement of the lamellar body and based on pH changes, the surfactant then undergoes structural changes, taking the form of a mesh work known as tubular myelin [11]. Surface-active surfactant containing surfactant proteins A, B and C is secreted into the airways as large aggregate forms and create a surfactant film with saturated phosphatidylcholine at air and water interface on the alveolar surface. Squeeze and expansion of the surfactant film by respiration disassociate surfactant lipid from surfactant proteins and become small aggregate lipid vesicles containing only the lipids [6, 20]. Small surfactant aggregates are not surface active and are preferably uptaken by AECII and alveolar macrophages, which equally contribute towards surfactant uptake [20]. While surfactant uptake by alveolar macrophages is less dependent on the physical form of surfactant or presence of surfactant proteins, its uptake by AECII is more selective [6].

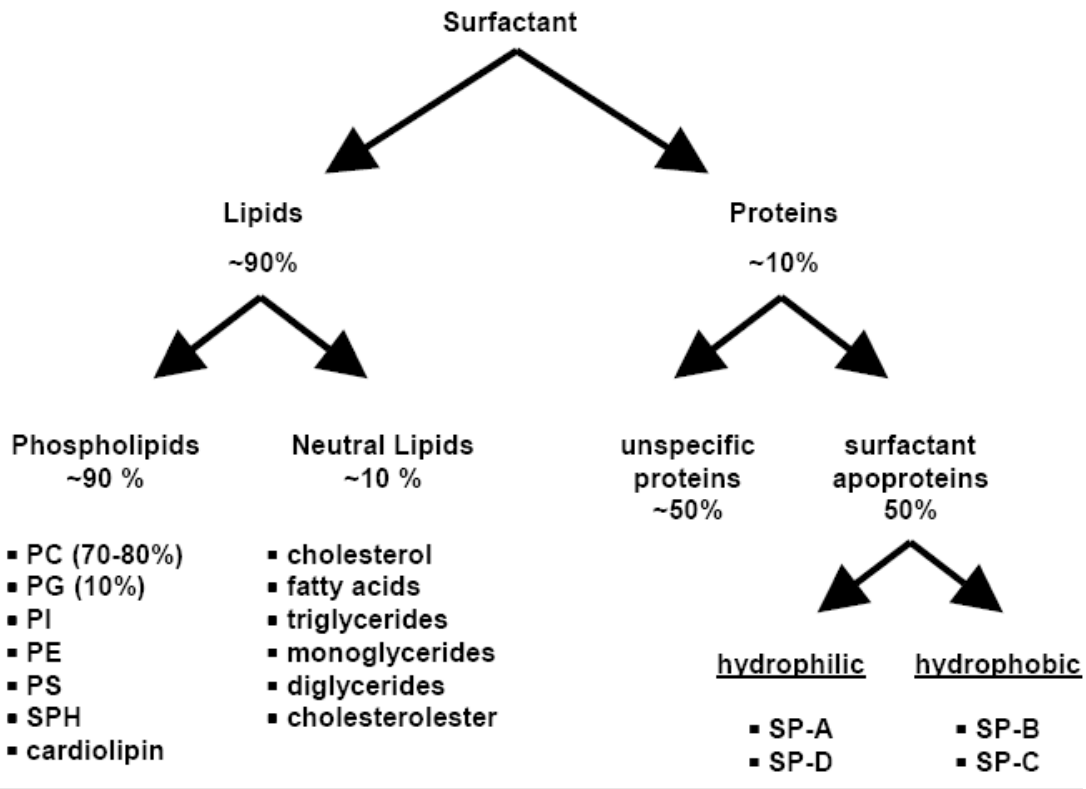


Figure 1: Biochemical composition of pulmonary surfactant.

PC = phosphatidylcholine, PG = phosphatidylglycerol, PI = phosphatidylinositol, PE = phosphatidylethanolamine, PS = phosphatidylserine, SPH = sphingomyelin

1.1.2. Surfactant lipids

Phospholipids form a predominant class of surfactant lipids, with a minor amount (~10 – 20%) of neutral lipids. Among phospholipids, phosphatidylcholine (PC~80%) is the major phospholipid class and contains an unusually high amount of saturated fatty acids, mainly palmitic acid (16:0) [8, 11, 21-23]. About 50-70% of all PC molecules are dipalmitoylated (DPPC), thus representing the most abundant surfactant component [6]. A high DPPC content is known to be an absolute requirement for the high compressibility of the phospholipid film during expiration and lowering of the surface tension to values near zero mN/m at end-expiration [24]. The rest of the PC is composed of monoenoic and dienoic fatty

acids at the 2-position, with only minor amounts of short chains or polyunsaturated acyl groups [25, 26].

Phosphatidylglycerol (PG), which accounts for about 10% of total phospholipids, is the second major surfactant phospholipid [8, 11]. Compared with other tissues, PG is over-represented in lung surfactant. PG is characterized by a high content (40-50%) of oleic acid (18:1) residues [25,27,28]. PG also contains a high amount (20-50%) of palmitic acid, but the content of dipalmitoylated molecular species is markedly lower. Because of its relative high content of unsaturated fatty acids, PG alters the fluidity of DPPC and displays favourable adsorption characteristics [29, 30].

Phosphatidylethanolamine (PE), phosphatidylserine (PS), phosphatidyl-inositol (PI), and sphingomyelin (Sph) are regularly found at low percentages. Their precise function in surfactant remains, however, unclear [8, 11, 21-23].

Cholesterol is the major component (80-90%) of the neutral lipids, presumably contributing to the biophysical surfactant activity by increasing fluidity and improving film respreading. Mono, diacyl and cholesterol esters are found at low percentages and are the minor components within this lipid fraction [31].

1.1.3. Surfactant proteins

Proteins account for approximately 10% of pulmonary surfactant dry weight. Plasma proteins (mainly albumin) and secretory IgA make up about half of the proteins and four apoproteins (SP-A,-B,-C and -D), make up the rest. SP-B and SP-C are extremely hydrophobic low-molecular weight proteins, whereas SP-A and SP-D are hydrophilic high-molecular weight glycoproteins [6].

1.1.3.1. The hydrophilic surfactant proteins, SP-A & SP-D

SP-A is the first identified surfactant protein and is the most abundant surfactant protein by weight (3-4% of the surfactant mass). Both SP-A and SP-D are water soluble and structurally similar, with an N-terminal collagen like domain, involved in trimerization, and a C-type lectin domain in the C-terminus [6] that can bind a

number of ligands in a calcium dependent fashion and based on specific carbohydrates. Both “collectins” therefore significantly contribute to the pulmonary innate host defense by acting as opsonins to coat bacteria and viruses, thereby promoting phagocytosis by macrophages resident in the alveoli [32], or by directly binding and aggregating viruses or bacteria. Although SP-A had been suggested to exert a feedback control that limits surfactant secretion *in vitro*, SP-A *-/-* mice show normal alveolar and tissue surfactant pool sizes, suggesting that SP-A is not critical for regulation of surfactant homeostasis [33]. In contrast, SP-A *-/-* mice are prone to respiratory infection through a variety of infectious agents and then undergo increased inflammation. SP-D *-/-* mice on the other hand, show a strikingly different phenotype: These mice seem to have a normal host defense, but develop progressive alveolar proteinosis and distal air space dilation, associated with increased levels of tissue and macrophage-associated metalloproteinases, macrophage derived oxidants and phospholipids [34]. SP-D has therefore been suggested to control alveolar surfactant homeostasis, most likely on the level of macrophage based phagocytosis [34-38].

1.1.3.2. The hydrophobic surfactant proteins, SP-B & SP-C

Being extremely hydrophobic, the SP-B and SP-C are soluble in organic solvents like chloroform/ethanol or acetonitrile/water mixtures. Both these proteins are synthesized and secreted by alveolar type-II cells and require specialized intracellular processing events to reach maturity without being of harm to the AECII [6].

Processing of SP-B occurs during its transit through the secretory pathway in type-II pneumocytes. The SP-B preproprotein consists of 381 amino acids. A 23 amino acid signal peptide is located at the N-terminus of the proprotein, which translocates SP-B into the lumen of endoplasmic reticulum. This signal peptide, on translational cleavage, yields a proprotein which contains an N-terminal propeptide (residues 24-200), a mature peptide of 79 amino acids (201-279), and a C-terminal propeptide (residues 280-381). This C-terminal propeptide is glycosylated on asparagine 311 [39]. This process, with the molecular weights of

different processing intermediates is depicted in Fig. 2. Recent studies have led to the understanding of the involvement of different enzymes in the post translational processing of SP-B.

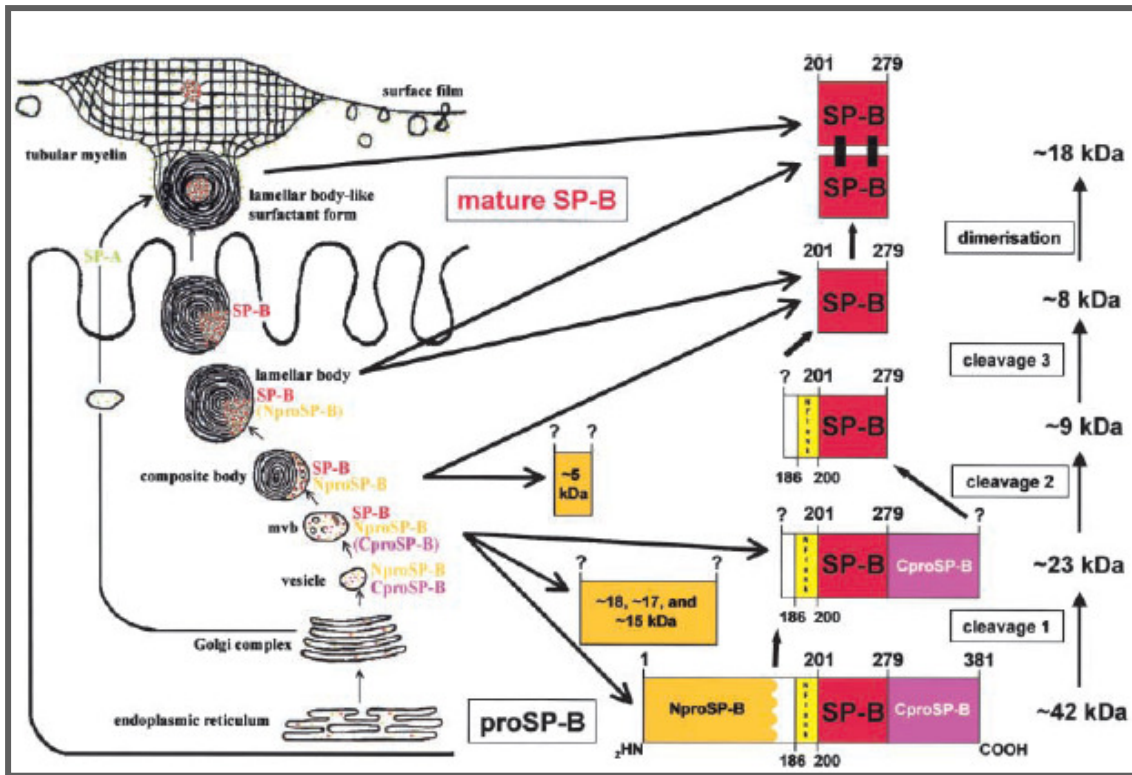


Figure 2. Processing, trafficking, and distribution of SP-B in type II pneumocytes and intra-alveolar surfactant forms in human lungs: Post-translational processing of proSP-B to mature SP-B is at least a three-step process with two distinct cleavages of the N-terminal propeptide and one of the C-terminal propeptide. The processing of proSP-B to mature SP-B occurs between Golgi vesicles and multi vesicular bodies. The colocalization of fragments of the N-terminal propeptide (*ocher dots*) and mature SP-B (*red dots*) in multivesicular, composite, and some lamellar bodies (LB) and the identification of a 5-kDa fragment of the N-terminal propeptide in LB provide evidence for the concept that the N-terminal propeptide of proSP-B is involved in the transport of mature SP-B to LB. In human lungs, mature SP-B is involved in the structural organization of LB by the formation of a projection core. Mature dimeric SP-B is secreted via the LB in the intra-alveolar space, whereas SP-A (*green dots*) largely bypasses the LB. After secretion, the outer membranes of unwinding LB become enriched with SP-A when tubular myelin formation is initiated. Taken from **Brasch et al., American Journal of Respiratory, Cell and Molecular Biology. Vol. 30, pp: 449-458, 2004.**

The membrane bound, aspartyl protease Napsin A, and a cysteine protease Cathepsin H, were reported to be responsible for the N-terminal cleavages of SP-B [40]. A type-II cell specific aspartyl protease, Pepsinogen C was recently identified as another necessary protease involved in SP-B processing [41].

SP-C is a 21 kDa propeptide, synthesized by type-II pneumocytes and is proteolytically processed to a 4.2 kDa dipalmitoylated protein. Previous studies showed that the processing of the 21 kDa proSP-C through 16-, 7- and 6- kDa intermediates, finally leading to mature SP-C is a four-step process, requiring atleast two distinct cleavages of the C-terminal propeptide followed by atleast two cleavages of the N-terminal propeptide (Fig.3). Cathepsin H has been indicated in the first N-terminal processing step of SP-C. Infact, this cysteine protease is the only enzyme that is known to be involved in SP-C processing [42].

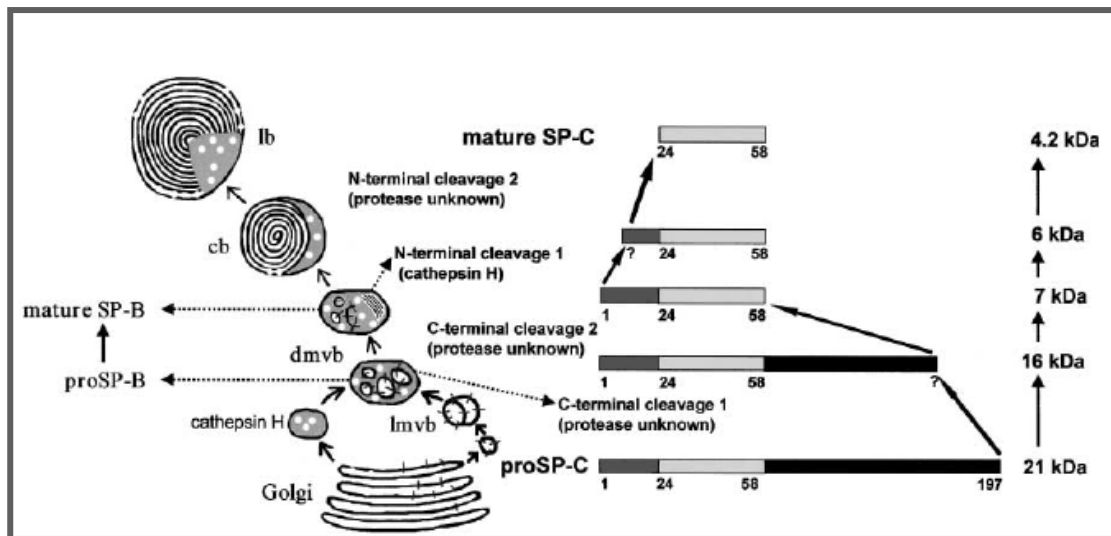


Figure 3. Model of intracellular processing of SP-C: SP-C is synthesized by type II pneumocytes as a 21-kD propeptide (proSP-C) which is proteolytically processed to a 4.2-kD dipalmitoylated protein on the route from its site of synthesis to the lamellar bodies. *In vivo*, the proteolytic processing of the 21-kD proSP-C through 16-, 7-, and 6-kD proSP-C intermediates to mature SP-C is a four-step process requiring at least two distinct cleavages of the C-terminal propeptide followed by at least two cleavages of the N-terminal propeptide. In the human lung, cathepsin H is involved in the first N-terminal processing steps of proSP-C in electron dense multivesicular bodies of type II pneumocytes after. Taken from **Brasch et.al., Am. J. Respir. Cell Mol. Biol., Volume 26, Number 6, June 2002 659-670.**

1.2. Disorders of the pulmonary surfactant system

Surfactant alterations and mutations in the surfactant protein encoding genes have been implicated in several diseases. It has long been studied that shortage of surface active material due to lung immaturity is the driving cause for the infant respiratory distress syndrome (IRDS) [5]. Under these conditions the elevated alveolar surface tension at the air-liquid interface in the lungs results in greatly reduced compliance and impaired gas exchange. Since the implementation of

transbronchial surfactant therapy, the lethality of this condition could be reduced by 50% [43]. Persistent respiratory distress may also be found in term infants, excluding immaturity of AECII as underlying reason. In some of these patients, deficiency of SP-B has been established as a first genetic cause of lethal IRDS [44], shedding light on its indispensable role in postnatal survival. Parallely, SP-B $-/-$ mice showed normal respiratory efforts, but failed to inflate the lungs and rapidly died due to severe respiratory failure. Furthermore, neither proSP-B nor SP-B proteins were detected, no tubular myelin and lamellar bodies were found in the lungs of these mice [45]. Interestingly, aberrant processing of SP-C was detected, indicating the essential role of SP-B in proteolytic processing of SP-C [46]. A similar phenotype has been encountered in infants and some few older patients with mutations of the ABCA3 gene.

In adult patients, surfactant alterations have been implicated to contribute to the Acute Respiratory Distress Syndrome (ARDS), where substantial changes in the surfactant composition and inhibitory events, rather than a lack of surface active material, similarly results in an increase in alveolar surface tension and thus induction of ventilation-perfusion mismatch, arterial hypoxemia and respiratory failure [47].

Alterations in the surfactant system have been also been implicated in the development of interstitial lung diseases (ILD). All diffuse parenchymal lung diseases (DPLD) caused by surfactant alterations are tabulated under the section: "Genetically defined disorders that may end up in progressive lung fibrosis".

1.3. Idiopathic Pulmonary Fibrosis

Idiopathic pulmonary fibrosis (IPF) is an interstitial lung disease of unknown etiology. It is a devastating disease process, which is characterized by fibroblast accumulation, excessive collagen deposition, matrix remodelling and distortion of the alveolar architecture. The progressive decline in lung function and impairment in gas exchange causes dyspnea during exercise, later at rest and

enforces nasal oxygen therapy at final stages. In face of a lack of an effective treatment, patients usually die 2-4 years after diagnosis [48]. On the histological level, temporal and spatial heterogeneity exist, resulting in still regular appearing septae adjacent to disease-defining areas such as fibroblastic foci, honeycomb changes with dense fibrosis and hyperplastic epithelium (Fig.4).

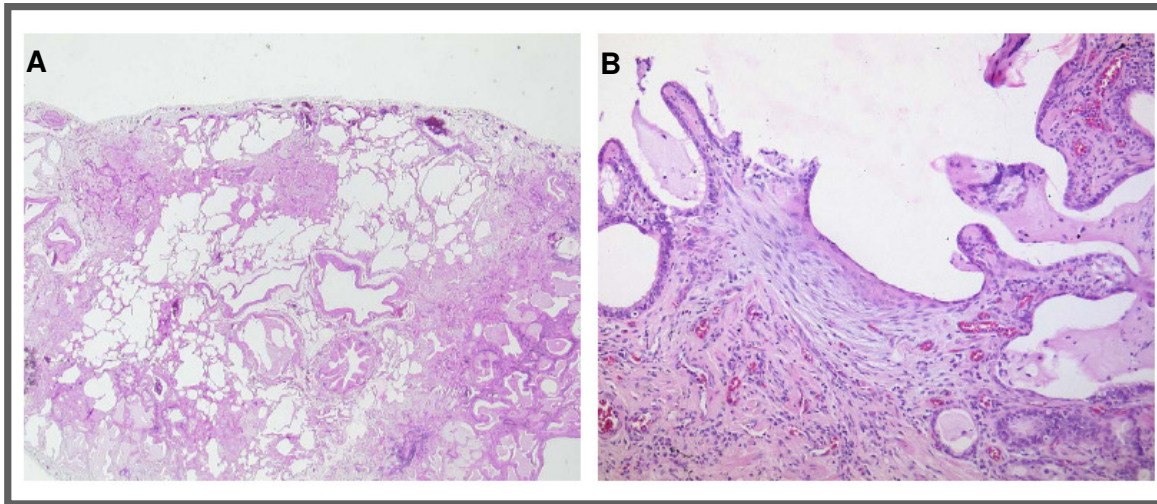


Figure 4. Idiopathic pulmonary fibrosis. H&E staining of lung tissue from a human patient with IPF showing **A)** heterogenous pattern, with still regular appearing septae adjacent to areas of dense fibrosis and honey combing, **B)** typical fibroblast foci and cellular infiltration.

The pathogenesis of this incurable, chronic respiratory disease remains unknown. However, two theories have been proposed for the development of IPF. **1)** The (older) inflammatory hypothesis and **2)** The (more recent) alveolar epithelial cell injury hypothesis.

1) The older hypothesis suggested that IPF results from chronic inflammation in response to a yet undefined stimulus, and, if left untreated, would lead to progressive lung injury and ultimately fibrosis [48]. Such reasoning was based on the obvious signs of inflammation on histological (lymphoplasmacellular infiltrates), BAL (marked neutrophilic alveolitis) and radiographic (enlarged lymph nodes, modest ground glass opacities) findings. However, anti-inflammatory therapies largely failed to gain any meaningful clinical effect, thereby providing

evidence that the inflammation events encountered in IPF seem neither to play a causative role nor do they seem to substantially contribute to the progression of the disease.

2) According to a more recent hypothesis, IPF primarily results from an epithelial injury, followed by a misguided wound healing. Failure to re-epithelialize the injured alveolar epithelium perpetuates and induces proliferation of interstitial fibroblasts, which then transform into myofibroblasts and produce excessive amounts of extracellular matrix (ECM) which ultimately leads to fibrosis [49, 50].

In line with this notion, increased apoptosis of type-II pneumocytes has been found in areas of remodelled regions replaced by fibrous tissue adjacent to ECM-producing myofibroblasts and also frequently in regions of lung with intervening normal or nearly normal alveoli [51, 52].

Pulmonary fibrosis may be a manifestation of various genetic disorders, which are defined briefly in the following section.

1.4. Genetically defined disorders that may end up in progressive lung fibrosis

1.	Hermansky Pudlak Syndrome	platelet degranulation disorder, hypopigmentation, colitis, interstitial lung disease.
2.	Chediak-Higashi Syndrome	platelet degranulation disorder, hypopigmentation, severe immunodeficiency.
3.	Griscelli Syndrome (mutated Rab 27)	hypopigmentation, immunodeficiency, normal platelet function.
4.	Mutated ABCA 3	Infant respiratory distress syndrome, Interstitial lung disease.
5.	Mutated SP-C	Interstitial Lung Disease
6.	Lipid storage diseases like Nieman Pick disease	Interstitial Lung Disease

1.5. Hermansky Pudlak Syndrome (HPS)

Hermansky-Pudlak syndrome (HPS) dates back to 1959, when two Czechoslovakian physicists, F. Hermansky and P. Pudlak first defined the syndrome as oculocutaneous albinism, associated with hemorrhagic diathesis and pigmented macrophages in the bone marrow of two unrelated albinos. They found that unusual reticuloendothelial cells in the bone marrow were packed with blackish or greenish blue granules, a histochemical study of which revealed their lipid nature [53]. Later on, several clinical case reports revealed that HPS is a group of autosomal recessive disorders, which share the clinical findings of oculocutaneous albinism, platelet storage pool deficiency, ceroid lipofuscinosis and an early death caused by severe fibrotic lung disease [54 - 57]. The cellular bases of these serious complications are unclear, but they seem to correlate with the defects in the lysosome related organelles (LROs). Thus, the study that started to analyze bleeding disorders has evolved into a much more complex investigation, thereby becoming a subject of interest not only to clinicians, but also to geneticists and cell biologists.

Mutations in the HPS gene are mostly prevalent in northwest Puerto Rico, and are estimated to occur in about 1 in 1,800 persons, with a carrier frequency of 1 in 21 persons [58 - 60], proving that this is the home for largest group of known HPS patients. However, some sporadic cases have been described in a variety of backgrounds from Mexico, Holland, Sri Lanka and Japan and many patients have been identified in the United States [61, 62]. It is otherwise an extremely rare disease, occurring with a prevalence of 1 in 500,000 - 1,000,000 persons [63, 64]. How the HPS mutations came to originate in Puerto Rico is unknown.

There are 7 known HPS genes in humans [63 – 70] and at least 16 HPS genes causing the HPS-mutant phenotype in the mouse have been identified so far [69, 71 – 74]. These genes encode the following known proteins involved in vesicle trafficking **1)** the nine novel BLOCs (Biogenesis of Lysosome Related Organelle Complexes), **2)** the Adaptor Protein (AP)-3 and **3)** the Vacuolar Protein Sorting Complex (VPS) 33a (see Fig.5). Their sequences offer few clues to their

functions or to the mechanisms by which they orchestrate the biogenesis and trafficking of LROs (Lysosome Related Organelles). Apart from effecting the different LROs, these genes control a wide range of physiological processes like immune recognition, neuronal functions and lung surfactant trafficking [75].

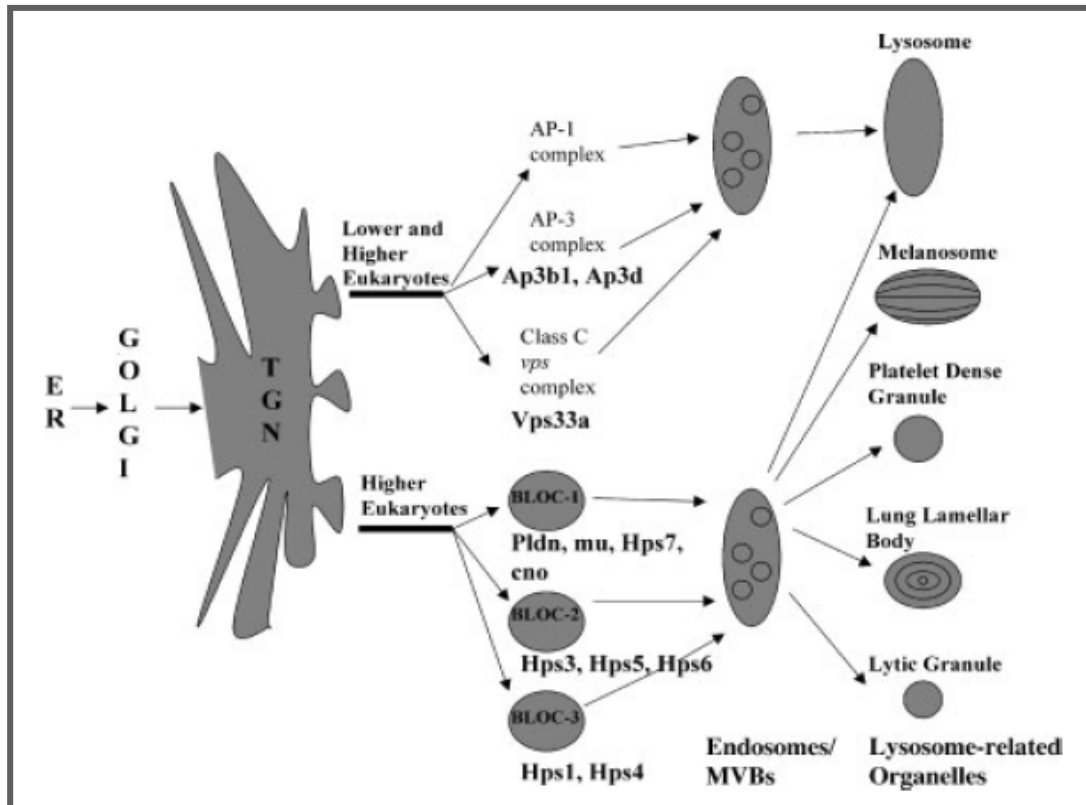


Figure 5: HPS proteins in vesicle trafficking. HPS proteins act in the endocytic pathway to affect the synthesis of a variety of lysosome-related organelles. The Ap3b1, Ap3d and Vps33a proteins function in both lower and higher eukaryotes while the nine novel proteins of BLOC-1 – BLOC-3 are found only in higher eukaryotes. For simplicity, these complexes are depicted as participating only in the synthesis of lysosomes, though they are involved in the synthesis of other lysosome-related organelles in higher organisms. The exact subcellular sites of action of most HPS proteins are uncertain. While they are depicted here as acting between the trans-Golgi network(TGN) and endosomes/MVB's (Multi Vesicular Bodies), it is possible that they act at other subcellular sites. Taken from **Li.et.al., BioEssays 26: 616-628, 2004.**

1.5.1. The BLOC complex: The biogenesis of lysosome related organelle complex (BLOC) has been extensively studied in several organisms and found to be linked to the secretory and endocytic pathways for protein and lipid trafficking. Most known genes that are mutated to cause HPS in patients and mouse models encode polypeptides, belonging to the BLOCs-1, -2 and -3 complexes [76 – 81].

Several HPS mouse mutants are mimics in coat colour. This helped in predicting the protein products of these genes as components of common protein complexes termed as BLOCs. For example, the HPS-7, HPS-8, pallidin, muted and cappuccino mice have similar coat colours and belong to BLOC-1 complex [82 – 85]. Likewise, HPS3, HPS5 and HPS6 mutants that belong to BLOC-2 are highly similar in coat colour. Their gene products are also co-members of the BLOC-2 protein complex [86, 87]. The HPS1 and HPS4 mutants are similarly indistinguishable and their protein products are components of BLOC-3 complex [88, 89]. While BLOC-1 complex interacts with the cytoskeleton [89], BLOC-3 has been shown to function in fibroblasts to regulate the intracellular location of lysosomes [91]. The three BLOCs have been found in soluble (cytosolic) forms as well as associated to membranes as peripheral membrane proteins. The identity of the membrane-bound compartment(s) to which BLOC-1 and -2 associate is unknown. On the other hand, BLOC-3 has been localized by immuno - fluorescence and immunoelectron microscopy to tubulovesicular and vesicular structures near the golgi complex (in pigmented and non pigmented cells) as well as to the membrane of maturing melanosomes, providing proof of the involvement of this protein in trafficking [92]. Several binding partners like syntaxin 13, SNARE-25, VAMP-2, are described for BLOC-1; but only one candidate was reported for BLOC-2 and none for BLOC-3 [73]. The molecular mass of the complex has been estimated to range from ~ 130 to 150kDa up to 200kDa in melanoma-derived cell lines [92]. Different types of HPS proteins and mice models belonging to this complex are described in detail in the coming sections.

1.5.2. The AP-3 complex: The AP-3 is the only known HPS gene product, whose structure and functions are well characterised. Adaptor proteins are heterotetrameric complexes that facilitate cargo selection and coated vesicle budding from different membrane compartments. Four such complexes have been identified in mammals, AP-1 through 4. Of interest is the AP-3 complex, which plays a prominent role in mediating cargo protein selection into transport vesicles and trafficking those membrane proteins to lysosomes [93].

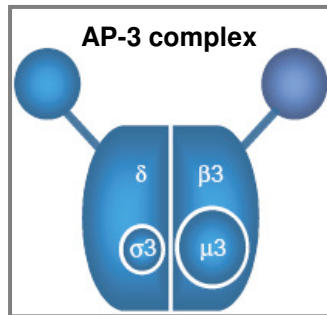


Figure 6: Structure of AP-3: AP-3 is a heterodimer consisting of two large subunits ($\beta 3A$ and δ), a medium subunit, ($\mu 3$) and a small subunit ($\sigma 3$). The $\beta 3A$ and δ subunits have three domains: the head or core region the hydrophilic hinge region and the ear or appendage region. The carboxy-terminal domains of the two large subunits project as 'ears', connected to the 'head' of the complex by flexible hinges. Taken from **Di Petro et.al., Current Opinion in Cell Biology 2001, 13:444–453.**

AP-3 is structurally and functionally related to the AP-1, AP-2 and AP-4 complexes. The head or the core region (Fig.6) is responsible for protein-protein interactions. Yeast two-hybrid experiments have shown that the δ subunit interacts with the σ subunits, that the β subunits interact with the μ subunits and that the two large subunits interact with each other. It plays a crucial role in sorting specific membrane proteins and facilitating carrier vesicle formation at the *trans*-golgi network. These vesicles are then targeted to their specific subcellular destinations like the lysosomes and lysosome related organelles [94].

Two naturally occurring mouse mutants have been identified with mutations in AP-3 subunits. The first is the mocha (mh) mouse, which has a null mutation in the δ subunit of the complex, leading to severe neuronal abnormalities [95]. The second one is the the pearl (pe) mouse, which has an effectively null mutation in the $\beta 3A$ subunit (HPS-2) [96].

BLOC-1 interacts physically and functionally with AP-3 to facilitate the trafficking of a known AP-3 cargo, CD63 and of tyrosinase - related protein-1 (Tyrp1). This study also showed that BLOC-1 also interacts with BLOC-2 to facilitate Tyrp1 trafficking by a mechanism being apparently independent of AP-3 function [97]. Although an interaction between BLOC-1, BLOC-2 and AP-3 has been suggested in several investigations, there is no experimental evidence regarding a direct interaction between BLOC-3 and AP-3.

1.5.3. Hermansky - Pudlak Syndrome associated Interstitial Pneumonia

Severe pulmonary fibrosis, manifesting in the 3rd or 4th decade of life, has been shown to be the most serious complication of the disease, accounting for premature death in 50% of HPS patients, generally by the 5th decade [98]. HPS1 and HPS4 individuals are known to show a greater degree of lung involvement, with an estimate of about 80% of HPS1 subtypes afflicted [99 – 101]. Studies evaluating pulmonary disease in other subtypes are lacking, disabling any interpretation on the development of pulmonary fibrosis in other subtypes.

Numerous investigations have shed light on pathologic features which demonstrated patchy fibrosis, alveolar septa displaying florid proliferation of type-II pneumocytes with characteristic foamy swelling / degeneration and lymphocytic and histiocytic infiltration around honey combing (Fig.6). Histochemical examination revealed an over accumulation of phospholipids and a weak positivity for Surfactant Protein-A (SP-A) (Fig.7).

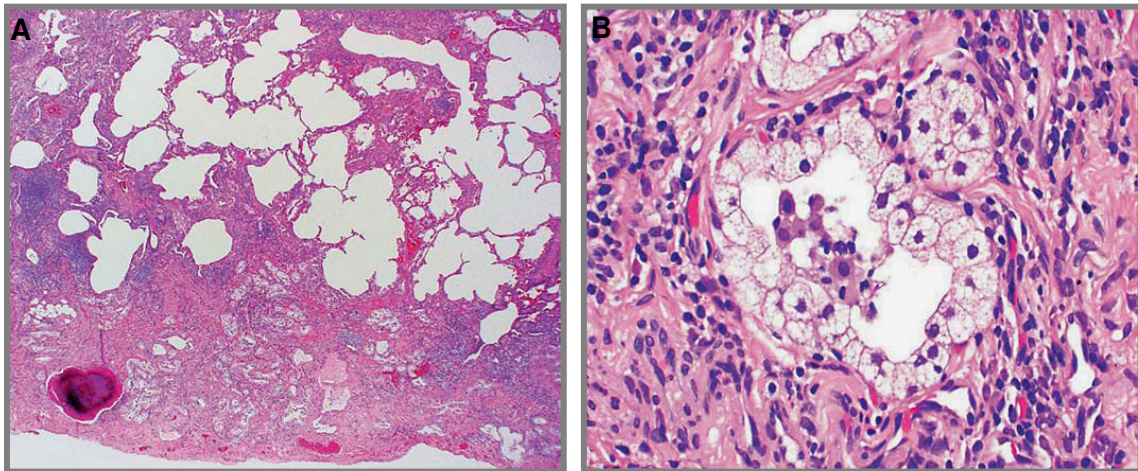


Figure 7. H&E staining of lung tissue section from a patient with HPSIP, showing **A)** Advanced lung remodeling with fibrosis, typically without an easily characterized distribution. **B)** Accumulation of foamy type II pneumocytes and alveolar histiocytes laden with ceroid, an insoluble lipoprotein substance, which is distinctive for HPSIP. Taken from **Pierson et.al., Respiration 2006;73:382–395.**

An ultrastructural study of these enlarged type-II pneumocytes revealed giant lamellar bodies that compressed the nucleus. Accumulation of surfactant, termed as “giant lamellar body degeneration”, is a prominent finding. Occasionally,

cytoplasmic disruption, suggestive of cellular degeneration was encountered (Fig.8) [57]. With the exception of these AECII specific features, the overall histopathological pattern of HPSIP appears quite similar to the usual interstitial pneumonia pattern usually observed in IPF.

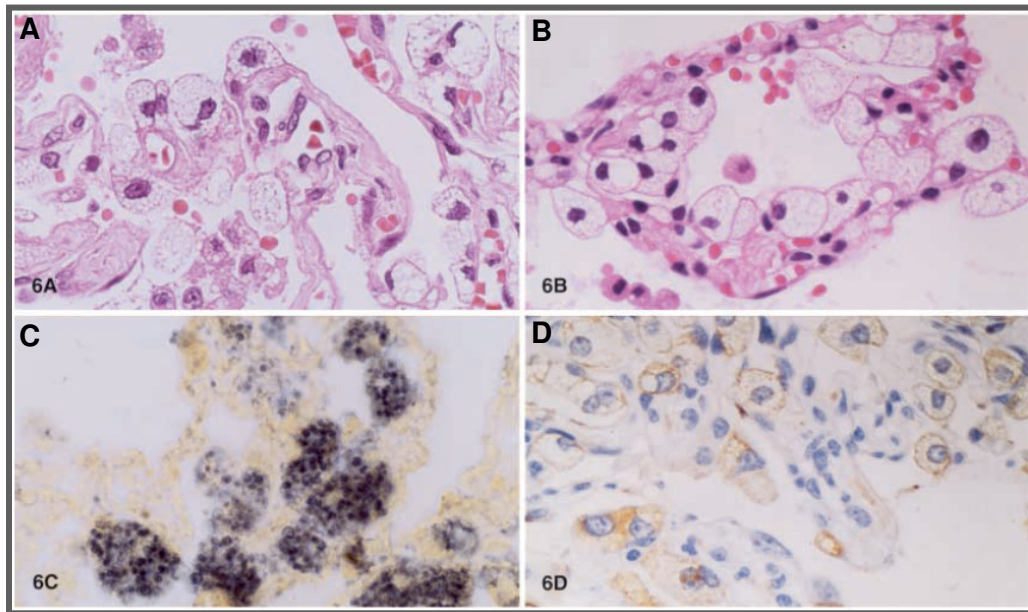


Figure 8: Histochemical analysis of lung tissue from 2 HPSIP patients: A) & B) Depicted are H&E stains of the two patients. Type II pneumocytes are shown with characteristic foamy swelling / degeneration, and some showing small vanishing nuclei. **C)** Acid hematin staining showing numerous cytoplasmic globules positively stained (blue/black) for phospholipid. **D)** Immunostaining for surfactant protein A showing relatively weak positivity. Taken from **Nakatani et.al., Virchows Arch (2000) 437:304–313.**

The pathogenesis of HPSIP is poorly understood. It has however been speculated that intracellular disruption of type II pneumocytes by ceroid could trigger inflammation, cytokine production and fibroblast proliferation, ultimately culminating in the development of fibrosis. Hence, it appeared more likely that the alveolar epithelium is the driving force in HPSIP development. HPS mouse models serve as invaluable tools, in order to further study the role of AECII in driving the disease.

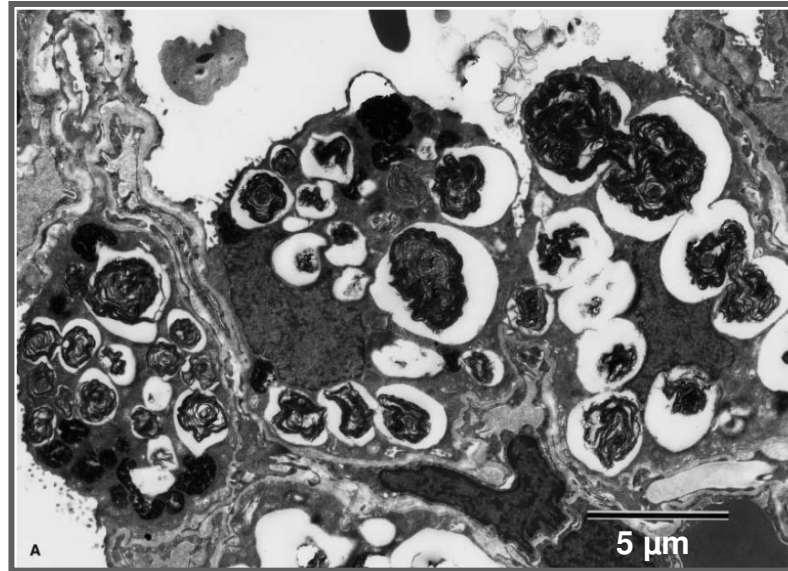


Figure 9: Electron microscopy of type II pneumocytes showing giant lamellar bodies constantly in fusion with each other in the cytoplasm. The complex multilamellar pattern suggests the formation of the giant lamellar body by fusion of smaller ones. Taken from **Nakatani et.al., Virchows Arch (2000) 437:304–313.**

1.5.4. Types of HPS and corresponding mouse models

Initially bred for their attractive coat colours, the HPS mice mutants phenocopy their human counterparts with one exception; i.e. there are no reports till date revealing sporadic development of pulmonary fibrosis in any of the HPS mice models. However, several studies showed the development of progressive pulmonary emphysema in some of the mono and double mutant mice. As mentioned below, about 16 genes causing a HPS-like phenotype in mice have been identified so far. 8 of these genes have disease relevance to human HPS (see Table 1), a detailed description of which is as follows:

Table1: List of human and mouse HPS genes (Taken from a review by Juan S.Bonifacino, Ann. N.Y. Acad. Sci., 2004, 1038: 103–114).

Human	Mouse	Product
HPS1	Pale ear	BLOC-3 Subunit
HPS2	Pearl	AP-3 β 3A Subunit
HPS3	Cocoa	BLOC-2 Subunit
HPS4	Light Ear	BLOC-3 Subunit
HPS5	Ruby eye-2	BLOC-2 Subunit
HPS6	Ruby eye	BLOC-2 Subunit
HPS7	Sandy	BLOC-1 Subunit
	Mocha	AP-3 δ Subunit
	Pallid	BLOC-1 Subunit
	Muted	BLOC-1 Subunit
	Cappuccino	BLOC-1 Subunit
	Reduced pigmentation	BLOC-1 Subunit
	Gunmetal	Rab geranylgeranyl transferase α subunit
	Buff	Vps33A
	Subtle gray	

HPS type 1: The human HPS 1 gene is present on chromosome 10, comprising 20 exons. The gene was identified by positional cloning and encodes a novel, ubiquitously expressed 700-residue protein, which displays no homology to any protein of known function. More than 20 disease causing mutations have been reported in HPS 1 gene, the most common being a 16 bp frame shift duplication in exon 15 [73]. Pale ear strain (*ep*) is the corresponding mouse model and the mouse sequence is 81% identical to human amino acid sequence and 89% similar [73, 88]. Previous reports indicate that mutations in HPS 1 gene in humans lead to the development of abnormal organelles in their melanocytes and development of severe pulmonary fibrosis. HPS 1 mutant mice mimic the human disease with the exception of the development of pulmonary fibrosis. Biochemical characterization using specific antibodies revealed that the HPS 1 protein exists as both cytosolic and peripheral membrane protein in both, humans and mice. It was reported to be associated with HPS4 protein in the 200kDa cytosolic BLOC-3 complex, with a minor proportion also found to be membrane associated. The HPS 1 and the HPS 4 proteins were co-

immunoprecipitated, but the yeast two-hybrid analysis revealed no direct binding between them, suggesting the presence of at least one other subunit in the complex [100].

HPS type 2: This subtype is very unique because it is the only HPS subtype, whose product (AP-3) has been assigned to a definite function. A candidate gene approach was followed to identify the gene responsible for HPS-2. The pearl (*pe*) gene, designated *AP3b1* and its human orthologue, *ADTB3A*, encode the β 3A subunit of the Adaptor Protein-3 sorting complex [96]. The gene encoding β 3A consists of 3968 bp comprising 27 exons. The HPS-2 mutation has a tandem duplication of 793 bp at the cDNA level, originating from the corresponding duplication at the genomic level. The genomic analysis revealed that the mutation contains a tandem duplication of six entire exons (exons 18–23) and associated introns. The identical duplicated units are linked by a unique junction intron that retains the upstream 5.6 kb of the 3' intron (intron 23) and downstream 1.6 kb of the 5' intron (intron 17), which are separated by a 0.2-kb partial mouse transposon (MT) [102]. Patients with HPS-2 can be distinguished from those of the other forms by the presence of neutropenia and susceptibility to recurrent respiratory illnesses. The pearl mice exhibit pigment dilution, prolonged bleeding and impaired kidney and platelet lysosomal enzyme secretion. Interestingly, the pearl strain was suggested also as a model for human congenital stationary night blindness, as it exhibits a reduced sensitivity in the dark-adapted state. The β 3A transcripts of pearl mice were significantly decreased in quantity and produced a β 3A protein with a truncation of 130 amino acids of the C-terminus of the 1,105-amino acid subunit, making it undetectable at the protein level. This suggests that the expression and function of the β 3A protein are significantly affected in pearl mice tissues. Interestingly, in the brain tissue as well as in the melanocyte cell line of pearl mice, the μ 3 subunit levels were undetectable, while both δ 3 and σ 3 were detectable at reduced levels. Moreover, immunofluorescence studies in pearl cells using δ -subunit specific antibodies revealed diffuse cytoplasmic labeling unlike the typical punctate pattern in control cells, indicating that although δ subunit is present in

pearl cells, it is unable to associate with membranes in the absence of the β 3 and / or μ 3 subunits [103].

HPS type 3: The cocoa strain (*coa*) is the murine model for HPS-3 [86]. The HPS 3 gene contains 17 exons, encoding for a protein with 1002 amino acids, with a molecular mass of 113 kDa and is ubiquitously expressed. In humans, more than twenty patients with HPS-3 have been reported with eight mutations described [101]. Most commonly, these patients are homozygous for a large 3904 bp deletion, encompassing the whole exon 1 with more than 2 kb of upstream sequence and 600 bp of intron 1. HPS-3 is clinically mild both in humans and mice and it has been shown that the cocoa mice do not have a defect in basal levels of secretion of lysosomal enzymes, although immature melanosomes were found in retinal pigment epithelium and choroid. The most important observation is that the HPS3 protein is associated with the HPS5 and HPS6 proteins in the multimeric protein complex, BLOC-2 [78].

HPS type 4: The mouse model for HPS-4 is the light ear strain (*le*). The gene consists of 14 exons. The mouse light ear protein is predicted to have 671 amino acids with a molecular mass of 72.7 kDa [89]. Two isoforms of RNA transcripts are detectable in light ear tissue, 3.6 and 3.1 kb in size. Cell lysosomal activity was shown to be elevated in a cell line from light ear mouse skin. Many patients with HPS-4 were reported and 10 different mutations in the HPS-4 gene were identified. Lung biopsy from a HPS-4 patient suffering from pulmonary fibrosis revealed an increased number of type II pneumocytes with foamy cytoplasm [61]. There are however, no reports till date, exhibiting lung abnormalities in light ear mice.

HPS type 5: The ruby eye-2 mouse strain (*ru-2*) is the model for HPS-5 [87]. The HPS-5 gene is found on chromosome 11 in humans and on chromosome 7 in mice. The gene has 23 exons and encodes for a protein length of 1129 amino acids with a molecular mass of 127kDa in humans. In mice, the gene has an open reading frame of 3381 bp with 23 exons, encoding a 1126 amino acid

protein, with a molecular mass of 126.3 kDa. It shares 81% homology with human sequence. Seven disease causing mutations in HPS-5 were identified [104]. All patients had visual impairment and increased cholesterol levels. None of them had shortness of breath and showed minimal to no impairment by pulmonary function testing. On a biochemical level, the HPS-5 molecule was reported to bind to the α 3A integrin [105]. The *ru-2* mice copy the human HPS-5 disease. In choroids, several multi-melanosomal bodies were observed, which is unique to the *ruby eye-2* and *ruby* mutants [101].

HPS type 6: Ruby eye (*ru*) is the mouse model for HPS-6. The human HPS-6 gene is found on chromosome 10 with a single exon and a protein length of 775 amino acids. The mouse HPS-6 gene is found on chromosome 19 [87], and is similar to human gene, containing a single exon with a protein size of 88.8kDa. It shares an 80% homology with the human HPS6 protein. Four allelic ruby eye strains were reported, out of which two strains (*ru*, *ru^{4j}*) have inframe deletion of 3 amino acids H187 to P189 and 22 amino acid deletion L65 to W86, respectively. Reports indicate that HPS-6 patients showed typical oculocutaneous albinism, but no pulmonary fibrosis. The *ru* mouse model mimics human disease with no major pulmonary alterations, although decreased kidney lysosomal enzyme secretion after testosterone treatment was reported [101].

HPS type 7: The gene that is defective in HPS-7 is *DTNBP1* (Dysbindin) and sandy strain (*sdly*) is the corresponding murine model. It encodes dysbindin protein on chromosome 6 with 10 exons. The *Dtnbp1* defective gene encodes a 51 kDa, 352 amino acid protein with a predicted coiled coil region. In *sdly* mice, an inframe deletion from genomic nucleotides caused deletion of 52 residues (119-172 amino acids) comprising exons 6 and 7 including the majority of the predicted coiled coil region. Dysbindin was confirmed to be component of BLOC-1, but the functional significance is not yet clear. Six non-disease causing polymorphisms and a single mutation have been reported in human patients. Patients showed oculocutaneous albinism, mild shortness of breath and decreased lung compliance, but otherwise normal pulmonary function. Studies in

sdv mice showed markedly abnormal melanosomes and decreased retinal pigment, with little insight into the lung abnormalities [82].

HPS type 8: Defect in the BLOC1S3 has led to the identification of HPS-8. The reduced pigmentation (*rp*) mouse gene is its orthologue. The mouse gene is found on chromosome 7 containing 2 exons encoding a 195 amino acid protein. Studies showed that BLOS3 is a component of BLOC-1 when in the phosphorylated form. Patients have been identified to have a homozygous germline frameshift mutation. They showed incomplete oculocutaneous albinism and mild platelet dysfunction with easy bruising, frequent epistaxis and prolonged bleeding after surgery or child bearing, requiring blood transfusion in some cases. The *rp* mouse was reported to have increased kidney lysosomal glycosidase activities, increased bleeding times, decreased platelet dense bodies, immature melanosomes, decreased melanin and abnormal intracellular tyrosinase distribution [67].

Other important models of HPS: Attempts to create a mouse model that more severely mimics the human HPS disease, resulted in the development of some HPS double, triple and quadruple mutant mice. This was done by intercrossing the different HPS mono mutant mice. Mouse model homozygously recessive for both HPS1 and HPS2 (*ep/pe*) displayed pathologic findings similar to the human HPS. Type II cells of these mice showed giant lamellar body degeneration with intracellular organelles demonstrating florid foamy degeneration of surfactant material aberrantly produced and secreted. A more recent study on these double mutant mice showed that they exhibited developmentally increased tissue phospholipid concentration from postnatal day-2 to postnatal day 70. This study focused on very young HPS1/2 mice, which showed an increase in mature hydrophobic surfactant proteins in lung tissue and decreased stimulated secretion by type II cells isolated from these mice [106]. Another important model is the pale ear – ruby eye (*ep/ru* or HPS 1/6) double mutant, which exhibited air space enlargement and honeycomb structure at the age of about 2 years [106]. Prominent lung abnormalities were observed in many combinations of

double/triple mutants, but sporadic development of lung fibrosis has yet not been reported in any of the murine strains investigated. Noteworthy information is the development of giant lamellar bodies with combinations of any BLOC with AP-3, which was supported by the increased phospholipid concentrations in their respective lung tissues [80].

2. Aim of the study

It is now known that severe pulmonary fibrosis is found in some patients with HPS (HPSIP) and that the occurrence of HPSIP then largely dictates a poor prognosis. However, despite the fact that there are 16 different murine HPS strains mimicking the human HPS gene defects there is, up to now, no report on development of lung fibrosis in mice. Likewise, the underlying pathomechanistic principle for development of HPSIP is yet not known. The aim of this study was therefore to screen different murine HPS models (HPS1,2,6,1/2,1/6) for development of lung fibrosis and to undertake genotype / phenotype correlations with special emphasize on impaired lysosomal trafficking and the cellular consequences of which in alveolar type II cells. For this purpose, the following questions were addressed.

- Is pulmonary fibrosis, which is found in some patients with HPS, also found in some murine forms of HPS, pending on the genotype?
 - Does HPS result in impairment of lysosomal trafficking in alveolar type II cells, thereby inducing defective surfactant metabolism? If yes, would there be differences in dependency of the genotype?
 - Does the extent of altered surfactant metabolism correlate with phenotype?
 - What would be the cellular consequences of such altered lysosomal transport in the alveolar type II cells? Does the altered lysosomal transport induce lysosomal or ER stress and cause apoptosis?
 - Finally, as development of apoptosis was suggested to represent a key event in Idiopathic Pulmonary Fibrosis, another ultimately lethal interstitial lung disease, would the extent of epithelial apoptosis in the various HPS models correlate with the development of lung fibrosis?
-

3. Materials

3.1. General materials

Manufacturer	Products
Carl Roth, Karlsruhe, Germany.	Tris, NaCl, Rotipherose, Sacharose, APS, Glycine, Agarose, BSA.
Sigma Aldreich, Steinheim, Germany	EDTA, Triton X-100, Tween20, β -mercaptoethanol, DNase.
Fluka chemie, Buchs, Switzerland.	Sodium deoxy cholate, TEMED, Skimmed milk powder, Methanol, Chloroform, Acetic acid.
Merck, Darmstadt, Germany.	Sodium dodecyl sulphate, Perchloric acid, Bromophenol blue, NaOH, HCl, Ascorbic acid, KH_2PO_4 , Na_2HPO_4 , KCl.
Amersham, Brunswick, Germany	Hybond PVDF membrane, ECL western blot detection system, ECL hyperfilms.
Whatman GmbH, Dassel, Germany.	Whatmann papers, 3mm.
Wak chemie, Steinbach, Germany.	RNA Zol-B.
Applied Biosystems	Random hexameres, RNase inhibitor
Fermentas	dNTP mix.
GIBCO/Invitrogen, Germany.	DMEM, RPMI, L-Glutamine, Pencillin/ Streptomycin.
PAA Laboratories GmbH, Marburg, Germany.	FCS.
BD Biosciences, Belgium.	Dispase.

3.2. Materials for animal work

Manufacturer	Products
Braun Melsungen, Germany	Use and throw syringes and needles.
Beckton-Dickinson, Germany	Tracheal cannulae, (Kanuele 26G)
Pfizer, Karlsruhe, Germany.	Ketamin hydrochloride (100mg/ml) (KetavetR)
Bayer, Leverkusen, Germany.	Xylazinhydrochloride (RopumR)
Ethicon GmbH, Norderstedt, Germany.	Surgical threads, non absorbable
Martin Medizintechnik, Germany.	Surgical instruments.

3.3. Materials for histology

Manufacturer	Products
Fischer scientific, Germany.	Ethanol 70%, 95%, 99.6%, Formaldehyde, alcohol free.
Carl Roth, Karlsruhe, Germany.	Rotihisto (Xylolersatz), Xylol, Haemalaun.
R. Langenbrinck, Teningen, Germany.	Histologic glass slides.
Menzel, Braunschweig, Germany.	Cover slips, 24 x 36 mm
Feather, Japan.	Microtome blades.
Dako cytomation, Hamburg, Germany.	Glycerol mounting medium.
Leica Microsystems, Nussloch, Germany.	Automated microtome, flattening for paraffin sections, tissue embedding cassettes, cooling plate.

3.4. Kits

Manufacturer	Products
Zytomed systems, Berlin, Germany.	Zytochem AP Fast red kit, broad spectrum – for immunohistochemistry.
Roche, Germany.	In situ cell death detection kit, Flourescein.
Pierce, Germany.	BCA protein assay kit.
Qiagen, Hilden, Germany.	Omni transcript RT kit for Reverse transcription. Hot start taq DNA polymerase kit for PCR. DNeasy blood and tissue kit for genomic DNA isolation.

3.5. List of primers

<u>WT HPS1-forward</u>	5' AGCTAGAACACTGTCCAAAGATAGC 3'
<u>WT HPS1-reverse</u>	5' GTATGAGAGAAGGCACTGGAAGAAG 3'
<u>HPS1-forward</u>	5' AGCTAGAACACTGTCCAAAGATAGC 3'
<u>HPS1-forward</u>	5' ATGTAAGAATAAAGCTTTGTGCGCAG 3'
<u>WT HPS6-forward</u>	5' ACATCCTGCTACACCATTGCCCC 3'
<u>WT HPS6-reverse</u>	5' CATGTCCAGTAGTTCCAAGGTGGAG 3'
<u>HPS6-forward</u>	5' CACCCACATCCTGCTACACCTTTTTG 3'
<u>HPS6-reverse</u>	5' CATGTCCAGTAGTTCCAAGGTGGAG 3'
<u>HPS2-forward</u>	5' GAAATGGGGCTGCACATAG 3'
<u>HPS2-reverse</u>	5' GAACCCTCACACAGGACTCG 3'
<u>Cathepsin D-forward</u>	5' GGTACCTGAGCCAGGACAC 3'
<u>Cathepsin D-reverse</u>	5' CCGTGGTAGTACTTGGAGTC 3'
<u>β – actin-forward</u>	5' CTACAGCTTCACCACCACAG 3'
<u>β – actin-reverse</u>	5' CTCGTTGCCAATAGTGATGAC 3'

3.6. List of antibodies

Name of the antibody	Dilution	Company
Rabbit X Human proSP-B	1:1000 (WB)	Chemicon
Rabbit X Sheep mature SP-B	1:1000 (WB)	Chemicon
Rabbit X Human proSP-C	1:1000 (WB,IH)	Chemicon
Rabbit X Human mature SP-C	1:100 (WB)	Altana pharma
Rabbit X Mouse β -actin	1:5000 (WB)	Abcam
Rabbit X Mouse CHOP	1:200 (WB)	Santacruz
Goat X Mouse Cathepsin D	1:1000 (WB) 1: 50 (IH)	R&D systems
Rabbit X Human Cathepsin D	1:200 (IH)	Abcam
Rabbit X Human Cleaved Caspase-3	1:50 (IH)	Trevigen
Rabbit X Mouse CHOP	1:50 (IH)	Santacruz
Mouse X Human CHOP	1:50 (IH)	Abcam
HRP conjugated secondary antibodies (anti-rabbit or anti- goat)	1:2000 (WB)	Dako cytotation
Rat X Mouse CD16/32	15 μ l/10ml RPMI (panning antibody for AEC isolation)	BD Biosciences
Rat X Mouse CD44	15 μ l/10ml RPMI (panning antibody for AEC isolation)	BD Biosciences

3.7. Equipment & software

Manufacturer & Type	Products
Applied Biosystems, PCR system 2400	Thermocycler
Bio-rad, Trans-blot SD, semi dry electrophoretic transfer blot	Transfer machine for Western blots.
Tecan Spectraflour plus; MTX lab systems Inc.	ELISA plate reader.
Magellan Tecan Inc.	Software for ELISA reader
Alphalnotech, Alphaease.	Gel biodoc for UV light .
Alphaease FC	Software for densitometry.
Carl Zeiss Micro Imaging Inc.	Mirax micro digital slide scanner with viewer software, Light microscope.

4. Methods

4.1. Animals

Breeding pairs of all HPS mono mutant mice, HPS1/6 double mutant mice were bought from Jackson laboratories. Breeding pairs of HPS1/2 double mutant mice were obtained from the lab of Dr. Richard Swank, Roswell park, Buffalo, NY. The background strain for HPS1, HPS2, HPS6 and HPS1/2 mice was C57Bl/6J. The HPS1/6 mice were on B6C3Fe background. All these mice were mated and maintained in the central animal housing facility under SPF (specific pathogen free) conditions. All HPS mice along with WT controls used in this study were sacrificed at the age of 3 months and 9 months.

HPS mice can be generally identified by their different coat colours. In spite of this, all HPS mice were genotyped for the mutated gene with the primers mentioned in the list of primers in 'Materials' section. Genomic DNA for this purpose was isolated with DNeasy kit according to the manufacturer's protocol. All mice were tested periodically and were free of known viral and bacterial pathogens. Mice were sacrificed by injecting an overdose of anesthesia (Ropum solution - 2% of the injecting solution, 100mg/ml ketavet; a final volume of 100µl per mouse). Thorax and abdomen were then disinfected with Braunol^R. Each mouse was then fixed, a small slit was made near abdomen, the skin and belly were cut open upto the mentum. The diaphragm was carefully teared and the rib and elbows were spread apart and fixed laterally. Within the ventral neck region, trachea was seen covered with connective and muscle tissue which were carefully teared apart without damaging the trachea. An incision was made in the trachea with a blunt tweezer into which, a tube (braunuele) was inserted and fixed. The left main bronchus was clamped and the right lung was washed (lavaged) three times with 350µl 0.9% NaCl each time. The lavage was done with same volume and in the same way for both HPS and control mice. This lavage (broncho alveolar lavage or BAL) was collected in an eppendorf cup and centrifuged for 10 minutes at 300xg, at 4°C. The supernatant was transferred to a new vial and shock frozen in liquid Nitrogen. The clamp from the left main bronchus was removed and fixed to the right main bronchus. The bronchus was

cut distal from the clamp and the right lung was excised and shock frozen. Before taking the left lung for histology, the lung was flushed to make it free from blood via the right ventricle. Formalin fixation was achieved by filling the lung with 3.7% Formaldehyde solution with a constant hydrostatic pressure of 20 cm H₂O. Following instillation the trachea was ligated, the lung was carefully removed and transferred into a cup and covered with Formaldehyde solution. After overnight incubation at 4 °C, the lung was transferred into an embedding cassette, buffered in PBS and stored at 4 °C. This lung tissue was processed in a Vacuum-dryer for dehydration and then embedded in paraffin. 3µm thin sections were cut with a microtome for further analysis.

4.2. Histology

4.2.1. Hematoxylin & Eosin staining: H&E staining is a charge-based, general purpose stain, widely used for routine histological examination of tissue sections. It is a two-stage stain for cells, in which hematoxylin is followed by a counter stain of red eosin. The hematoxylin stains acidic molecules, which gives shades of blue and eosin stains basic materials and gives shades of red, pink and orange, thereby, staining the nuclei with a deep blue-black and the cytoplasm with pink, respectively. The staining protocol is summarized as follows:

Staining time(minutes)	Reagents
2x 10	Rotihistol
1 x 5	Rotihistol
2 x 5	Ethanol (absolute)
1 x 5	Ethanol (96%)
1 x 5	Ethanol (70%)
1 x 2	Aqua.dest
1 x 20	Hemalaun (acidic)
5	Running water
1	Ethanol (96%)
4	Eosin (alcoholic)
washing	Aqua.dest

2 x 2	Ethanol (96%)
1 x 5	Ethanol (99.6%)
1 x 5	Isopropyl alcohol (99.8%)
2 x 5	Rotihistol
1 x 5	Xylol
	Mount with pertex, which is a xylol based mounting medium.

4.2.2. Trichrome staining: A staining method utilizing a combination of three different dyes to identify different cell or tissue elements. This method is especially suitable for studying connective tissue. Nuclei are normally stained blackish brown, cytoplasm is stained brick red, erythrocytes are stained yellow / orange and mucous substances and collagen are stained in green. Following is the protocol in a table format for trichrome staining.

Staining time(minutes)	Reagents
2 x 10	Rotihistol
2 x 5	Ethanol (absolute)
1 x 10	Weigert hematoxylin
1 x 5	Warm, running tap water
1 x 10	Ponceau acid fuschin solution
4-5x	1% acetic acid until nonspecific shades are washed off.
1 x 5	Orange-G solution
4-5x	Wash in 1% acetic acid
1 x 20	Light green solution
2 x 5	Ethanol (99.6%)
2 x 5	Rotihistol
1 x 5	Xylol
	Mount with pertex.

4.3. Western blot analysis

Homogenization of mice lungs: The right halves of the snap frozen lung tissues were pulverized by mortar and pestle. The pulverized tissue was treated with lysis buffer containing protease inhibitor. The ground tissue treated with lysis buffer was incubated for about an hour on ice, followed by centrifugation at 13000 rpm at 4°C for 10 minutes. The supernatant was obtained and used for protein concentration determination by Bicinchoninic acid (BCA) method.

Lysis buffer pH 7.4	Final concentration
Tris	50mM
NaCl	150mM
EDTA	5mM
Triton X-100	1%
0.5% Sodium deoxycholat	0.5%
PMSF	1mM

Poly Acrylamide Gel Electrophoresis of protein (SDS-PAGE): Protein sample from tissue extract was either non-reduced or reduced (by adding 10% β -mercaptoethanol) and denatured by heating to 95°C for 10 min in 4 x loading buffer, (5g SDS, 40ml glycerin, 25ml stacking gel buffer, 0.01g bromophenolblue for a final volume of 100ml) and then cooled on ice immediately. The samples were collected by brief centrifugation and then loaded on self casted polyacrylamide gels. In the presence of 1x electrode buffer (10x buffer: 25mM tris, 192mM glycin, 0.1%SDS) the electrophoresis was performed with 15mA constant and the gel was run till the bromophenol blue reached the bottom of the resolving gel. Then, the gel was used for Western-blot analysis.

SDS PAGE	Resolving gel buffer		Stacking gel buffer
	10%	15%	
Rotipherose	3.3ml	5ml	1.33ml
Dist.H ₂ O	3.2ml	1.53ml	6.57ml
10%SDS	100µl	100µl	100µl
Resolvinggel buffer (1.125M Tris/HCl, pH8.8, 30%sacharose)	3.33ml	3.33ml	-----
Stacking gel buffer (0.625M Tris/HCl, pH6.8)	-----	-----	2ml
10%APS	50µl	50µl	100µl
TEMED	10µl	10µl	10µl

Electro blotting of immobilized proteins: The separated proteins on the SDS-polyacrylamide gel were transferred to a polyvinylidene fluoride (PVDF) membrane by electro blotting. The PVDF membrane was activated by methanol before used. The transfer equipment was prepared in the following way: two layers of Whatmann 3mM filter paper washed with transfer buffer (20mM tris, 150mM glycin, 20% methanol) followed by activated PVDF membrane washed with transfer buffer were placed onto the electro blotting chamber. On the PVDF membrane, the gel and the other two layers of filter paper washed with transfer buffer were placed. Electro blotting was performed at constant current (2mA / cm²) for approximately 90 min.

Immunological determination of immobilized proteins: The membrane was blocked with 5% non fat dry milk in 1% TBST buffer at room temperature for 1h followed by incubation with primary antibody at 4°C overnight. After washing with 1 x TBST three times for 20 min each, the membrane was incubated with the respective secondary antibody at room temperature for 2 h followed by three

times washing with 1 x TBST buffer for 20 min each (10x buffer: 500mM tris, 500mM NaCl, 0.1% tween 20). The protein bands were detected by ECL (Enhanced Chemi-luminescence) treatment, followed by exposure of the membrane to ECL films in dark. Bands on the film were then visualized by dipping them in developing and fixing solutions.

4.4. Phospholipid analysis

Phospholipids were extracted according to the classical Bligh & Dyer method. 25µl of lung homogenate was used as a starting material. The volume was made upto 800µl with 0.9% NaCl. Phospholipids were isolated by adding 3ml Methanol : Chloroform (2:1) followed by a 30 minutes incubation at RT. The phospholipids were resolved by adding chloroform and methanol, 1ml each and centrifugation was performed at 2500xg, for 10 minutes at 4°C. Phase separation was observed and the upper chloroform phase was pipetted into a new tube followed by drying under liquid Nitrogen. Phosphate assay was performed by adding 200µl of perchloric acid into both standards and samples followed by cooking at 200°C for 1 hour. After cooling down the tubes to room temperature, 20µl (114mg/ml) ascorbic acid and 1ml Ammonium Molybdate (4.6mM) were added and allowed to develop colour at 60°C for 45 minutes. The tubes were cooled down and the absorbance of each sample was measured at a wavelength of 698λ. The OD values were noted and the concentration of phosphate was measured by means of a standard curve. Concentration of phospholipids was calculated by the formula: $\mu\text{g PL} / 1\text{ml} = [\mu\text{g Phosphorous}] \times 734/31 \times \text{dilution factor}$ (734: molecular weight of DPPC, 31: molecular weight of Phosphorous). The resultant values were normalized to 1 mg protein concentration of respective samples before analysis.

4.5. Lipidomics

Lipids were quantified by electrospray ionization tandem mass spectrometry (ESI-MS/MS) in positive ion mode as described previously (Brügger et al., Liebisch et al. 2004, Liebisch et al. 2006) (Tab. 1). Samples were quantified by

direct flow injection analysis using the analytical setup described by Liebisch et al. (Liebisch et al. 2004, Liebisch et al. 2006). A precursor ion scan of m/z 184 specific for phosphocholine containing lipids was used for phosphatidylcholine (PC), sphingomyelin (SM) (Liebisch et al. 2004) and lysophosphatidylcholine (LPC) (Liebisch et al. 2002). Neutral loss scans of m/z 141 and m/z 185 were used for phosphatidylethanolamine (PE) and phosphatidylserine (PS), respectively (Brügger et al.). PE-based plasmalogens were analyzed according to the principles described by Zemski-Berry (2004). Phosphatidylglycerol was analyzed using a neutral loss scan of m/z 189 of ammonium adduct ions (Schwudke et al.). Ceramide was analyzed similar to a previously described methodology (Liebisch et al. 1999) using N-heptadecanoyl-sphingosine as internal standard. Free cholesterol (FC) and cholesteryl ester (CE) were quantified using a fragment ion of m/z 369 after selective derivatization of FC using acetyl chloride (Liebisch et al. 2006). Correction of isotopic overlap of lipid species as well as data analysis by self programmed Excel Macros was performed for all lipid classes according to the principles described previously (Liebisch et al. 2004). Experiments concerning to lipidomic profiling were performed by Dr. Gerhard Liebisch, Department of clinical chemistry, University of Regensburg, Germany.

Lipid	MS - unlabelled
Phosphatidylcholine – PC Sphingomyelin - SPM	ESI+, PIS m/z 184
Lyso-PC - LPC	ESI+, PIS m/z 184
Phosphatidylethanolamine - PE	ESI+, NL m/z 141
PE based Plasmalogens	ESI+, PIS m/z 364 (O-16:1) PIS m/z 392 (O-18:1) PIS m/z 390 (O-18:2)
Phosphatidylglycerol - PG	ESI+, NL m/z 189
Phosphatidylserine - PS	ESI+, NL m/z 185
Ceramide (d18:1) - Cer	ESI+, PIS m/z 264
Cholesterol/Cholesteryl ester – FC/CE	ESI+, PIS m/z 369 Derivatisation

Table.2: Methods established for direct flow injection analysis of lipids with and without stable isotope labelling.

4.6. Isolation of RNA from mice lungs

RNA was extracted from cells using guanidine thiocyanate-acid phenol (RNAzol B, WAK-Chemie, Germany). RNA-Bee is a complete and ready-to-use reagent for isolation of total RNA from samples of human, animal, plant, bacterial and viral origin. A biological sample is homogenized or lysed in RNA-Bee and the homogenate/lysate is separated into aqueous and organic phase by the addition of chloroform. The subsequent centrifugation efficiently removes DNA and proteins from the aqueous phase containing RNA. The non-degraded, pure RNA is obtained from the aqueous phase by the isopropanol precipitation, washing with ethanol and solubilized in an appropriate solution. Snap frozen lung tissue was taken into a 15 ml falcon tube with 4ml RNAzol and homogenized on ice. Thereafter, 400 μ l of chloroform was added with mixing. The solution was incubated on ice for 30 min and centrifuged at 5000 rpm at 4°C for 45 min. The upper phase (~1ml) containing RNA was collected in a new 2ml eppendorf cup. The RNA was precipitated by addition of equal volume of isopropanol, incubating at -20°C for 1 hour and centrifuging at 13,000 rpm at 4°C for 10 min. The RNA pellet was washed once with 500 μ l 70% ethanol. The purified RNA was centrifuged again for 10 min at 13,000 rpm and dried at room temperature for 10 min. Finally, the pellet was dissolved in appropriate volume of RNase free H₂O. After measuring the RNA concentration, the samples were stored at -80°C. To determine the concentration and purity of the RNA, the extinction at 260 nm and 280 nm was measured. An OD of 1 at 260 nm corresponds to 40 μ g RNA/ml. The ratio of the OD at 260 nm and at 280 nm is a measure of RNA purity. In a protein-free solution the ratio OD₂₆₀/OD₂₈₀ is 2. Due to protein contaminations this coefficient is usually lower. In the experiments of this study, it was between 1.7 and 2.

4.7. Preparation of cDNA from RNA probes

For the preparation of cDNA, 2 μ g RNA per sample was used. RNA was copied to cDNA using reverse transcriptase (Qiagen, omnitranscript RT kit) with random hexamers. 15 μ l of the following master mix was added to 2 μ g / 5 μ l RNA.

10xBuffer	2 μ l
dNTPs	2 μ l
Randomhexameres	4 μ l
RNase-inhibitor	0.5 μ l
H ₂ O	5.5 μ l
RT	1 μ l

The denatured RNA mixed with master solution was then subjected for cDNA synthesis by incubating at room temperature for 15 minutes and then at 37°C for 1 hour.

4.8. Semi-quantitative RT PCR

The polymerase chain reaction (PCR) allows amplification of DNA fragments due to repetitive cycles of DNA synthesis. The reaction uses two specific oligonucleotides (primers), which hybridize to sense and antisense strands of the template DNA fragment, four deoxyribonucleotide triphosphates (dNTP's) and a heat-stable DNA polymerase. Each cycle consists of three reactions that take place under different temperatures. First, the double-stranded DNA is converted into its two single strands (denaturation at 94 °C).

PCR reaction	per 25μl
10xBuffer	2.5 μ l
dNTPs	0.5 μ l
Forward primer	1 μ l
Reverse primer	1 μ l
H ₂ O	17.75 μ l
Taq polymerase	0.25 μ l
cDNA	2 μ l

They function as templates for the synthesis of new DNA. Second, the reaction is cooled (50-60°C) to allow the annealing (hybridization) of primers to the

complementary DNA strands. Third, DNA polymerase extends both DNA strands at 72°C (DNA synthesis) starting from the primers. The PCR was performed in a thermocycler, programmed as follows:

Activation of Hotstart Taq	94 °C	20min
Denaturation	94 °C	30sec
Annealing	refer Table 3	30sec
Extension	72 °C	1 min
Cycles	30	
Final Extension	72 °C	10min

Table.3: Annealing temperatures of primers

Primers for	annealing temperature
HPS1	57°C
HPS2	59°C
HPS6	60°C
Cathepsin-D	55°C
Glucosylceramide synthase	57°C
β-actin	55 °C

After the amplification, PCR products (10 µl) were electrophoretically analyzed in a 2% agarose gel with 0.2 µg /100 ml ethidium bromide.

4.9. Agarose gel electrophoresis

The DNA sample was mixed with loading buffer (0.01% bromophenol blue, 40% glycerol, to a final volume with 10x TAE buffer) and loaded onto the 2% agarose gel. The electrophoresis was performed for 45-60 min with 5 V/cm. The negatively charged DNA migrated from the cathode (-) to the anode (+). To visualize DNA, the gel was treated with ethidium bromide (0.5 µg/ml), which intercalated between the bases of DNA double strands forming a complex

fluorescent under UV light. The size of amplified DNA was determined by a DNA molecular weight standard. The agarose gel was visualized by flourChem 8900, gel bio doc system.

4.10. Immunohistochemistry

Immunohistochemistry (IHC) is the localization of antigens in tissue sections by the use of labeled antibody as specific reagents through antigen-antibody interactions that are visualized by a marker such as fluorescent dye, enzyme, radioactive element or colloidal gold. Since immunohistochemistry involves specific antigen-antibody reaction, it has apparent advantages over other traditionally used special enzyme staining techniques that identify only a limited number of proteins, enzymes and tissue structures. There are numerous immunohistochemistry methods that may be used to localize antigens. The selection of a suitable method should be based on parameters such as the type of specimen under investigation and the degree of sensitivity required. Mice lungs were fixed in paraformaldehyde as described earlier and sections of 3µm thickness were used for immunohistochemical analysis in this study. Sections were deparaffinized at 60°C for 2 hours and then in xylene for 10 minutes. They were then rehydrated in descending alcohol concentrations (99.6%>96%>80%>70%>50%). Sections were washed in washing buffer (1x PBS) to remove traces of ethanol. Antigen retrieval was performed by detergent method, using 0.4% Triton X-100 in 1xPBS (10x buffer: 80g NaCl, 29g Na₂HPO₄×12.H₂O, 2g KCl, 2g KH₂PO₄, 1L final volume with d.H₂O, pH7.4). Sections were immersed in this permeabilization buffer for 5 minutes and washed. The AP fast red kit was used for further steps. The sections were blocked for 10 minutes in the blocking solution followed by washing. Primary antibody solutions were prepared in 3% BSA solution with respective dilutions. A negative control was always used where primary antibody was omitted. Sections were placed in a humid chamber and incubated with primary antibody overnight at 4°C, followed by washing for 5 times. 50µl of biotinylated secondary antibody was added to each section and incubated for 10 min at RT, followed by washing.

Few drops of enzyme conjugate (streptavidin / alkaline-phosphatase conjugate) were added to each section with 10 min incubation at RT, followed by washing. Fast red tablets were used as substrate which was freshly prepared by dissolving one fast red tablet in one substrate buffer vial (naphtol-phosphate buffer). 50µl of this substrate solution was given to each section and allowed to develop in the dark, with constant monitoring for the pink colour development under light microscope. Enough care was taken that all HPS sections, control sections and negative control sections be treated in the same way, and developed for the same time in order to avoid false results. After developing, the reaction was stopped by immersing the slides in aqua.dest. Counterstaining was performed with haemalaun for 2 minutes followed by washing the slides under running tap water, which resulted in blue nuclei. Sections were then mounted with glycerol mounting medium and allowed to dry.

4.11. In-situ apoptosis assay

The terminal deoxynucleotidyl transferase-mediated dUTP-biotin nick end labeling (TUNEL) method labels fragmented DNA which is a characteristic of the apoptotic cells. The TUNEL method identifies apoptotic cells in situ by using terminal deoxynucleotidyl transferase (TdT) to transfer biotin-dUTP to these strand breaks of cleaved DNA. The biotin-labeled cleavage sites are then detected by reaction with HRP conjugated streptavidin and visualized by a substrate. The following protocol was used for detecting TUNEL positive cells in this study. Sections were treated and permeabilized in the same way as described in immunohistochemistry method in this section. After permeabilization, sections were placed in a humid chamber and 50µl of enzyme solution was given to all sections, except to the negative control where enzyme solution was omitted. In order to carefully spread the solution all through the sections and to avoid drying, parafilm was used to cover them. This chamber was incubated at 37°C for 1 hour, followed by washing. 50µl TUNEL AP (converter AP, conjugated with alkaline phosphatase) was then given to each section, covered with parafilm and incubated at 37°C for 30 minutes, followed by

washing. The substrate used here was Fast red, which was freshly prepared by dissolving one fast red tablet in 2ml 0.1M Tris-HCl, pH 8.2 and filtering through a 0.22µm filter. This substrate solution was given to all sections and allowed to develop in dark, carefully monitoring the colour development under light microscope. Reactions were then stopped by placing the sections in washing buffer. Counterstaining with haemalaun and mounting was performed in the same way as described in immunohistochemistry method in this section.

4.12. Microscopy

All stained sections were analysed by scanning each slide in Mirax scanner from Carl Zeiss. The mirax viewer software was used to analyze and make snapshots of the stained tissue sections.

4.13. Isolation of alveolar epithelial cells

Alveolar epithelial cells were isolated from 3 months old HPS1/2 double mutant mice and their background control mice. 3 mice per group were taken for one isolation and this was performed for 3 times. Panning antibody (CD16/44 and CD45) coated plates were prepared one day prior to the isolation procedure by addition of 15µl of each antibody in 10ml RPMI medium and stored at 4°C overnight. These plates were transferred to 37°C incubator just before beginning the isolation procedure. Mice were anesthetized and dissected in the same way as mentioned under the description of animals in this section. Once the trachea was revealed, a tubus was fixed into it. Lavaging was then down for 3 times. Thymus was removed and the right atrium was carefully opened. The lung was cleared from blood by flushing with 20ml 0.9% NaCl through the left ventricle. 1.5ml dispase was injected into the lung through the tubus. 0.4ml melted agarose was then injected into the lung. The lung was then carefully taken out of the thorax and incubated for 45 minutes in 1ml dispase at RT. 5ml of + medium was taken into a cell culture dish under the laminar flow. The heart, trachea, bronchus, etc were removed and the tissue was minced with the help of scissor and pipetted thoroughly until a cell suspension was reached. Suspensions from

all the three mice were pooled and filled to a final volume of 50ml. This suspension was then filtered through different filter gazes (10µm, 20µm and 100µm) and sufficient +medium was used to avoid conglomeration. Filtered suspensions were poured in 50ml falcon tubes and centrifuged at 200xg for 10 minutes at 14°C.

Culture medium	+Medium	-Medium
2% L-Glutamine	2% L-Glutamine	2% L-Glutamine
10% FCS	1% Pen/Strep	1% Pen/Strep
1% Pen/Strep	10mM HEPES	10mM HEPES
10mM HEPES	DMEM	DMEM
DMEM	4%(w/v) DNase	

After centrifugation, the supernatant was carefully removed and the pellet was resuspended in 1ml +medium. Suspensions were pooled and –medium was added to a final volume of 30ml. These suspensions were plated on CD coated dishes, which were prepared one day before by adding 50µl of CD45 and 30µl of CD16/32 antibodies per 10ml –medium and stored at 37°C / 4% CO₂. 5 plates coated with these antibodies were used for isolation of primary cells from 3 mice. After plating the suspensions, these plates were incubated for 45 minutes at 37°C / 4% CO₂ for 45 minutes, followed by transferring the suspensions onto non-coated dishes and incubating them at 37°C / 4% CO₂ for 30 minutes. Suspensions were then pooled and centrifuged at 300xg for 5 minutes at 4°C. The supernatant was then removed and the pellet was resuspended in an appropriate volume of +medium. Nile red staining was performed and the epithelial cells were counted. Purity of the cells was checked by immunofluorescence and the rest of the cells were frozen after a brief centrifugation.

4.14. Densitometry analysis

The densitometry analysis was performed using the spot denso software from Alpha Innotech. Integrated density Values of targeted proteins were first normalized against those of actin values. The values of controls were then assumed as 100% and the percent of increase or decrease of a target protein was calculated.

4.15. Statistics

Unless indicated otherwise, all data in the figures and text are expressed as means \pm SEM of 3-8 mice. Statistical evaluation was performed by unpaired t-test with subsequent Mann – Whitney test. Significance is indicated by * $p < 0.05$, ** $p < 0.005$, *** $p < 0.0005$.

5. Results

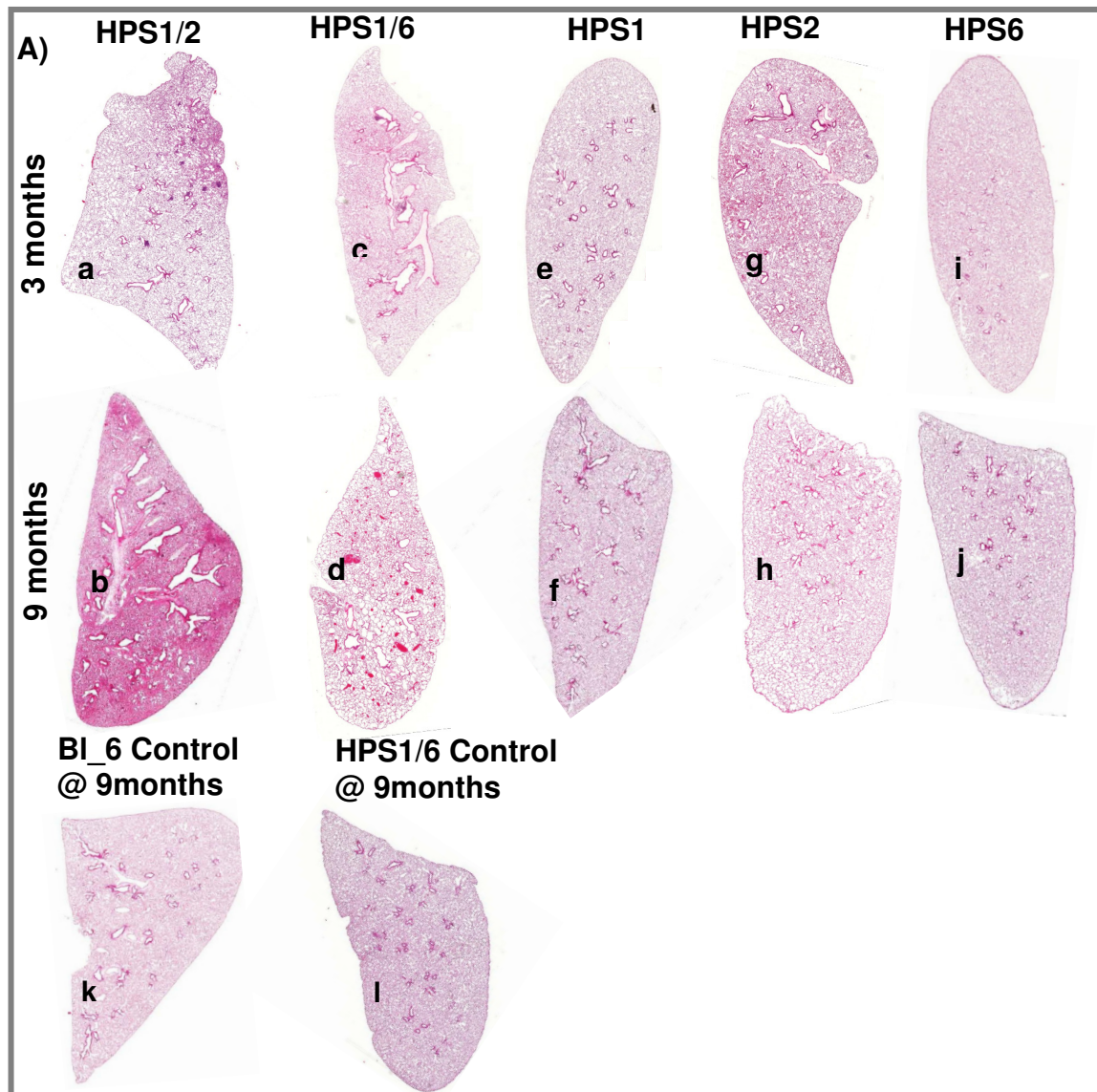
5.1. General appearance and phenotype of HPS mice

All the three mono mutant mice (HPS1, HPS2, HPS6) and the two double mutant mice (HPS1/2 and HPS1/6) mice were viable and showed a regular social behaviour until the end of the observation period of 9 months. Body weights of these mouse mutants were not significantly different from those of the respective control mice between the ages of 3 and 9 months. Pale ear was the phenotype of HPS1 mouse and the mouse imposed with a black coat colour. The coat colour was pearl white for HPS2 and black for HPS6 mutants. The eye colour was black for HPS1 and HPS2 mutants and deep red for HPS6 mutant, so the HPS1/2 and HPS1/6 double mutants revealed a phenotype of pale ear/pearl and pale ear/ruby eye, respectively. A major difference in breeding efficiencies was observed. The breeding efficiency of single mutants, where only one protein complex with either HPS1 (BLOC-3⁻), HPS2 (AP-3⁻) or HPS6 (BLOC-2⁻) was deficient, was uncompromised as compared with that of C57BL/6J control mice. Similarly, there was no difference in breeding efficiencies of homozygous double mutants involving the HPS1 and HPS6. In contrast, a significant drop in breeding efficacy was illustrated by the HPS1/2 (BLOC-3⁻, AP3⁻) homozygous mice.

5.2. Lung histology of HPS mice

To investigate the extent of lung disease in HPS monomutant (HPS 1,2,6) and double mutant (HPS 1/2, 1/6) mice, H&E and trichrome stainings of lung sections were performed. In the HPS 1/2 double mutant mice, but not in any of the other mice investigated, sporadic development of lung fibrosis was evident already at low magnification and at an age of 3 months (Fig.10A-a). Being patchy at the beginning, the extent of lung fibrosis progressed over time and at an age of large parts of the lungs were compensated (Fig.10A-b). At higher magnification, extensive cellular infiltration and extracellular matrix deposition was evident. With regard to the spatial distribution, the early fibrotic changes appeared to be more

prominent in the subpleural areas of the lungs. At a higher magnification, lung structure appeared to be roughly preserved in most areas, with lymphoplasmacellular infiltration and increased collagen content of septae (Fig.10B-k,l). However, in the most concerned regions dense fibrosis was prominent and did not allow further differentiation with regard to the basic alveolar structure. Especially in the younger HPS 1/2 mice still limited extent of fibrosis, alveolar type II cells could be evaluated and showed a distinct phenotype, with a dramatic increase in cell size, a “swollen” aspect and an apparently increased content of lamellar bodies (Fig.10B-a,b).



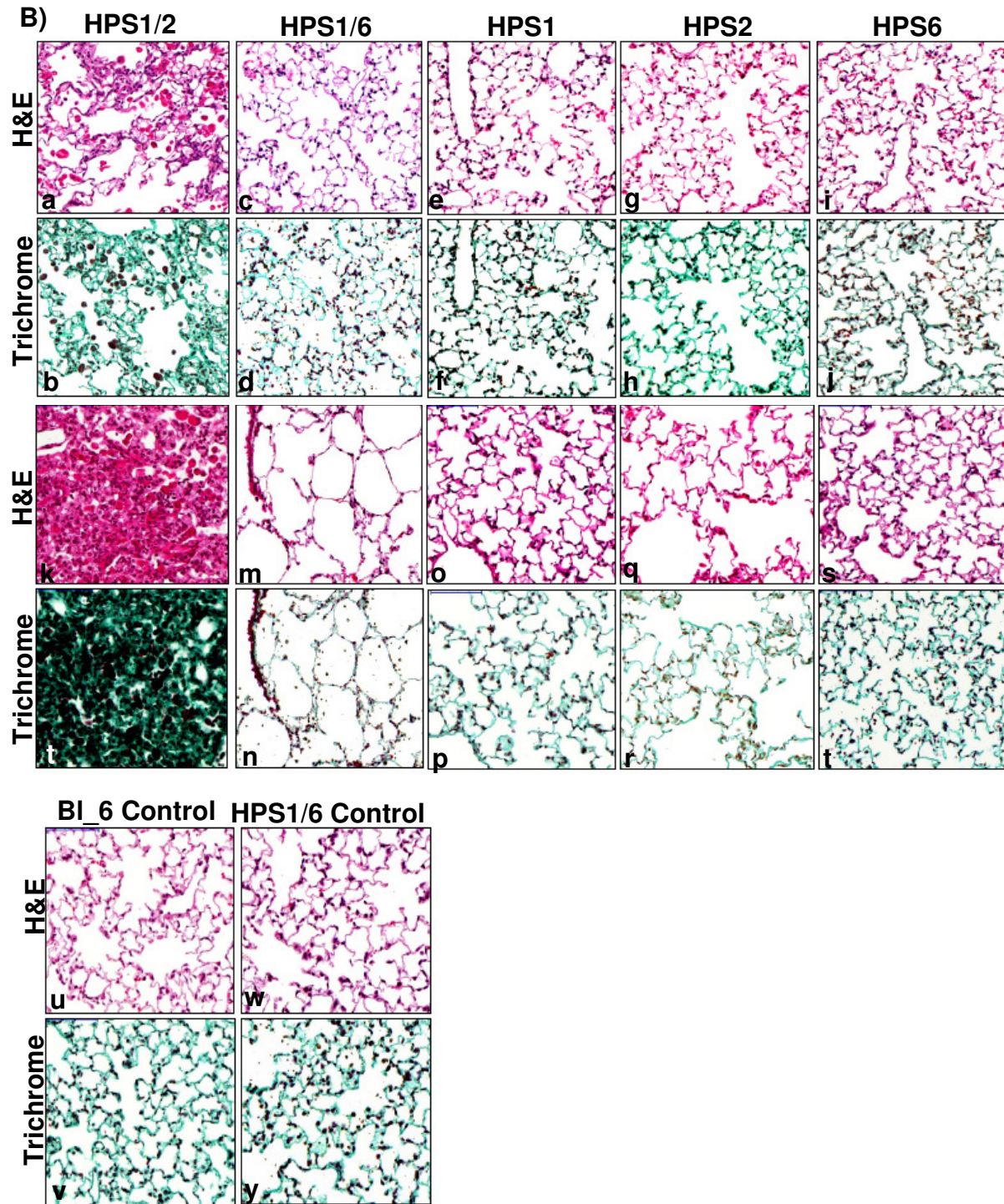


Figure 10: Histology of HPS mice **A)** Representative H&E stainings of complete right lungs of HPS mono mutant, double mutant, and their background control mice at 3 and 9 months age. **B)** Representative 20x magnification pictures of H&E and trichrome stained lungs of all the HPS mutants & WT controls analyzed in this study at (a-j) 3 months and (k-x) at 9 months (n=5-10 mice per group).

In the HPS 1 (Fig.10B-o,p) and 2 (Fig.10B-q,r) mono mutant, and even more in the HPS 1/6 (Fig.10B-m,n) double mutant mice, air space enlargement was a prominent finding. The HPS6 mice lungs (Fig.10B-i,j,s,t), however, showed normal structure when compared with their background controls (Fig.10B-u,v).

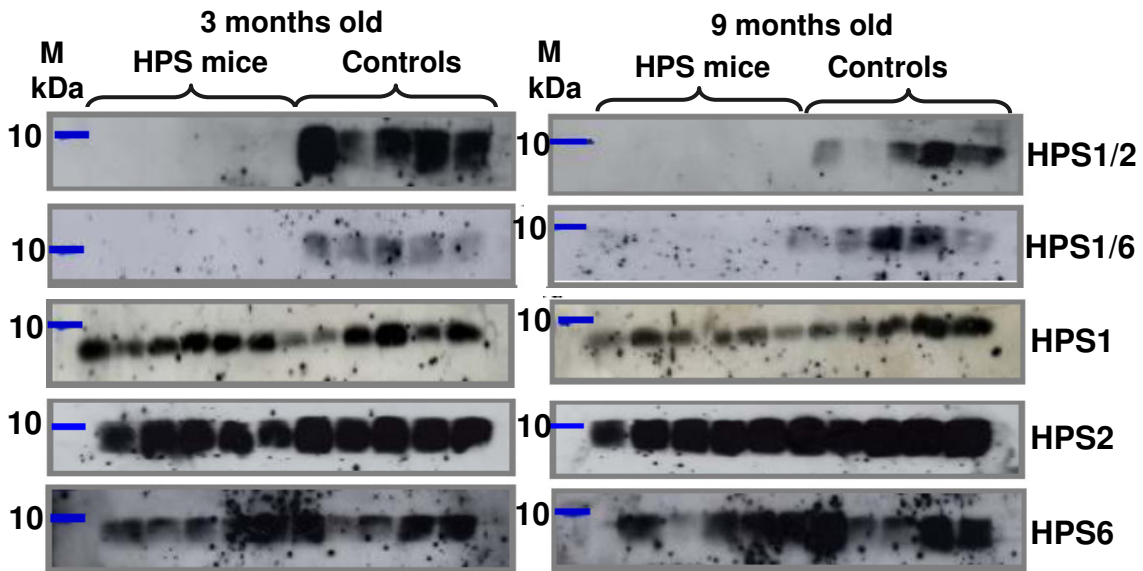
5.3. Surfactant alterations in HPS mice

5.3.1. Altered processing and transport of the hydrophobic surfactant proteins

In order to characterize surfactant metabolism in the HPS mouse models mentioned, a stepwise surfactant analysis starting with the surfactant proteins was performed, in particular, the hydrophobic surfactant proteins –B and –C in bronchoalveolar lavage fluid (BALF) as well as in lung tissue.

5.3.1.1. Reduction in mature SP-B & mature SP-C in BALF occurs almost exclusively in HPS1/2 mice: Equal volume of BAL fluids from all the HPS mice were subject to SDS PAGE and western blot analysis of mature SP-B and mature SP-C. While mature SP-B was undetectable already at the age of 3 months in HPS1/2 mice BAL fluid, it appeared to be reduced in HPS1/6 mice and remained unaltered in all the HPS mono mutant mice analyzed until the age of 9 months (Fig.11A). Similarly, significantly reduced levels of mature SP-C were observed in the HPS1/2 mice BAL fluid at the age of 3 and 9 months, but appeared unchanged in the HPS1/6 double mutant and all the single mutants analyzed until the age of 9 months (Fig.11B). As the mature hydrophobic surfactant proteins were found to be severely reduced especially in HPS1/2 mice BAL fluid, intracellular processing of these hydrophobic surfactant proteins in the lung tissue of HPS1/2 mice and all other HPS mice were further assessed.

A) SP-B



B) SP-C

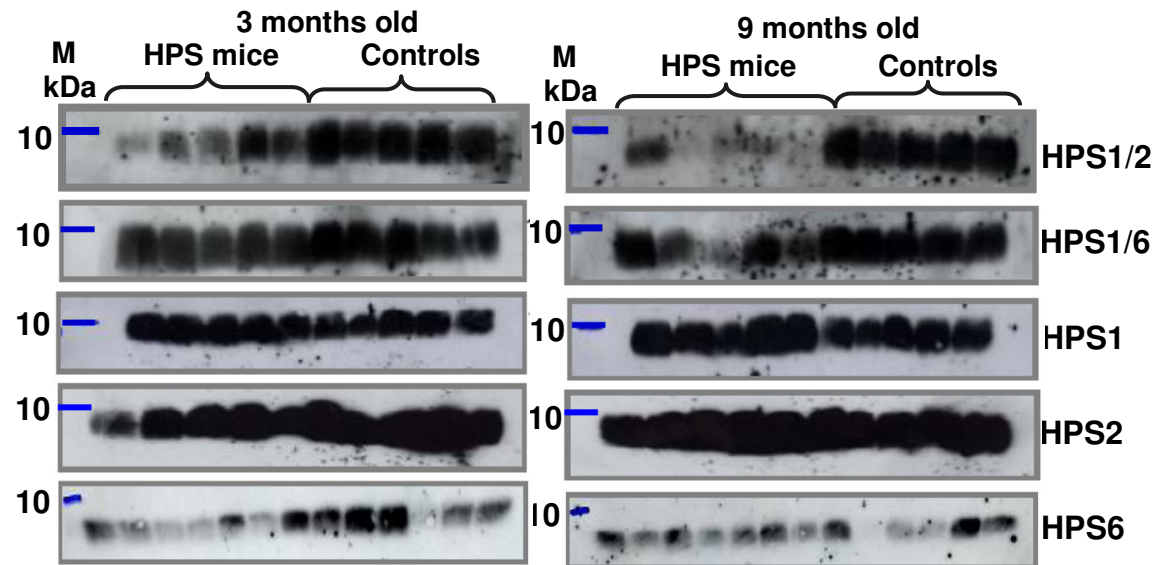


Figure 11: Mature hydrophobic surfactant proteins in BALF of HPS mice: Western blot analysis of **A)** mature SP-B and **B)** mature SP-C in BALF from all the double and mono mutant HPS mice along with their respective WT controls at the age of 3 and 9 months. Equal volume (20 μ l of BAL fluid per sample) was used for each analysis (n=5 mice per group).

5.3.1.2. Extensive intracellular surfactant protein accumulation in HPS1/2 double mutant mice: HPS1/2 and control mice lung homogenates were subjected to SDS-PAGE followed by western blotting for pro and mature forms of both SP-B and SP-C. This analysis revealed a prominent increase in the levels of

almost all forms of SP-B and SP-C when compared to their background controls (Fig. 12, 15). The 19kDa processing form of pro SP-B were already elevated in 3 month old HPS1/2 mice and at the age (Fig. 12) of 9 months. Similarly, a significant increase in the mature SP-B levels was already observed in 3 month old and it was much more severe in the 9 month old mice.

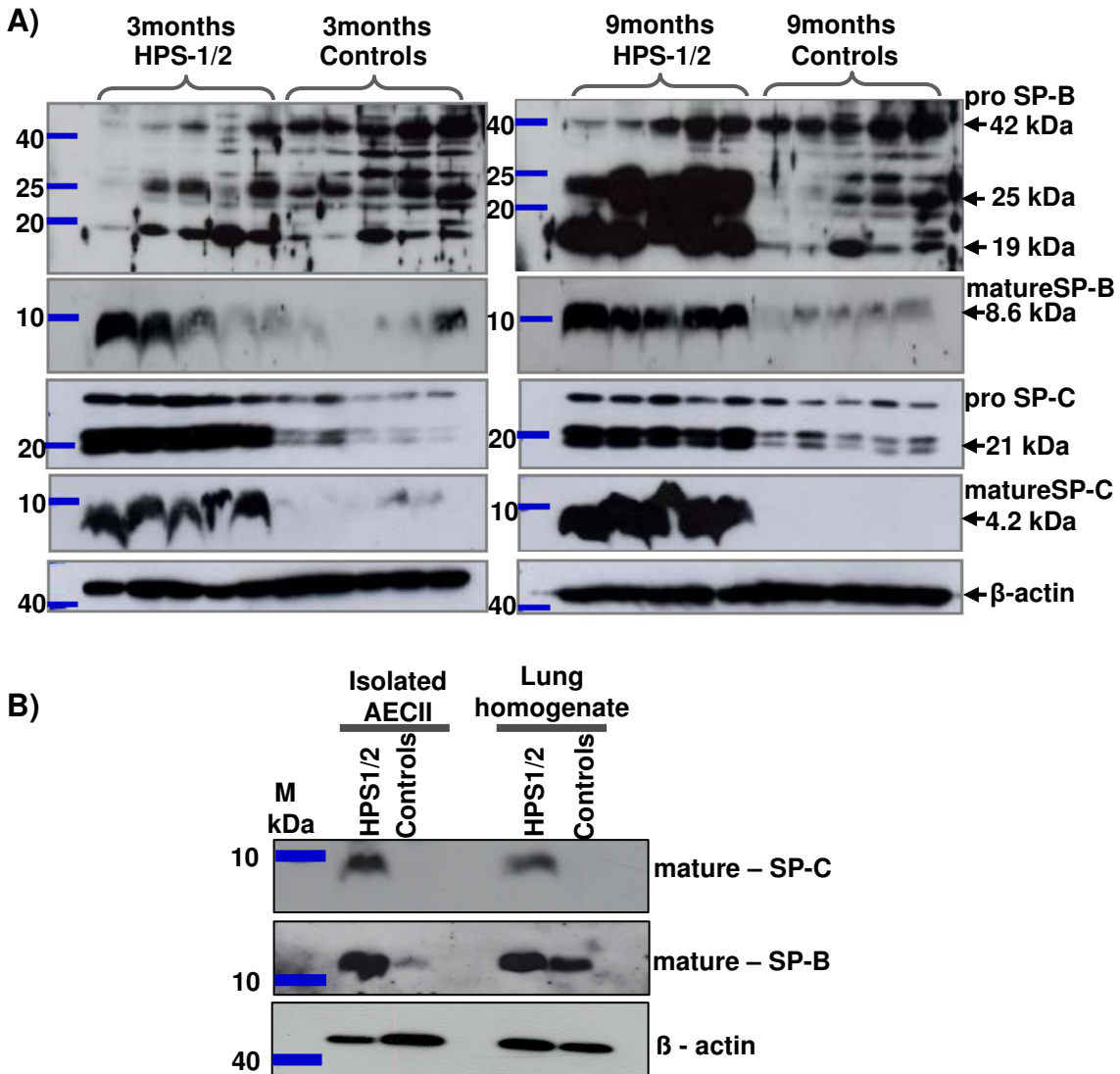


Figure 12: Alteration of surfactant proteins in HPS1/2 mice: A) Western blot analysis of lung homogenates of 3 month (left panel) and 9 month (right panel) old HPS1/2 double mutant and control mice (n=5 per group). Left panel shows 3 month old mice and right panel shows 9 month old mice. All forms of tissue hydrophobic surfactant proteins were analysed (proSP-B, mature SP-B, proSP-C, mature SP-C). **B)** Western blot analysis of isolated alveolar epithelial cells and lung homogenates from 3 month old HPS1/2 mice and WT control mice (n=3 mice per group). Please note that blots have been developed to show adequate staining for HPS1/2 mice samples, longer development forwarded staining for mature SP-C also in controls.

The pro SP-C and mature SP-C levels enormously increased both in 3 and 9 month old HPS1/2 mice (Fig.12A). This clearly illustrates a severe accumulation of hydrophobic surfactant proteins in the lung homogenates of these mice. To check if this increase particularly refers to an accumulation of surfactant proteins in AECII, alveolar epithelial cells were isolated from 3 month old HPS1/2 mice alongside with WT controls and analyzed these isolated cells for mature SP-B and mature SP-C, by western blotting. A clear accumulation of mature SP-B and mature SP-C was observed in AECII of HPS1/2 mice when compared with those of controls (Fig.12B). With such severe accumulation of surfactant proteins in AECII and drastic decrease in the levels of mature surfactant proteins in BAL, it was concluded that there is a severe defect in distal lysosomal transport and surfactant secretion by AECII in HPS1/2 mice.

5.3.1.3. Surfactant protein alterations in HPS1/6 double mutant mice :

Western blot analysis of HPS1/6 double mutant mice lung tissue revealed a significant increase in the 19kDa form of pro SP-B (Fig.13A), however, the tissue levels of mature SP-B, pro and mature SP-C were not significantly different from the background controls even at the age of 9 months (Fig.13A).

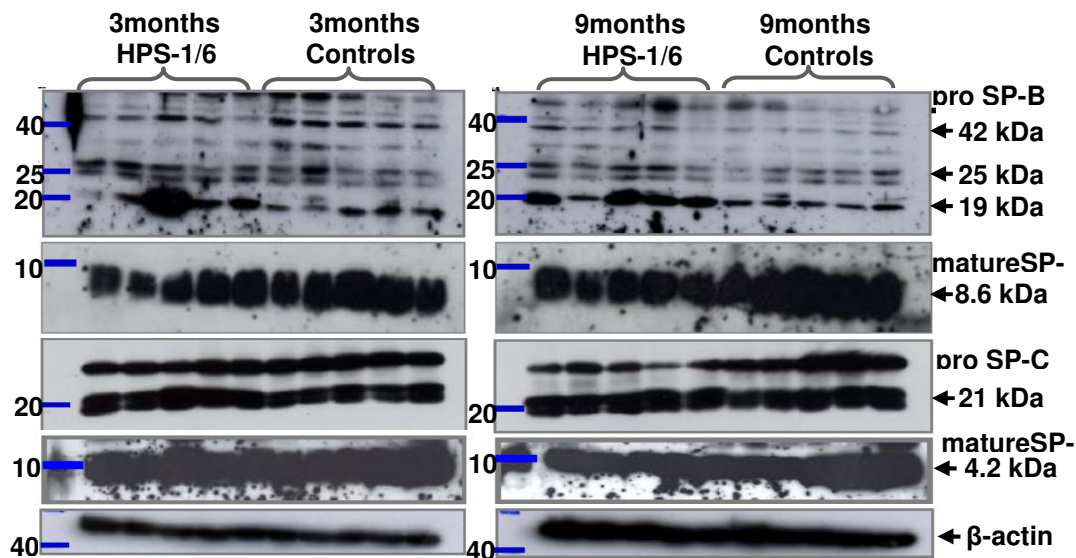
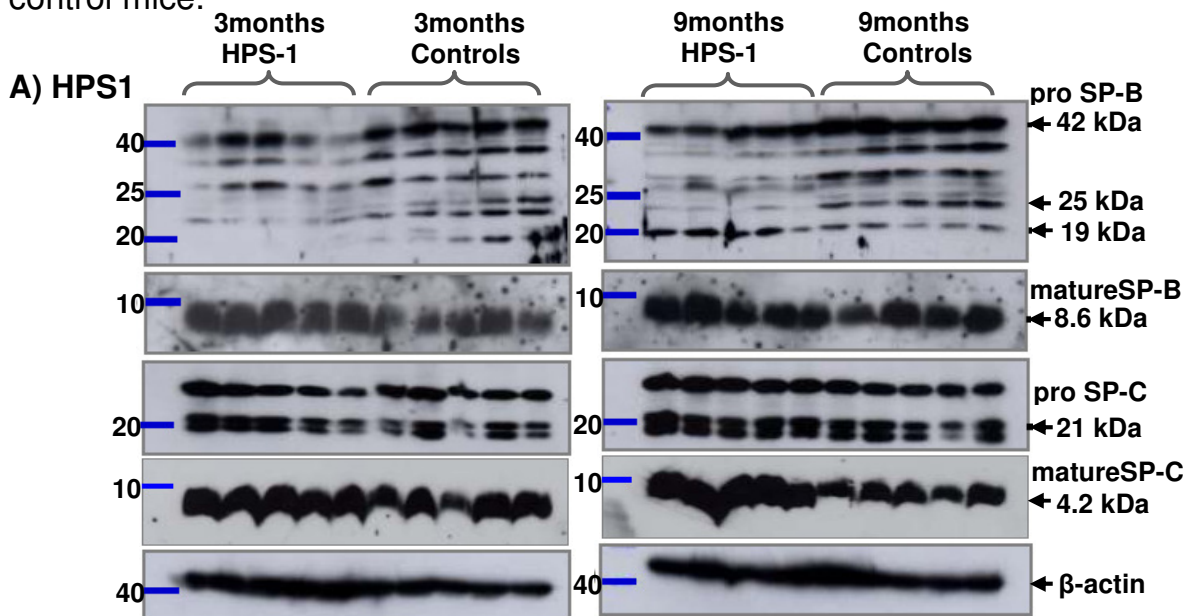


Figure 13: Alteration of surfactant proteins in HPS1/6 mice: Western blot analysis of lung homogenates of 3 month (left panel) and 9 month (right panel) old HPS1/6 double mutant and control mice (n=5 per group). Left panel shows 3M old mice and right panel shows 9M old mice. All forms of tissue hydrophobic surfactant proteins were analyzed (pro SP-B, mature SP-B, pro SP-C, mature SP-C).

5.3.1.4. Surfactant protein alterations in HPS mono mutant mice : HPS1, HPS2 and HPS6 along with control lung homogenates were subjected to SDS-PAGE followed by western blotting for pro and mature forms of SP-B and pro and mature forms of SP-C. An increase in the 19kDa pro SP-B processing intermediate was observed in lung tissues from 9 month old HPS1 mice. There was no significant increase in the levels of mature SP-B and pro SP-C. However, mature SP-C levels were slightly increased in the 9 month old HPS1 tissue (Fig.14A). In HPS2 mono mutant mice, a slight increase in the 19kDa pro SP-B processing intermediate was observed, but mature SP-B remained unchanged. In the same way, there was an increase in the pro SP-C levels as compared to controls, and no major changes were observed with regard to mature SP-C (Fig.14B). In HPS6 mono mutant mice, elevated levels of 19kDa form of pro SP-B in lung tissues of 9 month old HPS6 mice tissue was observed, but the levels of mature SP-B, pro SP-C and mature SP-C remained unchanged when compared with WT controls (14C). With these observations, it was concluded that the surfactant protein processing and transport were severely affected in HPS1/2 double mutant mice, partly in HPS1/6 mice and almost unaffected in the mono mutant mice as compared with WT control mice.



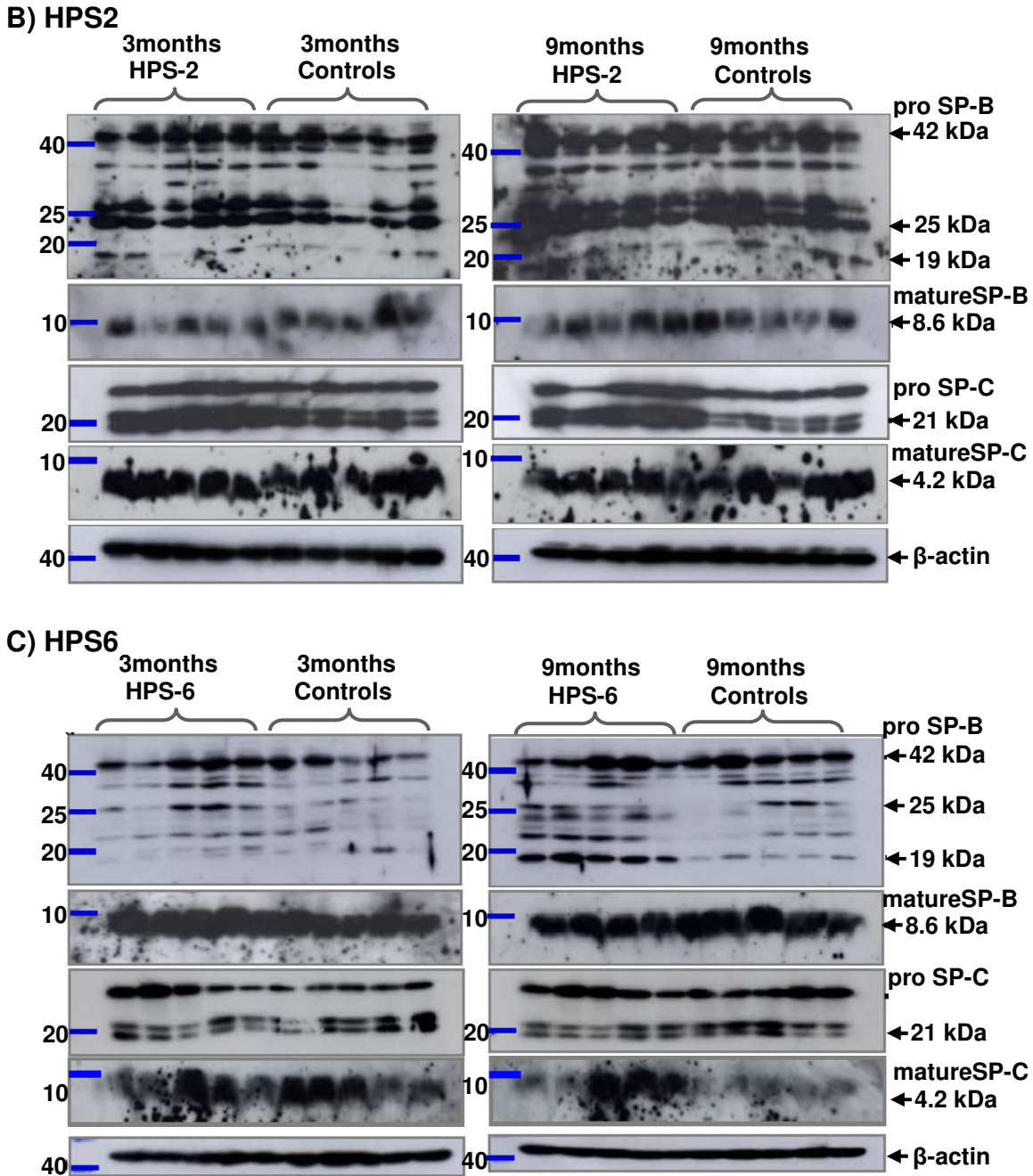
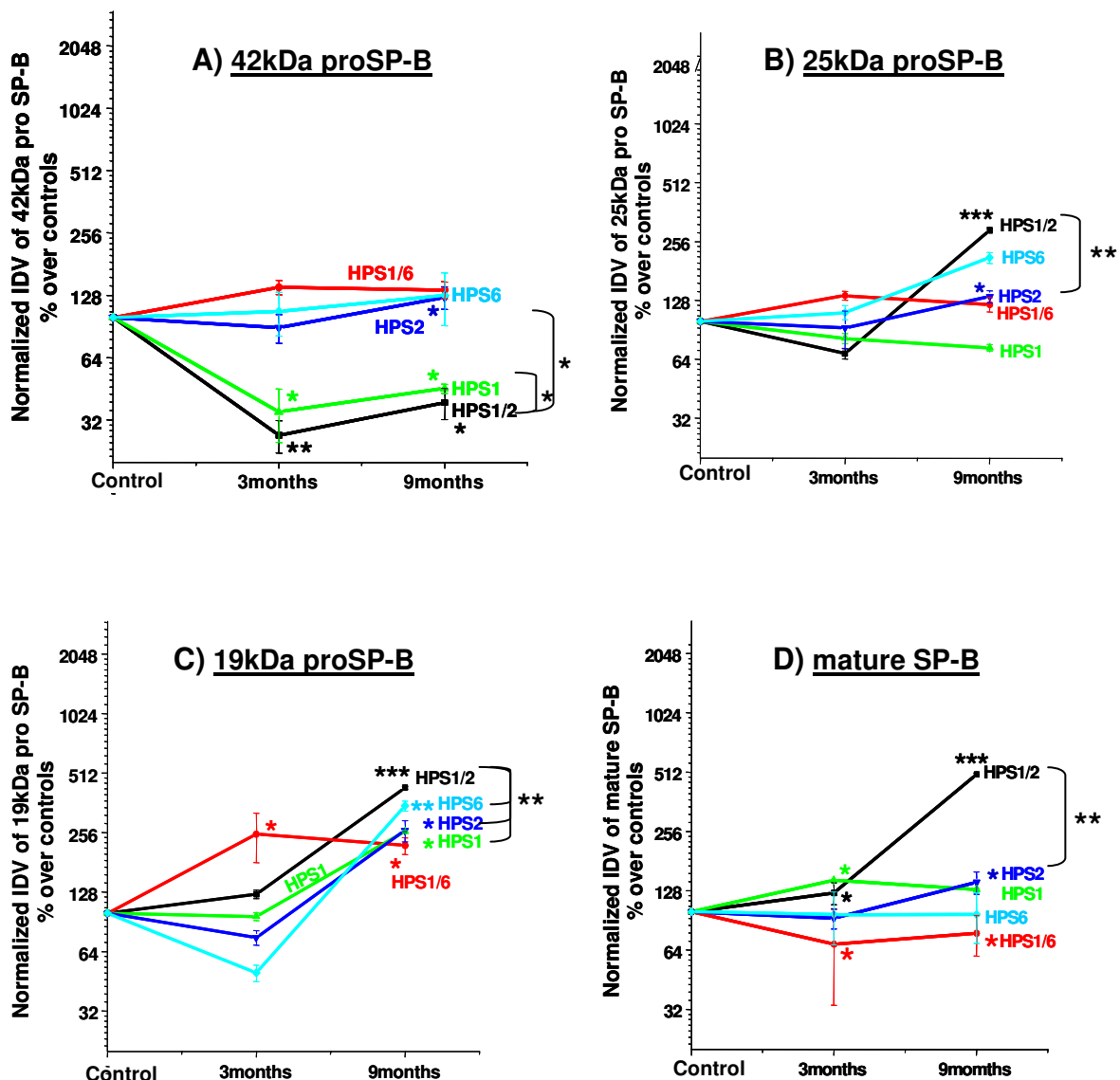


Fig 14: Alteration of surfactant proteins in HPS mono mutant mice: Western blot analysis of hydrophobic surfactant proteins for **A) HPS1 B) HPS2** and **C) HPS6** mono mutant and WT control mice. Left panel shows 3 month old and right panel shows 9 month old mice. Western blots were performed for pro SP-B, mature SP-B, pro SP-C and mature SP-C in lung tissue of these mice (n=5 mice per group).

5.3.1.5. Comparative analysis of surfactant protein alterations in HPS mice:

For better comparison between the different HPS strains, intensity of each pro and mature SP-B/C band of each HPS and control mouse lung homogenate was

assessed by densitometric analysis and referred to the b-actin band of the same SDS-PAGE. Expression of each protein form in HPS was then related to the band intensity of the respective control run on the same gel (Fig.15). Such comparative analysis forwarded almost unchanged or even reduced 42kDa pro SP-B levels in all HPS mice, a roughly threefold increase in the 25kDa (Fig.15B) and the 19kDa (Fig.15C) processing intermediates of pro SP-B, reaching significance for all HPS mice in case of 19kDa pro SP-B. With regard to mature SP-B (Fig.15D), a striking and fivefold increase was encountered in the lung homogenates of HPS1/2 mice, whereas mature SP-B did not change dramatically in the lungs of the other HPS mice.



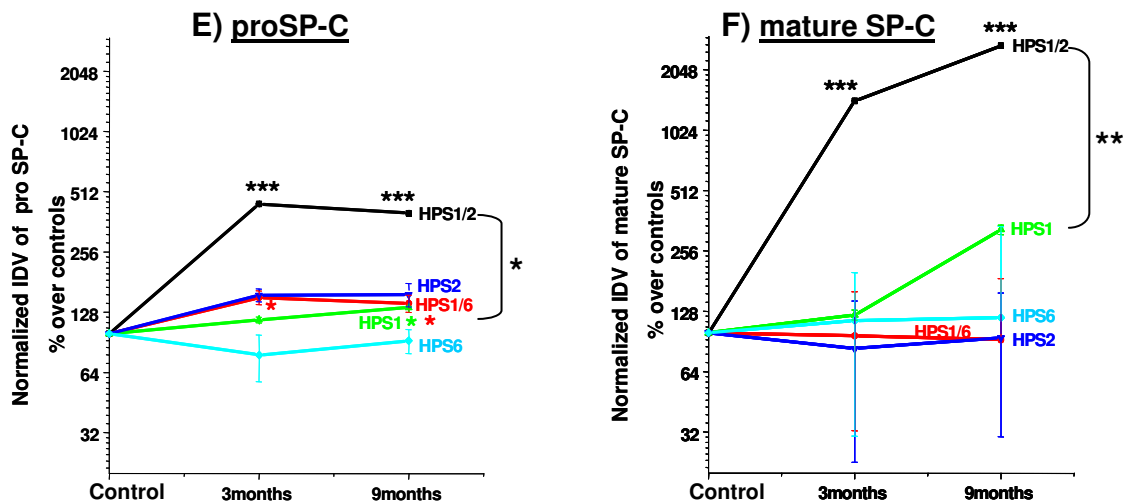


Fig 15: Alteration of surfactant proteins in HPS mice: Densitometric analysis of blot intensity of all forms of SP-B (A – D) and SP-C (E & F). Normalized IDV of blot intensities of respective proteins of HPS mice as percentage over control mice are given. (*p* value summary: **p*<0.05, ***p*<0.01, ****p*<0.001, n=5 mice per group).

With regard to SP-C, there were no significant changes of 21kDa pro SP-C and mature SP-C in the HPS 1/2/6 single and the HPS 1/6 double mutant mice, with the exception of a roughly threefold increase of mature SP-C in HPS 1 mice. However, in the HPS 1/2 mice, a dramatic increase of both, pro SP-C and mature SP-C was evident already at the age of 3months (Fig. 15 E & F). Whereas pro SP-C levels were already fivefold increased at that time point and did not increase anymore in the older HPS 1/2 mice, the mature SP-C levels were increased 15fold. This was paralleled by the severe accumulation of pro and mature forms of SP-C (Fig. 15 E & F respectively) in the same lungs. With the exception of accumulation of the 19kDa processing intermediate form of the pro SP-B in HPS1/6 double mutant mice lung homogenates (Fig.15C) and reduction in the mature SP-B in the same lungs (Fig.15D), the surfactant proteins otherwise remained unaltered in the lung homogenates of all the single mutant mice and the HPS1/6 double mutant mice.

5.3.2. Phospholipidosis in HPS mice

Since phospholipids represent bulk compounds of surfactant, total phospholipid content of lung homogenates was analyzed in all 3 and 9 month old HPS mono

mutant and HPS double mutant mice along with their background controls. Phospholipid content was increased in all HPS mice, however, with a varying extent. The weakest increase of phospholipids was encountered in HPS 1/6 (~1.5 fold), the strongest in HPS 1/2 mice (~ 3fold; Fig.16). Of note, there was a statistical significant difference between the HPS 1/2 and all other HPS mice with regard to the phospholipid content. In addition, it seems noteworthy to mention that in contrast to the changes in mature SP-B and SP-C, the phospholipids content of HPS 1/2 lung homogenates did not further increase beyond the age of three months.

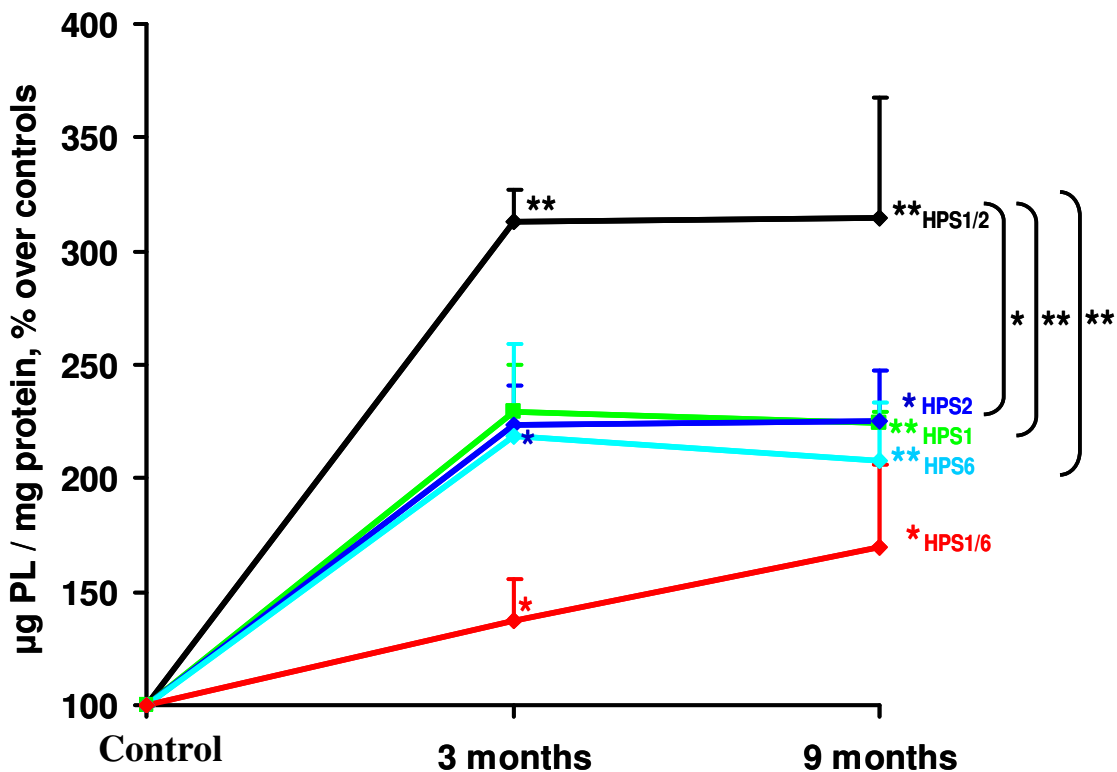


Figure 16: Alteration of surfactant lipids in HPS mice lung homogenates: Total phospholipids were extracted from lung tissue of all the 3 and 9 month old HPS mono and double mutant mice and their background controls (n=5 mice per group) according to Bligh & Dyer method, and phosphate assay was performed as described in methods. The resulting phospholipid concentrations were normalized against their respective protein concentrations and values are expressed as µg phospholipids per mg protein of respective sample. (*p value summary: * $p < 0.05$, ** $p < 0.01$, *** $p < 0.001$*).

5.3.3. Lipidomic profiling of HPS lung tissues

Lipidomic analysis of lung tissues from all 9 month old HPS and control mice was performed. As evident from Table 2, extensive alterations of the phospholipids were found especially in the HPS1/2 mice. HPS1/2 mice showed marked differences in almost all depicted phospholipids, when compared with controls. While significant increase in PC was observed, a reduction in the rest of phospholipid classes was observed in HPS1/2 lung tissue. As evident from Table.4, significant differences in different phospholipids were observed in all other HPS mice at varying levels.

	% PC	% SPM	% DihSPM	% PE	% PE-Pla	% PS	% PG	% LPC
Bl_6 Controls	53 ± 1.26	6.4 ± 0.16	0.3 ± 0.04	5.1 ± 0.12	25.1 ± 0.85	6.6 ± 0.2	0.8 ± 0.04	2.8 ± 0.16
HPS1/2	81.9 ± 1.02 ***	2.3 ± 0.17 ***	0.2 ± 0.03 **	2.2 ± 0.1 ***	8.9 ± 0.53 ***	2.1 ± 0.17 ***	0.8 ± 0.07 n.s.	1.7 ± 0.07 ***
HPS1	60.8 ± 0.8 **	5.2 ± 0.11 **	0.3 ± 0 n.s.	4.4 ± 0.17 **	19.6 ± 0.4 *	5.7 ± 0.4 *	1.3 ± 0.28 **	2.5 ± 0.23 n.s.
HPS2	59.2 ± 1.27 **	5.3 ± 0.23 **	0.3 ± 0 n.s.	4.7 ± 0.23 n.s.	21.2 ± 1.03 *	5.2 ± 0.05 **	1.3 ± 0.28 *	2.6 ± 0.11 n.s.
HPS6	54.2 ± 0.51 n.s.	6.5 ± 0.11 n.s.	0.3 ± 0 n.s.	4.3 ± 0.05 **	25 ± 0.4 n.s.	6.4 ± 0.17 n.s.	0.9 ± 0.05 n.s.	2.5 ± 0.05 n.s.
HPS1/6 Controls	53.6 ± 1.78	5.6 ± 0.11	0.2 ± 0.05	4.9 ± 0.23	24.7 ± 0.8	6.5 ± 0.46	0.8 ± 0.11	3.4 ± 1.96
HPS1/6	68.6 ± 1.15 **	3.7 ± 0.23 **	0.1 ± 0.05 *	3.6 ± 0.17 **	15.2 ± 0.75 *	4.1 ± 0.05 **	1.6 ± 0.05 **	2.8 ± 0.11 n.s.

Table 4: Phospholipid profile in lung homogenates from 9 months old HPS1/2 mice: Depicted here are different phospholipid classes in the tissue of HPS mice. Values are represented as ± standard error means. **pvalue summary:** **p*<0.05, ***p*<0.01, ****p*<0.001, *n.s.* = *not specific* (n=5 mice). SPM - Sphingomyelin; DihSPM - Dihydro Sphingomyelin, PC -Phosphatidylcholine; LPC - Lysophosphatidylcholine; PE - Phosphatidyl-ethanolamine; Pla - Plasmalogens, PE-Pla – Pe based plasmalogens; PG - Phosphatidylglycerol, PS – Phosphatidyl-serine.

5.3.3.1. Accumulation of PC and surfactant specific DPPC in HPS1/2 mice :

Analysis of different classes of phospholipids by GC-MS based lipidomics approach in lung tissues of all the HPS mutants revealed a significant increase in the saturated phosphatidylcholine fraction of HPS1/2 mice, followed by HPS1/6 mice (Table.4, Fig.17A). The increase in PC is mainly due to an increase in PC-32:0 (Fig.17B), which is dipalmitoylated fraction of PC and represents the most abundant single compound of the surfactant system.

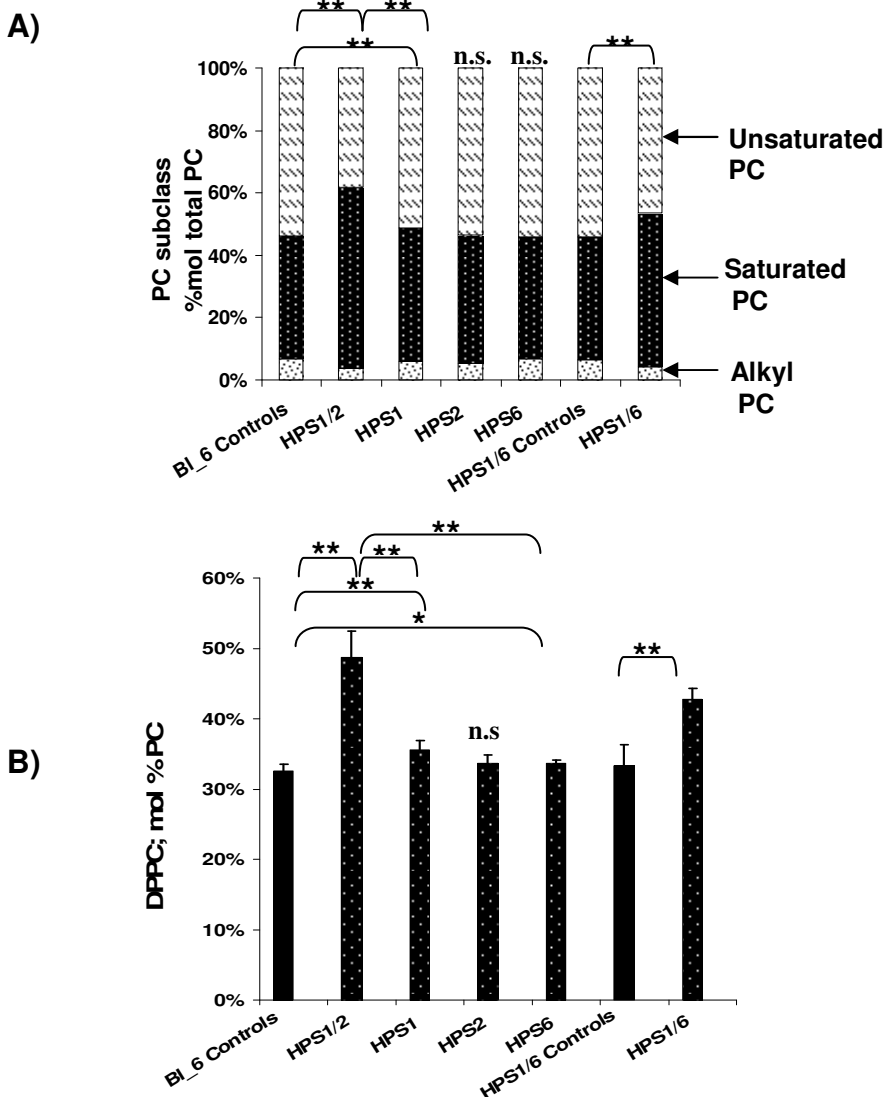


Fig 17: Phosphatidylcholine in HPS mice: A lipidomic study was performed as described in the methods section for both 3 and 9 month old HPS single and double mutant mice along with their background controls. Column graphs are depicted here representing **A)** subclass distribution of PC fraction **B)** relative content of DPPC within the PC fraction. The values are expressed as % mol of the respective lipid class, related to total PC. (* $p < 0.05$, ** $p < 0.01$, *** $p < 0.001$, n.s.=not significant; n=5 mice).

5.3.3.2. Glucosylceramides in HPS mice: Lipidomics study revealed that the glucosylceramides are significantly and specifically increased in 9 month old HPS1/2 mice tissue when compared with controls as well as with the other HPS mice (Table 3). These glucosyl ceramides are synthesized by intracellular glycosylation of ceramides, a reaction which is carried out by the enzyme glucosylceramide synthase. Since glucosyl ceramides were increased in HPS1/2 mice, a semi-quantitative RT-PCR was performed, to check if such increase in glycosylceramides could be ascribed to an altered regulation of the glucosylceramide synthase. However, any meaningful difference in the glucosylceramide synthetase mRNA expression in HPS1/2 versus control mice was not observed (Fig.18).

	SPM	DihSPM	Cer	GluCer
BI_6 Controls	90.0 ± 0.52	4.0 ± 0.53	4.8 ± 0.15	0.8 ± 0.08
HPS1/2	86.6 ± 1.6	5.9 ± 1.0	4.8 ± 0.31	1.5 ± 0.27 **
HPS1	88.4 ± 0.36	5.0 ± 0.8	4.5 ± 0.42	0.6 ± 0.06
HPS2	89.3 ± 0.4	4.2 ± 0.15	4.8 ± 0.13	0.6 ± 0.03
HPS6	90.5 ± 0.23	4.3 ± 0.51	4.4 ± 0.06	0.6 ± 0.05
HPS1/6 Controls	90.7 ± 0.73	3.4 ± 0.73	4.8 ± 0.11	0.5 ± 0.06
HPS1/6	91.0 ± 0.46	3.0 ± 0.11	4.7 ± 0.28	0.4 ± 0.11

Table 5: Increased glucosylceramides in HPS1/2 mice lung tissues: Each lipid here represents % mol of total lipids given in this table. Values are given as ± standard error means. Cer- Ceramides; Glucer- Glucosylceramides. Significant difference compared to the controls: (** $p < 0.01$); where significance is not mentioned, values are considered not to be significant. n=5 mice).

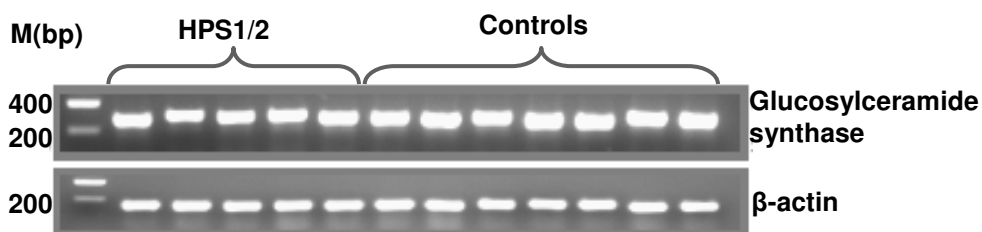
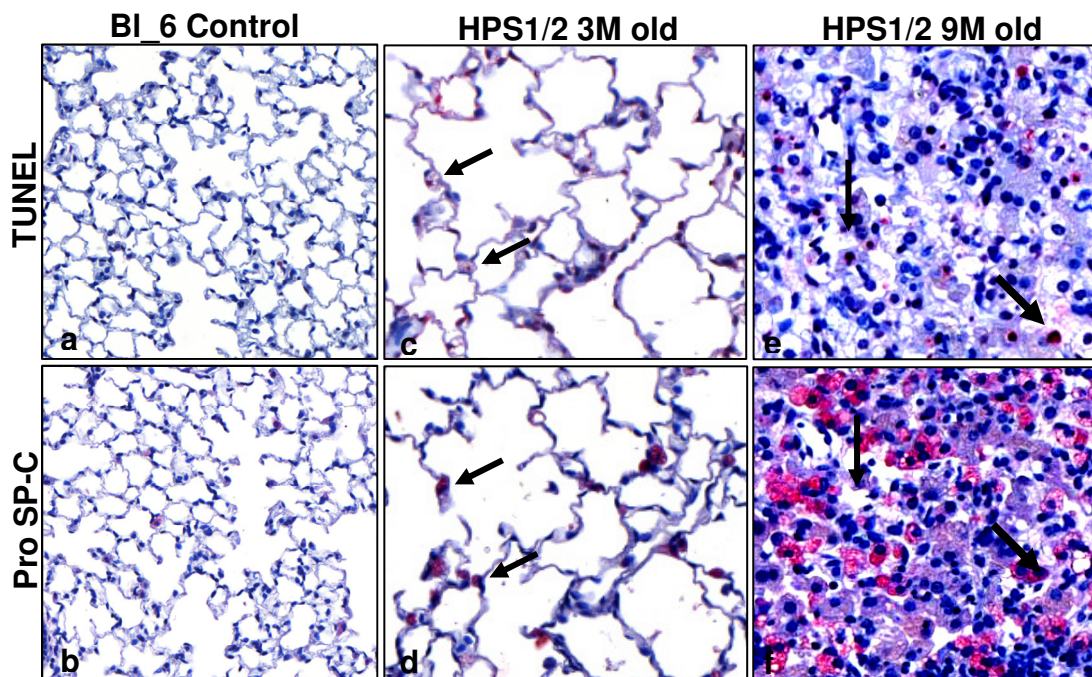


Fig 18: Glucosylceramidesynthase in HPS1/2 mice: Semi-quantitative RT-PCR was performed for glucosyl ceramide synthase and β-actin as described in the methods. Molecular weight is expressed in base pairs. (n=5-7 mice).

5.4. AECII undergo early and extensive apoptosis in HPS1/2 mice

Accumulation of surfactant in the AECII and its impaired secretion in HPS1/2 mice lungs might lead to cellular stress in the cell, ultimately leading to apoptosis, by various pathways. To identify apoptotic AECII in the lung tissue of these mice, TUNEL staining, alongside with immunohistochemistry for the AECII specific marker pro SP-C was performed on serial sections of all HPS and control mice. As depicted in Fig. 19A-c,e, numerous TUNEL positive AECII were evident in the lung tissue of HPS1/2 mice already at an age of 3 months, indicating that AECII apoptosis is an early event in the course of the HPS 1/2 induced lung fibrosis. TUNEL positivity was not observed in any of the controls (Fig.19A-a), the other HPS single (Fig.19B) or double mutant mice (Fig.19C) analyzed here.

A)



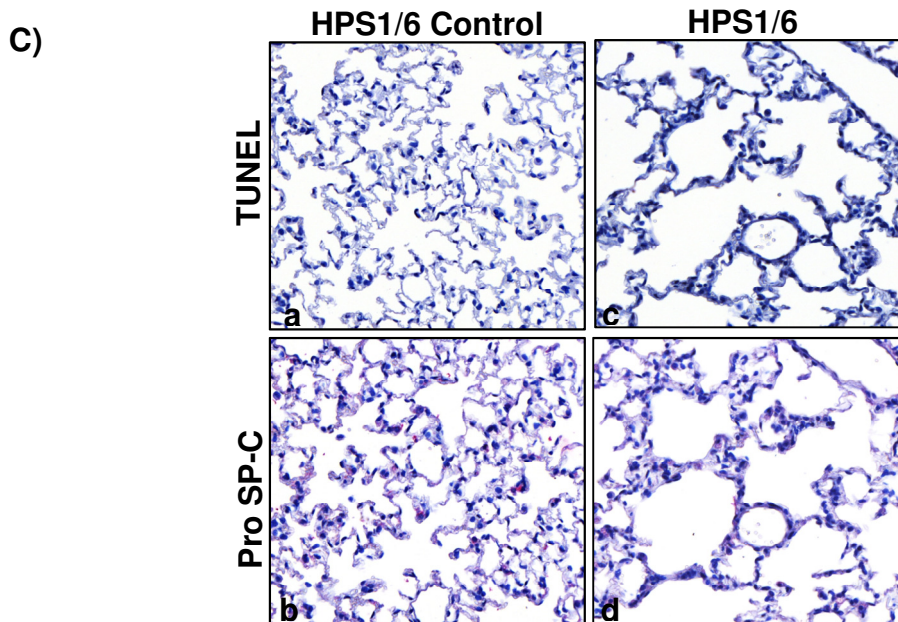
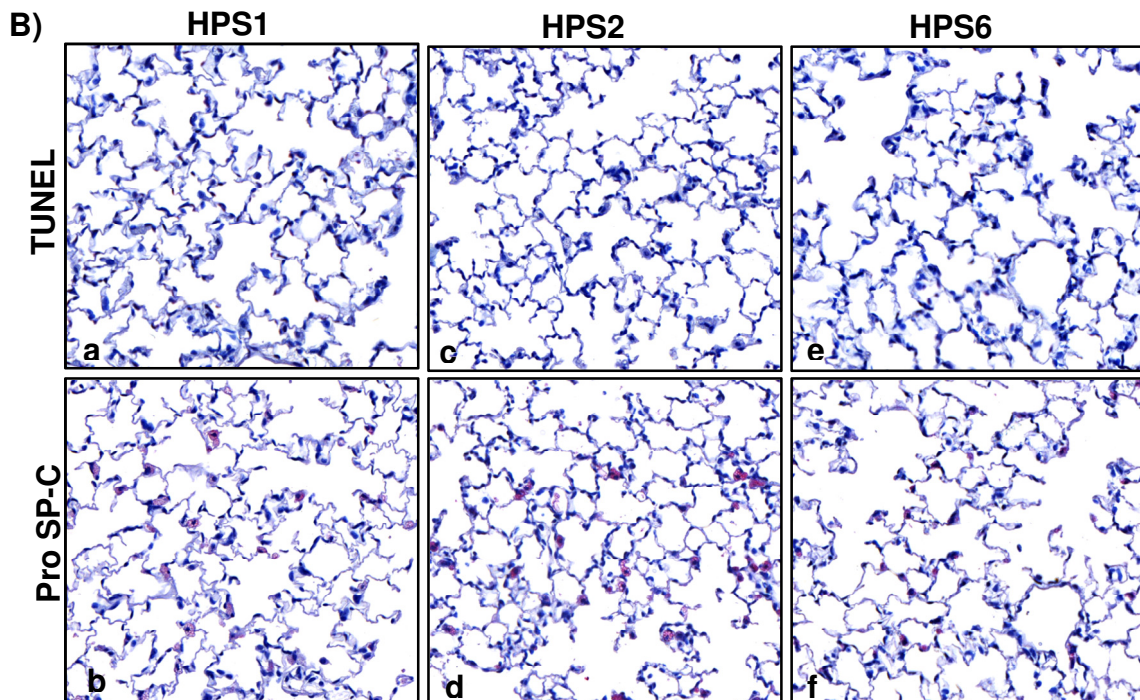


Figure 19: AECII apoptosis in HPS1/2 mice: 3 μ m serial sections were obtained from paraffin embedded lungs of **A)** HPS1/2 & WT controls **B)** HPS1, HPS2, HPS6 **C)** HPS1/6 and control mice. Serial sections were either stained for TUNEL assay (upper panel) or immunostained for pro SP-C (lower panel). Arrows indicate same cells stained positive for TUNEL and pro SP-C. **Magnification:** 20x; (n=3 mice per group).

In a complementary approach, apoptosis was assessed by performing immunohistochemistry for cleaved caspase 3, alongside with pro SP-C on serial sections of HPS1/2 and control mice lungs. It was found that the pro SP-C positive cells also stained positive for cleaved caspase-3 in HPS1/2 tissue sections (Fig. 20, right panel), while no signal for cleaved caspase-3 was detected in control mice tissue sections (Fig. 20, left panel). Thus, cleaved caspase 3 immunohistochemistry fully confirmed the TUNEL data and again suggests that AECII undergo apoptosis in a caspase-3 dependent manner in HPS 1/2, but not in the other HPS or control mice.

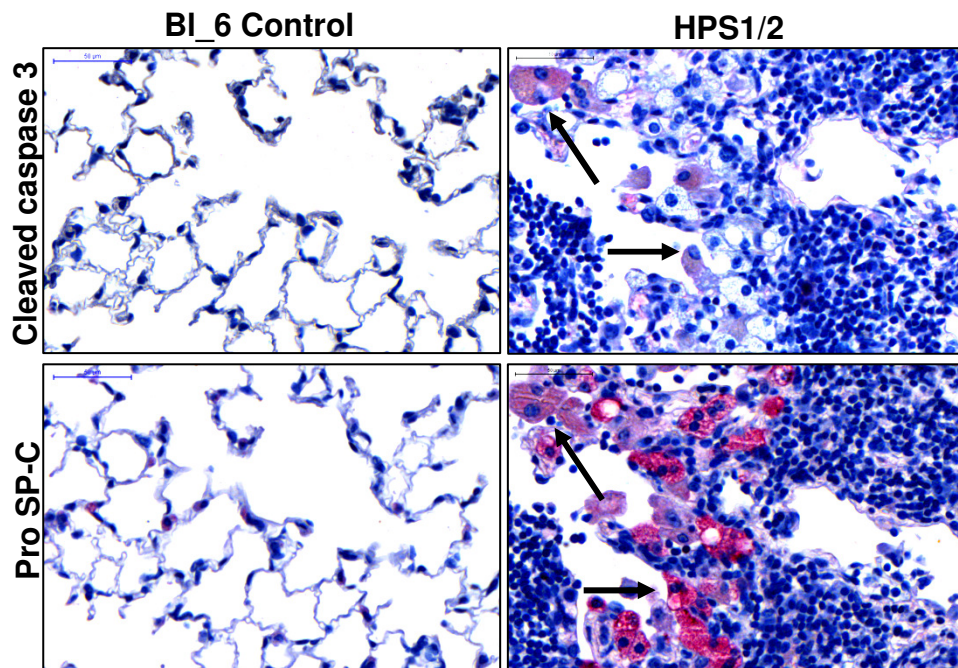


Figure 20: Caspase-3 dependent apoptosis of type II pneumocytes of HPS1/2 mice: 3µm serial sections were performed from paraffin embedded lungs of 9 month old HPS1/2 and control mice. Sections were immunostained either for cleaved caspase-3 (upper panel) or with pro SP-C (lower panel). (n=3 mice per group). Arrows indicate same cell stained for both cleaved caspase-3 and pro SP-C. **Magnification: 40x.**

5.5. Early lysosomal stress underlies AECII apoptosis in HPS 1/2 mice

As already described, lamellar bodies of AECII are lysosome related organelles and are the subcellular storage and secretion forms of surfactant in AECII. Observations till this point indicated that intracellular accumulation of surfactant was especially prominent in HPS 1/2 mice, which also spontaneously developed lung fibrosis, and may be related to the increased apoptosis of AECII in HPS 1/2. To further study the pathways that may interconnect surfactant accumulation and AECII apoptosis in HPS1/2 mice, it was hypothesized that such surfactant accumulation may primarily cause lysosomal stress in these mice. Therefore, a well known lysosomal aspartyl protease, cathepsin D, was analyzed by western blotting of lung homogenates of HPS1/2 and control mice. Increased levels of pro cathepsin D (44kDa), glycosylated form (54kDa) and subsequent cleavage products were observed in lung tissues from both 3 month and 9 month old HPS1/2 mice when compared with their controls (Fig.21A). In parallel, cathepsin D levels were analyzed also in AECII, isolated from both, HPS1/2 and control mice lungs at the age of 3 months. Interestingly enough, increased levels of pro cathepsin D, its glycosylated form and its cleavage products were found in these AECII of HPS1/2 mice when compared to those of controls (Fig.21B). To check if this was based on an altered cathepsin D gene expression level, semi-quantitative RT-PCR for cathepsin D was performed, but did not forward significant changes when compared with controls (Fig.21C).

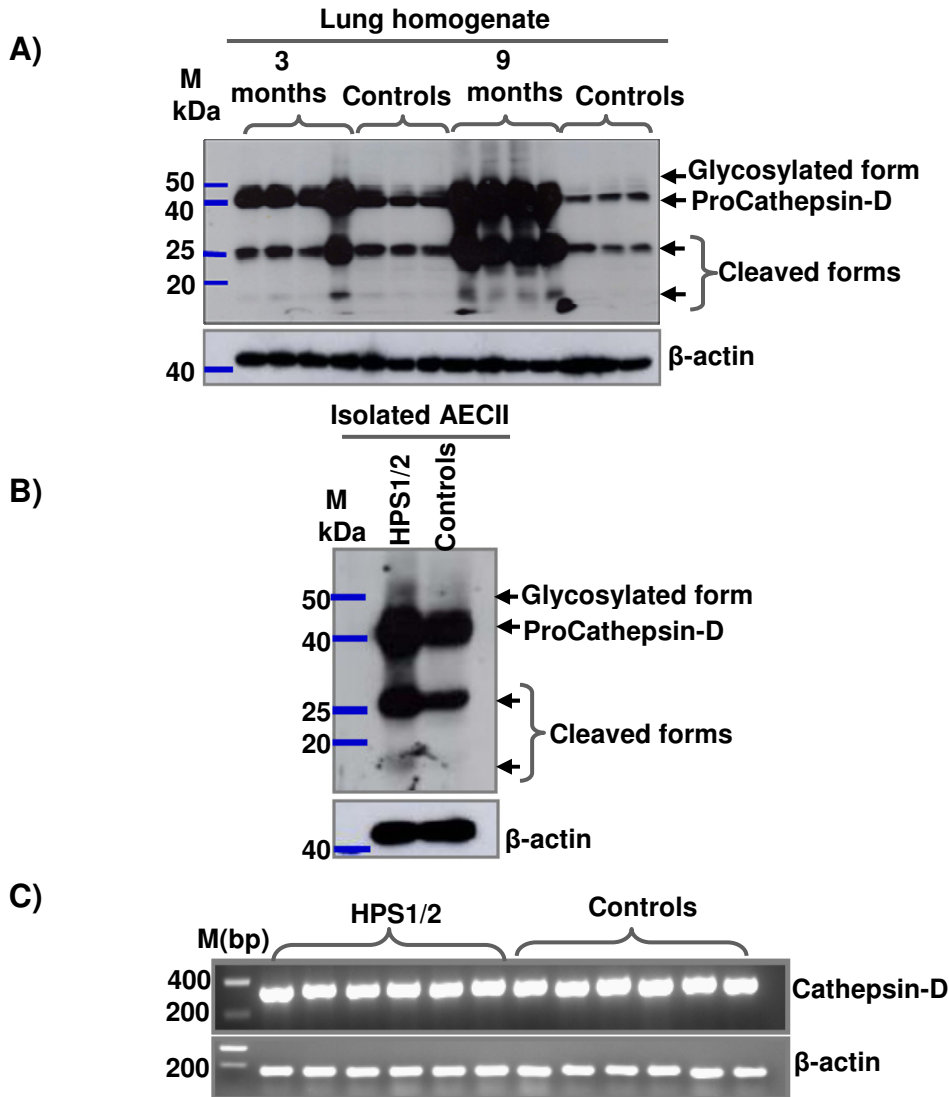


Figure 21: AECII specific lysosomal stress in HPS1/2 mice: Western blot analysis of cathepsin D in **A)** lung homogenates at the age of 3 and 9 months ($n=5$ mice per group) and in **B)** isolated AECII at the age of 3 months of HPS 1/2 and WT control mice ($n=3$ mice per group). **C)** A semi-quantitative RT-PCR analysis for the expression of cathepsin D and β -actin from HPS1/2 and control mice lung RNA ($n=6$ mice per group).

5.5.1. Lysosomal stress is specific in HPS1/2 mice

Since HPS in general is known to effect lysosome related organelles, it was further checked if lysosomal stress could be detected in all other HPS mutants. For this purpose, cathepsin D levels were analyzed by western blot in lung homogenates of all HPS mice mentioned in this study. Interestingly, it was

observed that up-regulation of cathepsin D forms was exclusively found in HPS1/2 mice (Fig. 22B), but in none of the other HPS mouse mutants (Fig. 22 A,B & C). This indicates the existence of a lysosomal stress response exclusively in HPS1/2 mice.

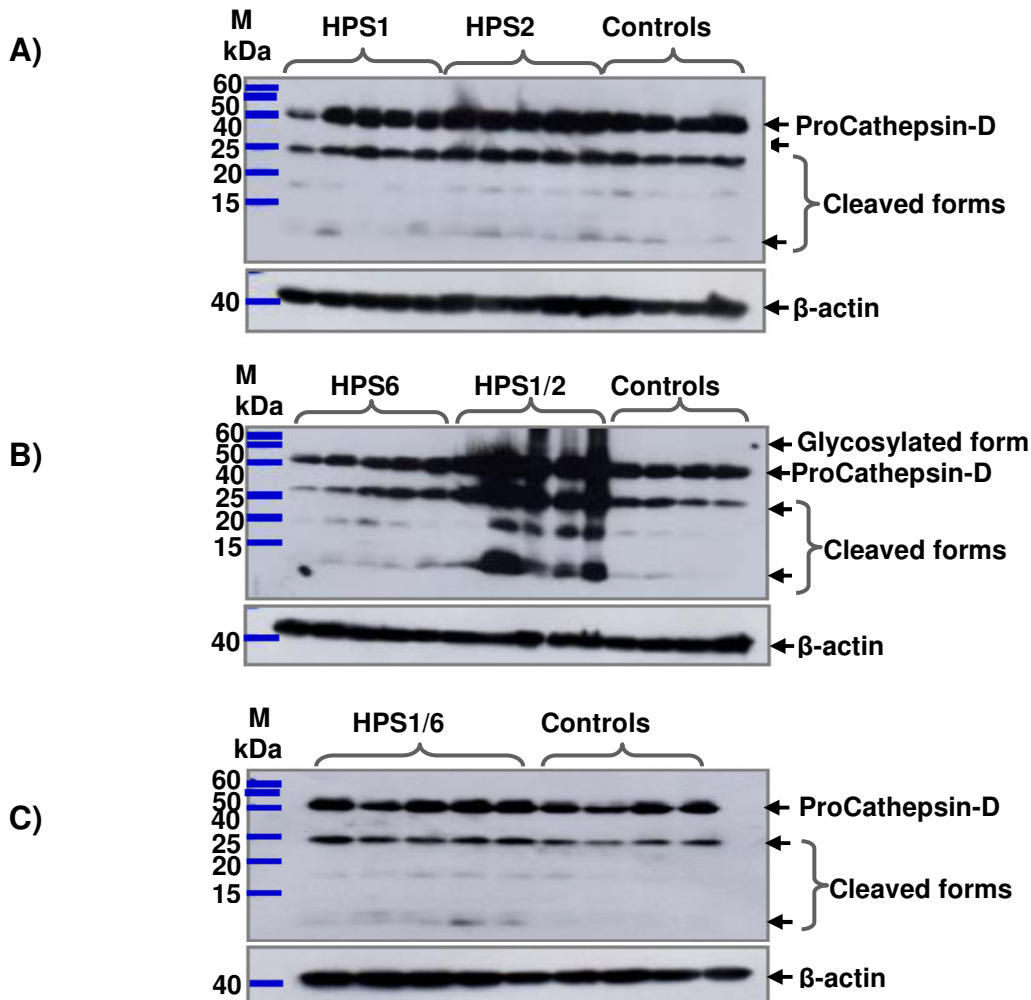


Figure 22: Lysosomal stress is specifically found in HPS1/2 mice: Western blot analysis for cathepsin D in reducing lung homogenate samples of 9month old **(A)** HPS1, HPS2 and WT controls **(B)** HPS6, HPS1/2 and WT controls **(C)** HPS1/6 and WT controls. Gels were run, blotted and developed under same conditions for all the samples. (n=5 mice per group).

5.5.2. Cathepsin D mediated apoptosis in HPS1/2 mice: To study if increased cathepsin D would colocalize with cleaved caspase 3 and pro SP-C in HPS1/2 lungs, serial sections were stained for all three proteins. Identical regions from HPS1/2 lungs on three different sections showed positivity for all the three

proteins (Fig.23a, b, c), proving that AECII are indeed showing colocalization of these markers with enhanced cathepsin D staining.

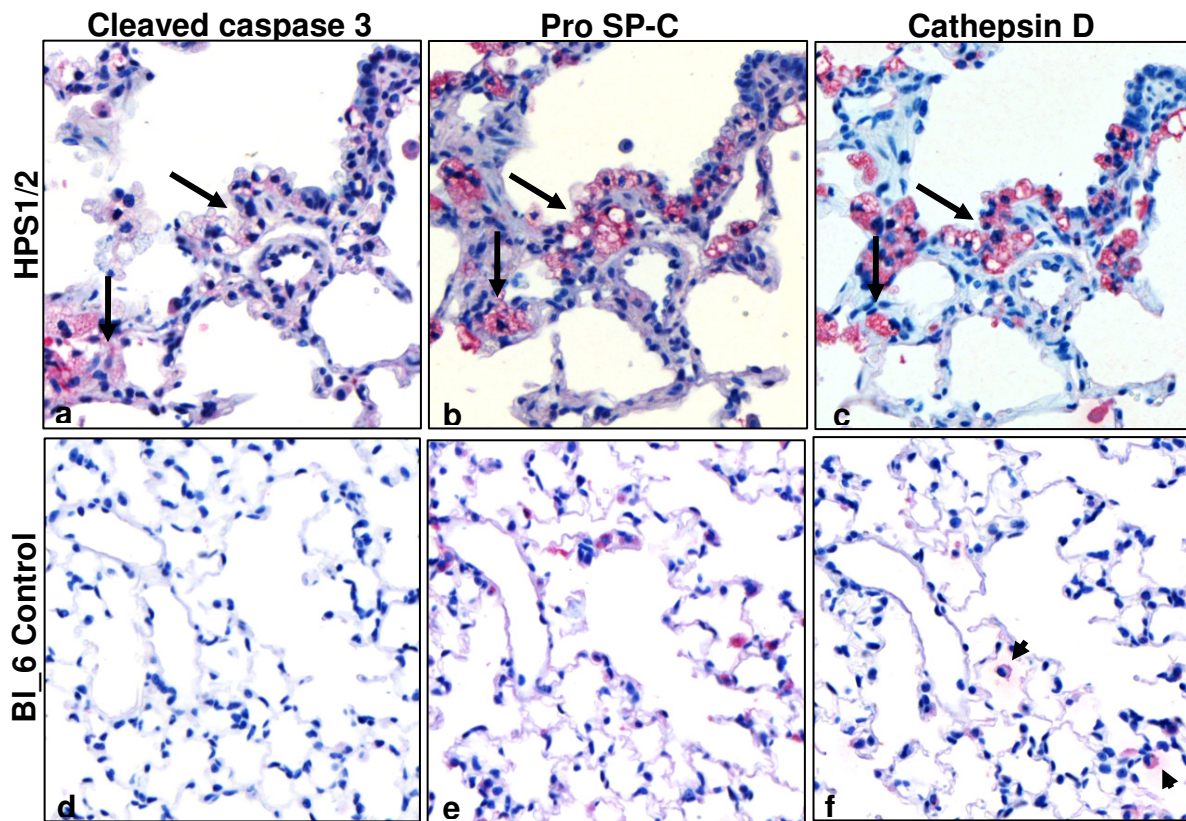


Fig 23: Cathepsin D mediated apoptosis of AECII in HPS1/2 mice: Immunohistochemistry on 3 μ m serial paraffin sections of HPS1/2 (upper panel) and WT (lower panel) mice for cleaved caspase 3 (a,d), pro SP-C (b,e) and cathepsin D (c,f) in HPS1/2 double mutant mice. Arrows indicate positive staining of AECII for all three proteins. Arrow heads (in f) indicate cathepsin D staining of macrophages in control mouse lung section. **Magnification:20x.** (n=3mice per group).

5.6. Induction of ER stress in HPS1/2 mice

Apart from the lysosomal stress response, the possible existence of an endoplasmic reticulum (ER) stress response was also assessed in the HPS mice. For this purpose, the late ER stress marker CHOP (GADD 153), which is involved in ER-stress induced apoptosis was studied. Western blot analysis of CHOP in HPS1/2 and control mice lung homogenates revealed that CHOP is indeed upregulated in HPS1/2 mice. Interestingly, only the 9 month old mice, but not the 3 month old HPS1/2 mice, showed an increase in CHOP protein level when compared to age matched controls (Fig. 24A). To check if CHOP is

expressed in AECII, immunohistochemistry of CHOP and pro SP-C was performed on serial sections of 9 month old HPS1/2 and control mice. Interestingly, these stainings illustrated that pro SP-C positive cells stained positive for CHOP in HPS1/2 mice sections (24B, right panel), while control mice sections showed no positivity for CHOP staining (Fig. 24B). Thus, it was concluded that AECII from HPS1/2 mice undergo ER stress during the later stage of the disease.

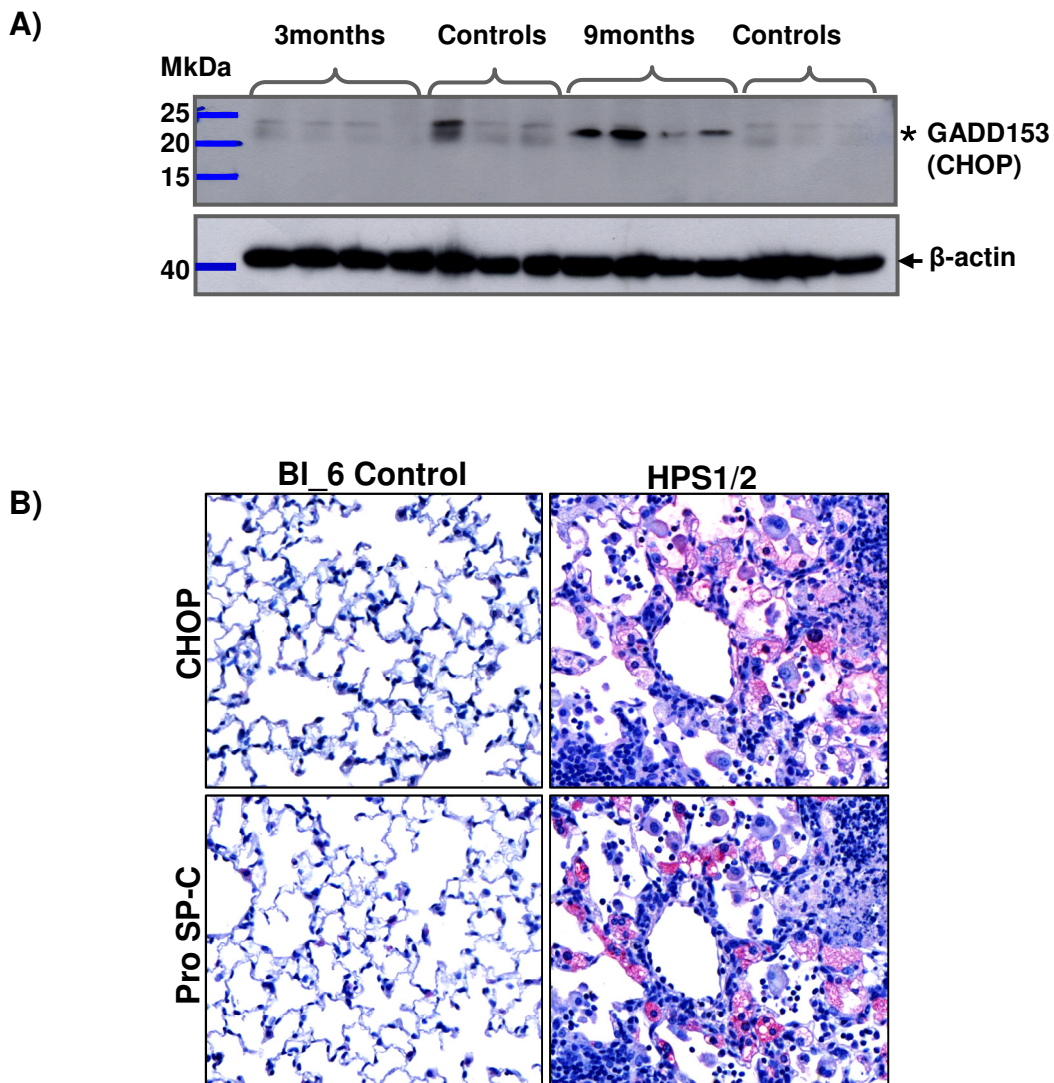


Fig 24: AECII specific induction of ER stress in HPSIP: A) Western Blot analysis for CHOP protein in lung homogenates of HPS1/2 mice and age matched WT controls (n=5 mice per group) **B)** 3µm serial sections were performed from paraffin embedded lungs of 9 month old HPS1/2 and WT control mice. Arrows indicate AECII stained positive for both CHOP and proSP-C. **Magnification: 20x** (n=3mice per group).

5.7. Alveolar type II cell apoptosis due to lysosomal and ER stress is a prominent finding in human HPSIP

Further, lysosomal and ER stress compounds in human HPSIP was characterized. Lack of frozen lung material from transplanted human HPS patients restricted the current work to the available paraffin sections, which were received from two HPS patients from the NIH. Hence, immunohistochemistry was performed on serial lung sections of these patients to assess lysosomal or ER stress in AECII. Interestingly, AECII from HPSIP patients not only showed much more pronounced immunohistochemical staining for pro SP-C as compared to donor lungs, (Fig.25A-b) but also showed a positive staining for both cleaved caspase 3 (Fig.25A-a) and cathepsin D (Fig.25A-c) in the AECII, confirming the data observed in the HPS1/2 mice. Noteworthy information here is that, in both WT control mice (Fig.23f) and healthy donors (Fig.25A-f), cathepsin D is found to localize more in the macrophages and not in the AECII, as indicated by arrow heads. ER stress was then studied on these sections again by immunohistochemistry on serial sections with CHOP and pro SP-C antibodies. It was observed that AECII of HPS1 patients (Fig.25B-b) showed positive staining for CHOP (Fig.25B-a) whereas AECII from donor lungs did not stain for CHOP at all (Fig.25B-b).

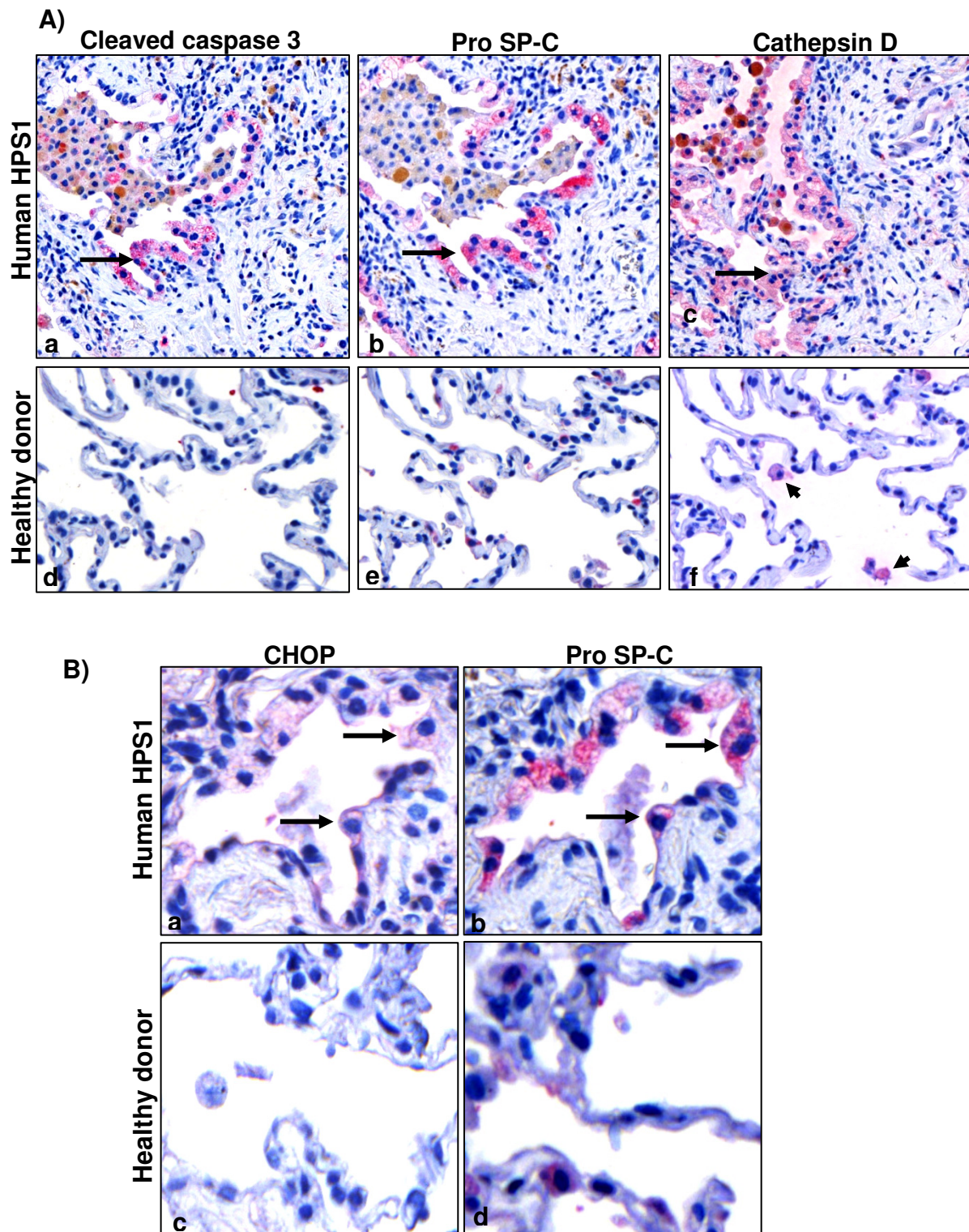


Fig 25: AECII apoptosis due to lysosomal stress and ER stress in human HPS1P: Immunohistochemistry on 3 μ m serial paraffin sections of one human HPS1 patient and healthy donors for **A)** cleaved caspase 3 (a,d), pro SP-C (b,e) and cathepsin D (c,f). **Magnification: 20x.** Arrow heads (in f) indicate cathepsin D staining of macrophages in healthy donor lung sections. **B)** CHOP (a,c) and pro SP-C (b,d). **Magnification:40x.** Arrows indicate positive staining of AECII for the proteins analyzed. (n=2 for both HPS1 patient sections and healthy donor sections).

6. Discussion

The initial focus of this study on HPS mice was to correlate their genotype and phenotype. For this purpose, the extent of lung disease was examined and surfactant processing and transport was characterized in HPS1/2, and HPS1/6 double mutant mice, their corresponding single mutant mice (HPS1, HPS2 and HPS6) and WT controls. HPS1/2 double mutant mice showed initial fibrotic changes at the age of 3 months and fully blown fibrosis at the age of 9 months. Another important observation is the appearance of emphysema as well as pulmonary fibrosis in this model. Air space enlargement, but not lung fibrosis was present to varying degrees in HPS1, 2, 6 and 1/6 mice. Surfactant analysis of both phospholipids and mature surfactant proteins revealed most severe accumulation in alveolar epithelial type II cells (AECII) in HPS1/2 mice both at 3 and 9 months of age and was found to be paralleled by extensive AECII apoptosis due to cellular stress mechanisms, which are discussed in the following sections. These key findings in mice could be fully reproduced in human lung sections from patients with HPSIP. Hence, these studies indicate that **a)** the magnitude of altered surfactant processing and transport correlates with the development of lung fibrosis, **b)** severe disturbance of surfactant processing and transport correlates with AECII apoptosis, **c)** age dependent accumulation of surfactant and severity of apoptosis correlates with the progression of fibrotic lung disease and **d)** distal lysosomal transport of surfactant is impaired, but not fully abrogated in HPS1/2 mouse model. The following aspects deserve extensive discussion:

6.1. Role of HPS gene products in surfactant processing and transport

Studies from other groups revealing abnormal appearance of alveolar structures [107, 108] and this study showing increased phospholipids in the lung tissues of both HPS1 and HPS2 mono mutant mice imply that the actions of AP-3 and BLOC-3 are possibly required in the distal compartments of AECII. Absence of

either BLOC-3 or AP-3 seems to retard surfactant transport or processing. It is not known if the gene product generated by the monomutant BLOC-3 or AP-3 gene in HPS1 or HPS2 respectively would result in a much more pronounced phenotype and alterations of surfactant processing, if its function could not be partially rescued by other proteins. In any case, absence or loss of function of both the protein complexes as in HPS1/2 double mutant mouse model, seems to result in an over additive effect, resulting in the extensive alterations of the intracellular surfactant pool and the severe phenotype illustrated herein.

AP-3 (muted in HPS2) has been suggested to cargo proteins from trans-golgi network (TGN) and early endosomes to late endosomes or lysosomes [109]. It is known to be recruited to membranes by ADP-Ribosylation Factor-1 (ARF-1) [110]. AP-3 binds to tyrosine sorting signals. It is essential for the normal melanosomal delivery of tyrosinase [111, 112]. It is also required for efficient localization of P-selectin to Weibel-Palade bodies, which are secretory granules of endothelial cells and a loss of AP-3 function as in pearl and mocha mouse mutants leads to a defective localization of P-selectin [113]. More than one AP-3 mediated lysosomal pathway exists. The first is the direct pathway from TGN to early and late endosomes. The second pathway is an indirect route, where AP-3 facilitates membrane traffic from TGN to lysosomes via an intracellular route, that bypasses early endosomes [114]. Depending on their sorting motifs, lysosomal membrane proteins exploit AP-3 to use these two different pathways. For example, the lysosomal delivery of endolyn, a lysosomal mucosialin, occurs predominantly via the indirect pathway [114], while the lysosomal delivery of CD63/LAMP3 occurs via the direct pathway [115]. When direct pathway was inhibited by chloroquine (a lysomotropic weak base and neutralizes the pH of endosomal compartments), the wild type CD63 (with GYEVM AP-3 binding motif) was trapped in early endosomes, while its mutant (with GYEVI AP-3 binding motif) was not at all found in early endosomes, but was trafficked via the indirect pathway [115].

The precise function of BLOC-3 (muted in HPS1 or HPS4) on the other hand, is unknown. But, it is implicated to regulate a) the movement or distribution of late endosomes and lysosomes and b) optimal attachment of late endocytic organelles to microtubule dependent motors. Binding partners or target proteins for BLOC-3 have not yet been identified, with the exception of one study, where decreased perinuclear staining of LAMP1 in late endocytotic organelles was observed in BLOC-3 deficient mouse skin fibroblasts [91]. In addition, mutations of BLOC-3 resulted in accumulation of stage-I melanosomes in mouse dorsal black follicular melanocytes. In mouse tail epidermal melanocytes, a more pronounced block in melanosome biogenesis leading to relatively decreased melanosomes was observed [101]. Thus, BLOC-3 seems to be differentially regulated in melanocytes.

But, how do defects in AP-3 and BLOC-3 affect lysosomal trafficking and lung lamellar bodies in AECII? It is proposed that BLOC-3 regulates endosomal and lysosomal movements, mediated by both microtubule and actin dependent mechanisms and to maintain normal function of several important proteins involved in the secretory pathway [92]. Hence, it could be speculated that one or more motility factors, which mediate attachment to or movement along microtubules are either decreased in amount or missing due to mistargeting in HPS. Another explanation could be that, factors which mediate events like vesicle docking, targeting or fusion at plasma membrane are missing.

As discussed earlier, there is an over additive affect in HPS1/2 mouse model. One immediate explanation for this effect could be that there is a direct interaction between BLOC-3 and AP-3. However, previous studies undertaking immunoprecipitation experiments in fibroblasts and B-lymphoblastoid cells did not show such interaction between the two protein complexes [72, 91]. Moreover, intracellular localization of AP-3 complex was not altered in fibroblasts from patients with HPS1 mutation. In addition, abnormal trafficking of lysosomal membrane proteins, like lysosome associated membrane protein-1 (LAMP-1), was observed in HPS2 mutant cells, but not in HPS1 fibroblasts [116]. In spite of

all this valuable information, a role of HPS1 protein in the AP-3 dependent pathway or vice-versa cannot be completely ruled out because all cited previous reports were performed in non-secretory or non lung secretory cells. In addition, cell type specific differences in lysosomal enzyme secretion of BLOC-3 mutants were reported [92]. Supporting this theory, studies dealing with a patient with HPS2 mutation (mutation on β 3A subunit of AP-3), demonstrated that lytic granules, which are lysosome related organelles of cytotoxic T lymphocytes, showed impaired microtubule dependent movement [117], a feature that has been ascribed to BLOC-3.

In case of a missing direct interaction between BLOC-3 and AP-3 in AECII, other binding partner(s) for these protein complexes, which may play a major role in surfactant secretion and the function of which may be more heavily affected, if both BLOC-3 and AP-3 are absent. Hence, additional experiments focussing on interactions between BLOC-3 and AP-3 and identification of binding partners specifically in the surfactant secretory pathway might enhance the understanding towards molecular pathways underlying the alteration of surfactant transport and processing in HPS1/2 mice.

6.2. Altered surfactant processing or transport occurs in other forms of ILDs, too

Surfactant alterations have been described in some other lysosomal storage disorders and interstitial lung diseases apart from HPS. Chediak-Higashi syndrome (CHS) is not only a lysosomal storage disease, but it also falls into the category of albinism, where patients are reported to show bleeding disorders and severe immune deficiency. The mouse mutant of CHS is the beige mouse, which also shows giant lamellar body degeneration soon after birth, with an increased severity at older ages. The older mice show signs of fibrosis, with an increased accumulation of lamellar body lipids [104, 118]. Another model that is not directly belonging to the group of HPS, but falls into the category of oculocutaneous albinism, is the chocolate mouse mutant which is caused by a mutation of the

Rab38 gene. Rab 38 encodes a small GTPase, which participates in regulating vesicular trafficking and is found at high levels in lung [119]. A human counterpart for the murine Rab38 mutation has not yet been reported. Nevertheless, in a recent study, enlarged airspaces in the lungs of these mice have been reported. As compared to wild type mice, the number and size of AECII, as well as the hydrophobic surfactant constituents were increased in the lungs [119]. However, there are no data yet with regard to the existence of lysosomal stress and epithelial apoptosis in these mice.

Another important lipid storage disorder is the Niemann-Pick disease that has also been associated with surfactant alterations. It was primarily identified as a neurovisceral lipid storage disorder, but lung involvement has been later identified in some types of the disease. The disease is primarily caused by sphingomyelinase deficiency (Niemann-Pick type C2; NPC2) [120]. Most interestingly, severe interstitial pneumonia has been observed in NPC2 neonatal patients [121]. Recent study in NPC2 patients showed the association of NPC type 2 with alveolar proteinosis. Foamy macrophages and enlarged AECII were observed, with accumulation of lipid rich material in the alveolar lumina and cytoplasmic inclusions of AECII [122]. In addition, progressive pulmonary infiltration has been observed in the concerned patients. In full accordance, ASM (acid sphingomyelinase) knock out mice lungs show cellular infiltration and significantly elevated levels of phosphatidylcholine, phosphatidylserine and phosphatidylethanolamine alongside with increased sphingomyelinase in both lung tissue and BAL fluid [123]. Histologic evidence of fibrosis development was not reported in ASM knockout mice, at any age [124].

In some few familial forms of idiopathic interstitial pneumonia, mostly with a usual interstitial pneumonia (UIP) or nonspecific interstitial pneumonia (NSIP) pattern, mutations in the SFTPC (surfactant protein-C) gene have been described [125, 126]. In these families, pro SP-C and active SP-C were either barely detectable, or COOH based missense or short deletion mutations resulted in the production of a misfolded protein [126]. In the latter patients, aberrant subcellular localization

of SP-C precursor protein was seen, with dense fibrosis and distorted AECII architecture [127,128]. In line with this study, in vitro trafficking experiments showed that constructs with mutations in BRICHOS domain of SP-C form large toxic intracellular aggregates, termed aggresomes, leading to cellular stress [129]. In addition, SP-C *-/-* mice, developed on a 129/sv background strain, showed a severe lung phenotype. Although lungs looked normal at birth, progressive emphysema, accumulation of lung tissue phospholipids and severe pulmonary fibrosis were observed at 2 months after birth [130]. Taken together, both the entire absence of SP-C or the production and accumulation of an abnormal, misfolded pro SP-C can result in the development of a diffuse parenchymal lung disease.

Finally, mutations in the ATP binding cassette subfamily A/3 (ABCA3) gene in pediatric patients have been reported to cause fatal surfactant deficiency as well as interstitial lung disease, depending on the phenotype. ABCA3 is specifically concentrated to the limiting membrane of lamellar bodies and is proposed to play a major role in the excretion of lipid fraction of pulmonary surfactant. Frameshift, nonsense mutations or mutations in the highly conserved regions of this gene lead to disturbed lipid trafficking in newborns [131 - 133]. Electron microscopy pictures revealed abnormally small and dense lamellar bodies in AECII of such patients. Recently, UIP pattern of pulmonary fibrosis has also been reported in an adolescent patient with ABCA3 mutations [134].

Taken together, disturbances of the delicate intracellular homeostasis of surfactant compounds seem to prone the AECII to chronic injury and appear to be responsible for the observed phenotypes (airway enlargement and fibrosis).

6.3. Lysosomal and ER stress reflect epithelial stress in HPS1/2 mice

6.3.1. Altered surfactant processing and trafficking as underlying reason for AECII injury: One of the key observations in this study is the extensive

intracellular accumulation of mature surfactant proteins and surfactant specific DPPC in the AECII of HPS1/2 mice. Although being still indirect in nature, the data set provided in this study strongly suggests a causative relationship between defective surfactant transport and processing, induction of AECII apoptosis and development of lung fibrosis in HPS1/2 mice. The following two cellular stress patterns need to be discussed as underlying reason for chronic AECII injury:

6.3.2. Lysosomal stress: Lysosomes are membrane bound organelles which contain hydrolytic enzymes for digesting macromolecules. Several proteases, nucleases and phospholipases, cathepsins (B, D, H, L, S, F, K, C, W, X, V, and O) are present in lysosomes, which optimally work at an acidic pH around 5. The limiting membrane of the lysosome contains a set of highly glycosylated, lysosomal-associated membrane proteins (LAMPs) such as LAMP-1, LAMP-2 and CD63/LAMP-3, the functions of which are still unclear. Morphologically heterogenous, the lysosomes often resemble other organelles of the endocytic and secretory pathways. These organelles share many traits of the lysosomes like the presence of mature acid-dependent hydrolases and LAMPs. They are however termed as “Lysosome Related Organelles” (LROs) [135], as they lack the lysosomal marker mannose 6-phosphate receptors (MPRs). Examples of LROs, as mentioned earlier are: melanosomes, lytic granules, major histocompatibility complex (MHC) II compartments, platelet dense granules, basophil granules and lamellar bodies of the lung. The shared traits of these specialized organelles may be biogenetically related to lysosomes, a relationship that has been further illuminated by the multiorganellar, lysosomal storage, genetic disorders such as the Hermansky-Pudlak and Chediak-Higashi syndromes.

As described previously, these genetic diseases can result in the accumulation/storage of undigested substances within the LROs, resulting in a severe “lysosomal stress”, with serious pathologic consequences. Programmed cell death might be one serious consequence of such severe stress. There is no

known marker for lysosomal stress till date. Of course, lysosomal enzymes and proteases offer as markers. Elegant studies from other groups showed increased activities of the lysosomal enzymes β -Glucuronidase and β -Galactosidase in the lungs and kidneys of HPS1/2 mice [136]. However, these studies did not relate the increased enzymatic activities to the AECII, nor did they associate these enzymes with apoptosis of AECII or any other cell type in this mouse model. In order to study the role of these lysosomal enzymes in driving the AECII into what is here described as “lysosomal stress” and subsequent apoptosis, the lysosomal aspartyl protease cathepsin D was opted. Cathepsin D has numerous functions within the lysosomal compartment, of which the best known is the proteolysis of endocytosed and autophagocytosed proteins at low pH. Much more interesting in the context of this investigation is, however, the observation that cathepsin D also plays a critical role in the induction of apoptosis, as previously shown in many cell types [137]. In addition, it has been shown under conditions of oxidative stress, that caspase-8 mediated apoptosis is dependent on cathepsins, especially cathepsins D and L [138]. Under conditions of bleomycin induced lung fibrosis, cathepsin D activates caspase-3 in bleomycin-induced apoptosis of alveolar epithelial cells, via the angiotensin (ANG II) pathway [139, 140]. The induction of apoptosis is based on two different major pathways, one being the extrinsic pathway, which involves the connection of appropriate ligand with the surface receptor (Fas), and which results in activation of caspase-8, -10 and -3. The intrinsic pathway is activated in case of mitochondrial dysfunction, which leads to release of caspase activators, that in turn yields activation of caspase-9, and, in consequence, caspase-3 [141]. In neuroblastoma cells subjected to oxidative stress, cathepsin D, and not cathepsin B, was shown to be responsible for the activation of the intrinsic pathway of apoptosis. Under these conditions, the action of cathepsin D was essential for the translocation of Bax from the cytosol to mitochondria and hence, the activation of the intrinsic pathway of apoptosis [142]. A combination of both the pathways results when caspase-8 induces proteolysis of Bid to truncated Bid (tBid). In addition, lysosomal destabilization in neutrophils triggered cleavage of pro-apoptotic Bcl2 protein Bid,

followed by a decrease in anti-apoptotic protein, Mcl-1 [143]. tBid is transported through mitochondrion where it initiates oligomerization of Bax and induces intrinsic pathway of apoptosis (Fig.26). Which of these pathways are activated in HPSIP has yet to be identified and it is currently a matter of research.

6.3.3. ER stress: The Endoplasmic Reticulum (ER) has a central role in the production of almost all lipids and proteins. All proteins designated for secretion and all proteins designated for the ER itself, the golgi apparatus, the lysosomes, the endosomes are first imported into the ER from the cytosol, or directly synthesized into the ER lumen by altered ribosomes. Proteins fold and oligomerize, disulphide bonds are formed and N-linked oligosaccharides are added within the ER lumen [144]. Proteins that do not fold or oligomerize correctly despite the action of chaperons are translocated back into the cytosol, where they are deglycosylated, ubiquitinated and degraded in proteasomes. If misfolded proteins accumulate excessively in the ER, they trigger an unfolded protein response (UPR), which under normal conditions activates appropriate genes in the nucleus to help the ER to cope. Similarly, extensive protein overload of the ER (eg. in the form of viral infection) results in an ER overload response [145].

Conditions interfering with the function of ER are collectively called ER stress. ER stress primarily aims to prevent further accumulation of proteins. However, if the stress cannot be resolved and the cellular responses fail to eliminate the unfolded proteins, the cell undergoes apoptosis [146, 147]. At present, the exact signalling mechanism underlying ER stress-induced apoptosis is poorly understood. Nevertheless, different pathways, a transcription factor, a caspase-dependent, and a JNK-dependent pathway have been identified. CHOP/GADD 153 has been shown to be activated via the cleavage of ATF6, ATF4, along with alternative XBP1 splicing, which are in turn induced by phosphorylation of PERK [148,149].

CHOP is a 168 amino acid (in rodents) protein, with a molecular weight of 20kDa. It is expressed ubiquitously at low levels. It is also known as DNA damage-inducible transcript-3, and growth arrest and DNA damage inducible gene (GADD). The CHOP protein is a heterodimer with C/EBPs. It comprises of an N-terminal transcriptional activation domain and a C-terminal basic-leucine zipper (bZIP) domain, consisting of a basic amino-acid-rich DNA-binding region followed by a leucine zipper dimerization motif [150, 151]. Furthermore, the CHOP protein contains two adjacent serine residues (79 and 82) which can serve as substrates for the p38 MAP kinase family. Deletion mutant analysis of CHOP revealed that bZIP domain is important for CHOP-induced apoptosis [149]. It is expressed ubiquitously at low levels and is strongly expressed by various factors like glucose deprivation and amino acid starvation [151]. Agents like tunicamycin, thapsigargin and dithiothreitol strongly induce CHOP expression. As discussed before, CHOP is regulated on a transcriptional level by distinct ER stress transducers. Overexpression of CHOP has been reported to cause cell cycle arrest, leading to apoptosis. Reduced apoptosis in response to ER stress has been reported in CHOP knock out mice. In addition, lymphocytes from spleen of CHOP knockout mice have been shown to be resistant to LPS-induced apoptosis [152]. These data prove that CHOP plays a prominent role in ER stress induced apoptosis.

Of late, ER stress has been implicated in the pathogenesis of many neurodegenerative disorders like Alzheimer's disease and Parkinson's disease [153]. A relation between surfactant and ER stress was first reported in a study which showed that a mutation in the BRICHOS domain of the SP-C precursor protein leading to the accumulation of its mutant protein in the ER, elicited ER stress followed by apoptosis in epithelial cell lines [154]. A recent study from our group focussing on sporadic cases of idiopathic pulmonary fibrosis has demonstrated the importance of ER stress in driving the AECII apoptosis, a feature that was not detected in COPD patients, but only in the IPF subjects [155]. In these patients, no mutations of the two hydrophobic surfactant proteins, SP-B and SP-C were observed, but defective intracellular processing of SP-B,

resulting in accumulation of proSP-B has been found to underlie the development of ER stress in these patients (unpublished).

6.3.4. Other possible mechanisms leading to lysosomal or ER stress: With respect to mouse models, a silver mutation, that is characterized as a recessive mouse mutant with progressive coat colour dilution has been reported to have a loss of ER export and endocytic signals, with altered melanosome morphology [156]. Apart from this, gangliosides, which are formed from precursor molecules ceramides, also act as apoptotic signals in ER stress response. These gangliosides mainly reside in the ER and regulate membrane dynamics and structure of this organelle; hence, changes in ganglioside compositions can have deleterious consequences like the induction of ER stress [157]. In addition, accumulation of G_{M1} ganglioside in a mouse model of G_{M1} -gangliosidosis, a lysosome storage disorder, was shown to activate the UPR, causing neuronal death [158]. Other important members of the ceramide super family are glucosyl and galactosyl ceramides, the accumulation of which causes Gaucher disease and Krabbe disease, respectively, which are LSDs [159, 160]. Gaucher's disease is caused because of excess accumulation of glucosylceramide, particularly via the deficiency of gluco-cerebrosidase or glucosylceramidesynthase. GlcCer are synthesized on the cytosolic surface of Golgi and may flip to the luminal leaflet of Golgi membrane where it can enter the luminal aspect of transport vesicles. Interestingly, GlcCer is a substrate of for the ABC-transporters MDR-1 P-glycoprotein and MRP1 [160]. Besides the well known lysosomal sequestration of GlcCer, an alternative pathway is supposed to exist to dispose it. In non-macrophage cells, GlcCer is believed to be transferred from lysosomes to other cell compartments by an unknown mechanism, where it is processed or even be accumulated to varying degrees. In line with these studies, elevated levels of GlcCer resulted in an increase in ER density, suggesting that GlcCer are also transported retrogradely to the ER [160]. In short, accumulation of GlcCer is possible either in lysosomes or in ER, thereby resulting in cellular stress mechanisms. However, lysosomal storage disorders have not yet been directly implicated to cause ER stress via ER overload in non-neuronal cells. But,

accumulation of GlcCer in HPS1/2 lung tissue in this study adds another proof to a possible cellular stress. Cell specific and/or sub-cellular organelle specific studies are however required in order to identify the organelle specific GlcCer accumulation in HPS model.

6.3.5. Integrative concept of induction of AECII apoptosis in HPS1/2 lungs:

This study discloses a prominent role of AECII in HPSIP in both mice and man. A simplified version of AECII of HPSIP in comparison with a healthy AECII is shown in the cartoon below (Fig.28). The AECII of HPS1/2 mouse is exceptionally big, with giant lamellar bodies. Important surfactant components like SP-B, SP-C and phospholipids are shown to be accumulated in such a cell. An overload of these surfactant components and their abnormal secretion leads to a severe cellular stress.

As indicated in the picture below, cathepsin D, CHOP and glucosylceramides were significantly increased with AECII of HPS1/2 mice, confirming the lysosomal and ER stress mechanisms in these mice, which were corroborated by human HPSIP tissue sections. Thus, this increase in different cellular stress markers is thereby eliciting the activation of caspases, finally leading to apoptosis of such an AECII in these mice. However, whether these cellular stress mechanisms orchestrate with each other or act independently to activate effector caspases and thereby apoptosis, has yet to be deciphered in HPSIP.

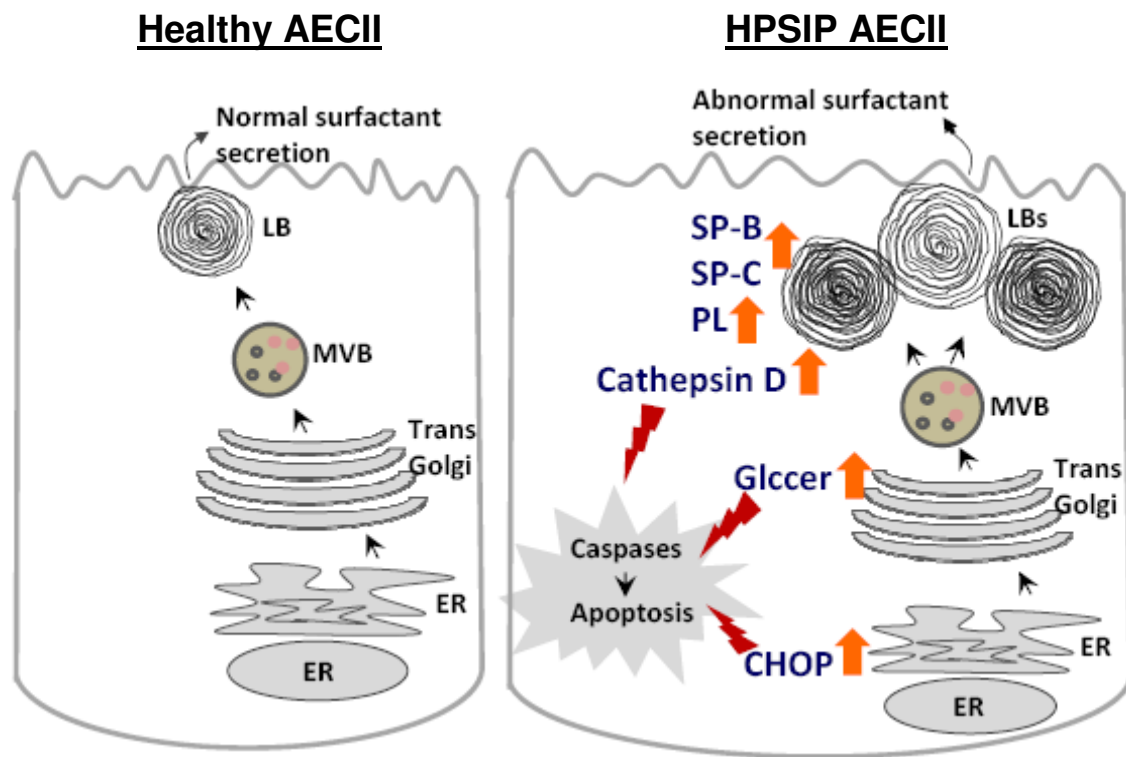


Figure 26: Induction of AECII apoptosis in HPSIP lungs: Cartoon depicting a healthy AECII where surfactant processing and secretion is normal and a HPSIP AECII, where giant lamellar bodies, altered surfactant transport and abnormal secretion of surfactant is shown. An increase in cathepsin D, GlcCer and CHOP are shown, all leading to apoptosis of the cell. Please note the size difference between the healthy AECII and the HPSIP AECII.

6.4. The role of AECII injury in the development of lung fibrosis in general and HPSIP in particular

6.4.1. AEC II injury underlies HPSIP: Several studies focussed on the cellular biology of HPSIP. Abnormalities have been reported in two major cell types, the AECII and alveolar macrophages. While macrophages are heavily loaded with ceroid material, AECII cells were shown to be enlarged, with giant lamellar bodies in HPSIP patients. In a HPS2 mouse model, activation of macrophages and baseline elevations in inflammatory cytokines was reported. The authors of that study showed that the alveolar macrophage activation seen in both HPS1 and HPS2 mouse mutants is not genotype specific [161].

Supporting this view, decreased lysosomal enzyme secretion from macrophages was observed in HPS1 mice [80]. Likewise, although macrophage activation was observed in HPS1 and HPS2 single mutant mouse models, development of pulmonary fibrosis was illustrated only after targeting AECII of these mice with bleomycin challenge [162]. The data from this work drive home the point that injury to and apoptosis of AECII in HPS1/2 double mutant mice represents the key event in HPSIP and it is forwarded by two cellular stress mechanisms, lysosomal and ER stress. Supporting this notion are data from human IPF as well as the herein described human HPSIP patients, where alveolar epithelial cell injury and cell death are a consistent finding. Precise mechanism(s) by which apoptosis of AECII may result in lung fibrosis is yet not settled, but may include the following mechanisms: downregulation of prostaglandin E₂ (PGE₂), increase in pro-fibrotic growth factors like transforming growth factor- β (TGF- β), epithelial to mesenchymal transition (EMT) or cell-cell contact.

6.4.2. Endogenous regenerative responses to the AECII injury in HPSIP:

Extensive loss of AECII as suggested in ALI / ARDS, causes a life threatening condition due to the denudation of basement membrane and the flooding of the alveolar space. However, alveolar edema is not a prominent feature of IPF, or HPSIP. It appears therefore reasonable, to anticipate a marked activation of progenitor or local stem cells in HPSIP lungs, in order to limit the pathophysiological consequences of AECII apoptosis. Hyperproliferation of AECII in IPF has been indicated, as a strategy to overcome the loss of epithelium. Wnt signalling is one such pathway that has been implicated in epithelial cell hyperplasia and proliferation in IPF lungs [163, 164]. Notch signalling is another pathway, which is involved in cell fate decisions [165]. Significant reduction in Notch protein and mRNA level were observed in the lung tissue of bleomycin induced lung fibrosis in mice [166]. Added to this, altered Notch signalling has been observed in the lungs of IPF patients (unpublished). In rat model of bleomycin induced lung fibrosis, transplantation of AECII from healthy rats proved to be effective, as the extent of lung fibrosis significantly reduced [167].

Apart from these considerations, the injured AECII lung may try to limit the consequences of distorted surfactant transport and processing in HPSIP, through activation of survival genes. For example, cells transfected with SP-C^{Δexon4} (which causes misfolded SP-C, leading to chronic ER stress), showed an increase in NF-κB activity [168]. Inflammation shown in HPS monomutant mice (HPS2 or example) [161], sublethal injury of AECII possibly causes inflammatory changes like activation of NF-κB and related survival genes, which help the AECII to survive. Because of an uncontrolled injury due to severe accumulation of surfactant and subsequent cellular stress where the function of survival genes is not sufficient, the AECII in HPS1/2 mice undergo apoptosis. Hence, it can be concluded that in murine HPSIP (HPS1/2), the AECII response pattern largely dictates the nature of the evolving lung disease.

6.4.3. Additional factors that possibly contribute to AECII apoptosis in HPSIP: An increase of the alveolar surface tension has been suggested to largely contribute to the loss of lung compliance and the impairment of gas exchange in patients with ALI / ARDS. According to more recent studies, extensive stretch of AECII, as it may occur because of the collapse of alveolar units due to increased alveolar surface tension or because of inappropriately high tidal volumes applied during mechanical ventilation, significantly adds to AECII apoptosis [169]. The underlying molecular mechanisms of such “over” stretch induced apoptosis of AECII still remain to be elucidated. However, it appears reasonable that increase in alveolar surface tension, as already shown for IPF patients, could contribute to the pathomechanism of HPSIP. Interestingly, such increase has very recently been disclosed in the HPS1/2 mice by our group (unpublished).

6.5. Murine HPSIP: A model for IPF and other “idiopathic” forms of lung fibrosis?

The present investigation is the first study to identify HPS1/2 double mutant mouse as a murine model for HPS associated interstitial pneumonia (HPSIP). Observations from this murine model are supported by those of human HPS1

patients. Apart from the development of pulmonary fibrosis in the mouse model, a first hand evidence was provided here, that AECII apoptosis, resulting from lysosomal stress and ER stress is involved in the development of HPSIP in mice and man.

The human HPSIP shares its prognosis with IPF. HRCT findings from HPSIP patients appear to be the same as those of IPF patients. Moreover, HPSIP demonstrates usual interstitial pneumonia (UIP) pattern, histologically. In spite of its genetic origin, the murine HPSIP model shares common features with IPF, and thus portrays as a new animal model of IPF. IPF is characterized by progressive deposition of fibrotic tissue in the pulmonary interstitium with minimal associated inflammation, a feature that is also seen in the HPS1/2 mice. Similar to IPF, alveolar epithelial cell injury, AECII hyperplasia and progressive loss of normal lung architecture can be attributed to murine HPSIP as well. On a biochemical level, altered surfactant processing and secretion has been observed in both IPF and murine HPSIP. In both cases, AECII injury appears to represent the primary trigger. Apart from this, the response of AECII indicating the induction of ER stress as well as activation of lysosomal enzymes [170] is similar in mice and man with HPSIP and IPF.

Upto now, bleomycin induced lung fibrosis in mice has been the standard model for most researchers in order to study the mechanisms underlying lung fibrosis in general and IPF in particular. This model however has its own drawbacks, like excessive inflammation prior to the onset of lung fibrosis and reversal of fibrosis after several weeks of bleomycin challenge. For this reason, the HPS1/2 double mutant mice may serve as an extremely valuable and important model not only to study further disease relevant patho mechanisms, but also to design, develop and scrutinize therapeutic strategies for patients with HPSIP as well as IPF.

6.6. Therapeutic strategies

As mentioned above, successful therapeutic strategies have not been developed for HPSIP, with lung transplantation remaining as the only curative, which is itself

not an uncomplicated approach for pulmonary fibrosis till date. Based on the observations from HPS mouse models in the present study, the following therapeutic options can be proposed. As indicated, HPS mono mutant mice present milder phenotype when compared with HPS1/2 mice. Hence, correction of phenotype of HPS1/2 mice by over expressing AP-3 in AECII specific manner might compensate some of the functions within the secretory pathway.

In addition, since apoptosis of AECII represents such a predominant finding in human and murine HPSIP, it may be worth to evaluate the therapeutic efficacies of PAN caspase inhibitors to modify the AECII stress response and thus, lung fibrosis. Apart from this, transplantation of stem cells has been proposed as a strategy for repair of lung fibrosis, but controversial results with this kind of approach restrict the potential use of these cells. An attempt to transplant AECII from healthy rats into bleomycin challenged rats forwarded positive results with regard to the extent of lung fibrosis [167]. Accordingly, syngenic transplantation of AECII from healthy WT littermates into HPS1/2 mice, following an experimental period of about 3 months, might possibly reverse the fibrosis in this mouse model and successfully result in the replacement of the AECII by the donor AECII. A potential therapeutic outlook for HPSIP patients could be the transplantation of ex vivo differentiated iPS (induced Pluripotent Stemcells) into AECII and subsequent transplantation.

7. Summary

Hermansky-Pudlak syndrome (HPS) comprises of a group of rare hereditary disorders primarily affecting transport within lysosome related organelles. Up to now, 16 (mice) and 8 (human) genes, respectively, have been found to cause this disease. Amongst other clinical symptoms, patients with HPS may develop lung fibrosis (HPS associated Interstitial Pneumonia; HPSIP). As a consequence of such organ involvement, quality of life is then greatly reduced and prognosis is poor. The underlying molecular reasons for the development of HPSIP had yet not been settled. However, on an ultrastructural level, patients with HPSIP impose with an abnormal enlargement and increased number of lamellar bodies, a lysosome related organelle of alveolar type II cells (AECII) that represents the intracellular storage and secretion form of pulmonary surfactant.

Drawn against this background, the genotype-phenotype correlation was analyzed in mice with different single and combined HPS mutations. This work primarily focussed on the extent of pulmonary fibrosis and performed an in depth surfactant analysis in the lungs of HPS1, HPS2, HPS6, HPS1/6, HPS1/2 and respective wild type mice. In addition, altered signalling pathways and cellular consequences were studied.

Histological studies, undertaken after 3 and 9 months of age, revealed that only HPS1/2 mice, but none of the other HPS mice, would develop lung fibrosis, being quite extensive by 9 months of age. In these mice, but in none of the other mice, AECII appeared swollen and seemed to contain more and larger lamellar bodies. On the other hand, especially the HPS1/6 mice revealed spontaneous development of airspace enlargement. Defective intracellular surfactant trafficking and secretion was a prominent finding in HPS 1/2 mice and caused a highly significant intracellular accumulation of the mature hydrophobic surfactant proteins SP-B and SP-C as well as phospholipids. Among the phospholipids, especially the dipalmitoylated phosphatidylcholine (DPPC), the most abundant surfactant compound, was significantly elevated in lung tissues of HPS 1/2 mice.

Isolated AECII from these mice revealed similar results. In contrast, although these above mentioned surfactant compounds appeared slightly increased in the mono mutant and the HPS 1/6 mice, there was a significant difference between HPS1/2 on the one, and the other mice on the other hand with regard to the extent of disturbed intracellular transport and accumulation of surfactant compounds.

As a possible consequence of such defective transport and secretion of surfactant, AECII apoptosis was observed extensively in 3 and 9 month old HPS1/2 mice by in-situ apoptosis assay and by immunohistochemistry of cleaved caspase 3. Hypothesizing that apoptosis of AECII in HPS1/2 mice would develop due to severe cellular stress, lysosomal and ER stress markers in these mice were investigated. The lysosomal protease, cathepsin D, was highly elevated in lung homogenates and isolated AECII of HPS1/2 mice, but, again, in none of the other mutant mice. Such increase in cathepsin D was already visible at the age of 3 months. These results indicate an early onset lysosomal stress specifically in HPS1/2 mice. Apart from this, HPS 1/2 mice also exhibited signs of severe ER stress at a later age (9 months). In detail, CHOP, a proapoptotic factor specifically induced by unresolved ER-stress, was found to be highly and exclusively elevated HPS1/2 mice. In addition, lipidomic profiling of 9 month old lung tissues from all HPS mice revealed increased levels of glucosylceramides only in HPS1/2 mice, which also hints towards a serious cellular stress in these mice.

Data from the HPS1/2 mouse model was aptly supported by those obtained from HSP1P patients. As compared to lung transplant donor lungs, paraffin sections of lungs from two HSP1P patients (HPS1 mutation) showed a highly increased immunostaining for cathepsin D in AECII, alongside with induction of caspase-3 and CHOP immunostaining in this cell-type, thereby confirming the cellular stress mechanisms as observed in HPS1/2 mice.

Taken together, this is the the first time to decipher HPS1/2 mice as a valuable animal model of human HPSIP. With regard to the clinical similarities and common pathomechanistic principles between HPSIP and patients with Idiopathic Pulmonary Fibrosis (IPF), HPS 1/2 mice also offer as the currently best available model of IPF. This study showed that defective intracellular surfactant trafficking in AECII of these mice leads to the development of lysosomal and ER stress, finally resulting in AECII apoptosis, and – at the end - development of lung fibrosis. Analysis of markers of lysosomal and ER-stress in human HPSIP samples fully corroborated such pathomechanistic concept and lends further credit to the general concept that apoptosis of the AECII represents a key step in the development of lung fibrosis in non-inflammatory triggered forms of Interstitial Lung Diseases. On the basis of these results, further elucidation of the molecular mode of action and the binding partners of the concerned HPS gene products (adaptor protein 3 and BLOC 3) appears reasonable and therapeutic strategies aiming to either restore the defective transport mechanism or to block the cellular stress response or AECII apoptosis are warranted.

8. Zusammenfassung

Das Hermansky-Pudlak syndrom (HPS) umfasst eine Reihe seltener und vererbbarer Erkrankungen, die primär alle zu einer Beeinträchtigung lysosomaler Transportprozesse führen und klinisch ein vergleichbares Spektrum an Beschwerden und Symptomen auslösen. Bis dato sind 16 (Maus) bzw. 8 (Mensch) verschiedene Gene bekannt, die im Falle einer Mutation die Erkrankung auslösen können. Neben vielfältigen anderen krankheitsdefinierenden Symptomen entwickeln viele betroffene Patienten eine Lungenfibrose (HPS associated Interstitial Pneumonia; HPSIP). In diesem Fall entwickelt sich eine deutliche Einschränkung der Lebensqualität und die Prognose der betroffenen Patienten ist schlecht. Die der Entwicklung der HPSIP zugrunde liegenden Pathomechanismen waren bis dato nicht bekannt, allerdings wurde in früheren post-mortem Analysen ein auffälliges Erscheinungsbild der alveolären Typ II Zellen (AECII) beschrieben, mit einer vermehrten Anzahl und einer Vergrößerung der Lamellarkörperchen, dem lysosomalen Organell der AECII, in dem pulmonaler Surfactant intrazellulär gespeichert wird.

Vor diesem Hintergrund war es das Ziel der vorliegenden Arbeit, eine Korrelation des Genotyps mit dem Phänotyp bei verschiedenen mono- oder doppelt mutanten HPS Mäusen (HPS 1, 2, 6, 1/2, 1/6) im Vergleich zum genetischen Hintergrund durchzuführen. Im Fokus stand hierbei zunächst die Frage ob auch bei murinen HPS Formen eine HPSIP auftritt und welche assoziierten Veränderungen des Surfactantsystems hierbei beobachtet werden können. Weiterhin wurden verschiedene zelluläre Stresspfade, wie lysosomaler Stress oder Endoplasmatisches Retikulum (ER)-Stress, untersucht und mit den anderen Befunden korreliert.

Die im Alter von 3 und 9 Monaten durchgeführten histologische Untersuchung ergaben, dass ausschließlich die HPS 1/2 Mäuse eine Lungenfibrose entwickelten, die mit 3 Monaten noch sehr diskret, mit 9 Monaten aber voll ausgeprägt war. In diesen HPS 1/2 Mäusen, nicht aber in den anderen HPS

Mäusen und Wildtyp Tieren, konnte auch ein den Patienten mit HPSIP entsprechendes Erscheinungsbild der AECII beobachtet werden, mit einer deutlichen Schwellung und einer Zunahme des Gehalts an Lamellarkörperchen. Die im Anschluß durchgeführte Analyse des pulmonalen Surfactantsystems ergab sowohl im Lungengewebe als auch in isolierten AECII der HPS 1/2 Mäuse eine hochsignifikante Störung des intrazellulären Transports von Surfactantkomponenten, die zu einer intrazellulären Akkumulation der muren hydrophoben Surfactant Proteine SP-B und SP-C sowie der Phospholipide führte. Bzgl. der Phospholipide konnte vor allem eine hochsignifikante Akkumulation des dipalmitoylierten Phosphatidylcholins (DPPC) in den Lungen der HPS 1/2 Mäuse beobachtet werden. Obwohl auch in den anderen HPS Mäusen eine moderate Störung der intrazellulären Surfactanthomöostase beobachtet werden konnte, war der Unterschied dieser Veränderungen zwischen den HPS 1/2 und den anderen HPS und den Wildtyp Tieren doch erheblich und ebenfalls hochsignifikant.

As mögliche Folge dieses hochgradig gestörten intrazellulären Surfactanttransports konnte ausschließlich in den HPS 1/2 Mäusen, und zwar bereits im Alter von 3 Monaten, eine Apoptose der AECII mittels der TUNEL Methode oder der Immunohistochemie (IHC) für gespaltene Kaspase 3 beobachtet werden. In den anderen HPS oder Wildtyp Tieren war dies in keinem Fall zu beobachten. Als zugrunde liegende zelluläre Stressreaktionen konnte zunächst eine Induktion des Kathepsin D in den AECII der HPS 1/2, nicht aber in den anderen HPS Mäusen, mittels Western Blot und ICH nachgewiesen werden. Dieser lysosomale Stressmarker war bereits im Alter von 3 Monaten erhöht. Noch nicht in diesem Alter, aber dann mit 9 Monaten ebenfalls prominent nachweisbar, war CHOP, ein proapoptotisch wirksamer Faktor, der infolge eines anhaltenden und nicht korrigierbaren ER-Stresses entsteht und zwingend mit der Entwicklung der Apoptose einhergeht Auch dieses Faktor wurde exklusiv in den AECII von HPS 1/2 Mäusen beobachtet. Schließlich fiel im Rahmen von Untersuchungen des

Lipidoms auch noch eine Erhöhung des relativen Anteils von Glukosylceramiden auf, ebenfalls ein Marker für eine schwerwiegende Stressantwort der Zelle.

Die in den HPS 1/2 Mäusen gewonnenen Daten konnten im Lungengewebe von zwei Patienten mit HPSIP vollständig reproduziert werden: auch hier fand sich im Vergleich zum Lungengewebe von Organdonoren eine deutliche Induktion von Kathepsin D und CHOP in den AECII, die zudem auch größtenteils Zeichen der stattfindenden Apoptose aufwiesen.

Zusammengefasst konnte mit den HPS 1/2 Mäuse werden ein murines Korrelat der am Patienten zu beobachtenden HPSIP beschreiben. Aufgrund der Ähnlichkeiten hinsichtlich des klinischen Beschwerdebildes und der Prognose dieser Patienten mit Patienten mit einer Idiopathischen Pulmonalen Fibrose (IPF), stellen HPS 1/2 Mäuse unserer Meinung nach außerdem das derzeit beste Modell der IPF dar. In diesen HPS 1/2 Mäusen bewirkt der gestörte intrazelluläre Transport und Sekretion von Surfactantkomponenten einen frühen lysosomalen Stress, gefolgt von einer späteren ER-Stress, die beide die Apoptose der AECII und – über noch zu definierende Schritte – die Lungenfibrose auslösen. Die Analyse von Markern eines lysosomalen und eines ER-Stresses in Patienten mit HPSIP bestätigen in vollem Umfang dieses pathomechanistische Konzept und stärken die Annahme, dass die unkontrollierte Apoptose der AECII ein Schlüsselvorgang bei der Entwicklung nicht-inflammatorisch getriggelter Formen der Lungenfibrose darstellt. Unsere Untersuchungen befürworten die weitere Aufdeckung der molekularen Wirkungsweise und intrazellulärer Bindungspartner der HPS 1/2 Genprodukte (Adaptor Protein 3, BLOC3) in den AECII. Darüberhinaus erscheint die therapeutische Korrektur des gestörten Surfactant-Transports wie auch die mögliche Blockade der lysosomalen- oder ER-Stress Antwort in den AECII als hoffnungsvoller therapeutischer Ansatz der Behandlung der HPSIP.

9. References

1. Scarpeli EM. The surfactant system of the lung. *Int. Anesthesiol Clin.*, 1977,15 (4) 19-60.
 2. von Neergard K. Retraktionskraft der Lunge, abhängig von der Oberflächenspannung in den Alveolen . *Z Gesamte Exp Med*, 1929, 66: 373-394.
 3. Pattle RE. Properties, function and origin of the alveolar lining layer. *Nature* 1995, 175: 1125-1126.
 4. Clements JA. Surface tension of lung extracts. *Proc Soc Exp Biol Med*, 1957, 95: 170-172.
 5. Gruenwald P. Surface tension as a factor in the resistance of neonatal lungs to aeration. *Am J Obstet Gynecol*, 1947, 53: 996-1007.
 6. Walter F. Boron, Emile L. Boulpaep. *Medical Physiology. A cellular and molecular approach.* Saunders imprint of Elsevier science, ISBN 0-7216-3256-4.
 7. King R. Isolation and chemical composition of pulmonary surfactant. In: Robertson B., van Golde L., Batenburg J. eds. *Pulmonary Surfactant.* Amsterdam: Elsevier Science, 1984, 1-15.
 8. Haagsman HP, van Golde LM. Synthesis and assembly of lung surfactant. *Annu Rev Physiol*, 1991, 53: 441-464.
 9. Hawgood S, Clements JA. Pulmonary surfactant and its apoproteins. *J Clin Invest*, 1990, 86: 1-6.
 10. Van Golde LM, Batenburg JJ, Robertson B. The pulmonary surfactant system: biochemical aspects and functional significance. *Physiol Rev*, 1988, 68: 374-455.
 11. Hawgood S. Surfactant: composition, structure, and metabolism. In: Crystal RG, West JB eds. *The lung*, chapt. 3.1.10. New York: Raven Press, Ltd., 1991: 247-261.
 12. Shelley SA, Paciga JE, Balis JU. Lung surfactant phospholipids in different animal species. *Lipids*, 1984, 19: 857-862.
 13. Post M, Batenburg JJ, Schuurmans EA, Laros CD, van Golde LM. Lamellar bodies isolated from adult human lung tissue. *Exp Lung Res*, 1982, 3: 17-28.
-

14. Magoon MW, Wright JR, Baritussio A, Williams M C, Goerke J, Benson BJ, Hamilton RL, Clements JA. Subfractionation of lung surfactant. Implications for metabolism and surface activity. *Biochim Biophys Acta*, 1983, 750: 18-31.
 15. Günther A, Schmidt R, Feustel A, Meier U, Pucker C, Ermert M, Seeger W. Surfactant subtype conversion is related to loss of surfactant apoprotein B and surface activity in large surfactant aggregates. Experimental and clinical studies. *Am J Respir Crit Care Med*, 1999, 159: 244-251.
 16. Wright JR, Benson BJ, Williams MC, Goerke J, Clements JA. Protein composition of rabbit alveolar surfactant subfractions. *Biochim Biophys Acta* 1984, 791: 320-332.
 17. L.M.G.Van Golde. Synthesis of surfactant lipids in the adult lung. *Annual Review of Physiology*, 1985, Vol.47:765-774.
 18. Stephen E. McGowan and John S. Torday. The pulmonary lipofibroblast (lipid interstitial cell) and its contributions to alveolar development. *Annu. Rev. Physiol.*, 1997. 59:43–62.
 19. J.S. Torday and V.K.Rehan. The evolutionary continuum from lung development to homeostasis and repair. *Am J Physiol Lung Cell Mol Physiol*, 2007, 292: L608–L611.
 20. Machiko Ikegami. Surfactant catabolism. *Respirology*, 2006, Volume 11, S24–S27.
 21. Shelley SA, Balis JU, Paciga JE, Espinoza CG, Richman AV. Biochemical composition of adult human lung surfactant. *Lung*, 1982, 160: 195-206.
 22. Hamm H, Fabel H, Bartsch W. The surfactant system of the adult lung: physiology and clinical perspectives. *Clin Investig*, 1992, 70: 637-657.
 23. Harwood JL. Lung surfactant. *Biochem Soc Trans*, 1987, 15I: 80S-89S (Suppl.).
 24. Veldhuizen R, Nag K, Orgeig S, Possmayer F. The role of lipids in pulmonary surfactant. *Biochim Biophys Acta*, 1998, 1408: 90-108.
 25. Schlame M, Casals C, Rustow B, Rabe H, Kunze D. Molecular species of phosphatidylcholine and phosphatidylglycerol in rat lung surfactant and different pools of pneumocytes type II. *Biochem J*, 1988, 253: 209-215.
 26. Kahn MC, Anderson GJ, Anyan WR, Hall SB. Phosphatidylcholine molecular species of calf lung surfactant. *Am J Physiol*, 1995, 269: L567-L573.
-

27. Adachi H, Hayashi H, Sato H, Dempo K, Akino T. Characterization of phospholipids accumulated in pulmonary-surfactant compartments of rats intratracheally exposed to silica. *Biochem J*, 1989, 262: 781-786.
 28. Hayashi H, Adachi H, Kataoka K, Sato H, Akino T. Molecular species profiles of acidic phospholipids in lung fractions of adult and perinatal rabbits. *Biochim Biophys Acta*, 1990, 1042: 126-131.
 29. Fleming BD, Raynor CM, Keough KMW. Some characteristics of monolayers of 1-palmitoyl-2-oleyl-phosphatidylglycerol with and without dipalmitoyl-phosphatidylcholine during dynamic compression and expansion. *Biochim Biophys Acta*, 1983, 732: 243-250.
 30. Meban C. Effect of lipids and other substances on the adsorption of dipalmitoyl phosphatidylcholine. *Pediatr Res*, 1981, 15: 1029-1031.
 31. Fleming BD, Keough KM. Surface respreading after collapse of monolayers containing major lipids of pulmonary surfactant. *Chem Phys Lipids*, 1988, 49: 81-86.
 32. Wright, J.R. Immunomodulatory functions of surfactant. *Physiol. Rev.* 1997, 77:931-962.
 33. Korfhagen TR, Bruno MD, Ross GF, Huelsman KM, Ikegami M, Jobe AH, Wert SE, Stripp BR, Morris RE, Glasser SW, Bachurski CJ, Iwamoto HS, Whitsett JA. Altered surfactant function and structure in SP-A gene targeted mice. *Proc Natl Acad Sci U S A*, 1996, 93: 9594-9599.
 34. Wert, S.E., et al. Increased metalloproteinase activity, oxidant production, and emphysema in surfactant protein D gene-inactivated mice. *Proc. Natl. Acad. Sci. USA*, 2000, 97:5972-5977.
 35. Carlos Botas, Francis Poulain, Jennifer Akiyama, Cindy Brown, Lennell Allen, Jon Goerke, John Clements, Elaine Carlson, Anne Marie Gillespie, Charles Epstein, and Samuel Hawgood. Altered surfactant homeostasis and alveolar type II cell morphology in mice lacking surfactant protein D. *Proc. Natl. Acad. Sci. USA*, 1998, V.95(20): 11869-11874.
 36. Korfhagen TR, Sheftelyevich V, Burhans MS, Bruno MD, Ross GF, Wert SE, Stahlman MT, Jobe AH, Ikegami M, Whitsett JA, Fisher JH. Surfactant protein-D regulates surfactant phospholipids homeostasis in vivo. *J Biol Chem.*, 1998, 273(43):28438-43.
 37. Palaniyar N, Clark H, Nadesalingam J, Shih MJ, Hawgood S, Reid KB. Innate immune collectin surfactant protein D enhances the clearance of DNA by macrophages and minimizes anti-DNA antibody generation. *The Journal of Immunology*, 2005, 174(11):7352-8.
-

-
38. William J. Janssen, Kathleen A. McPhillips, Matthew G. Dickinson, Derek J. Linderman, Konosuke Morimoto, Yi Qun Xiao, Kelly M. Oldham, R. William Vandivier, Peter M. Henson and Shyra J. Gardai. Surfactant Proteins A and D Suppress Alveolar Macrophage Phagocytosis via Interaction with SIRP α . *American Journal of Respiratory and Critical Care Medicine*, 2008, Vol 178. pp. 158-167.
 39. Frank Brasch, Georg Johnen, Alexandra Winn-Brasch, Susan H. Guttentag, Andreas Schmiedl, Nadine Kapp, Yasuhiro Suzuki, Klaus M. Müller, Joachim Richter, Samuel Hawgood and Matthias Ochs. Surfactant Protein B in Type II Pneumocytes and Intra-Alveolar Surfactant Forms of Human Lungs. *American Journal of Respiratory Cell and Molecular Biology*, 2004, Vol. 30, pp. 449-458.
 40. Takayuki Ueno, Stig Linder, Cheng-Lun Na, Ward R. Rice, Jan Johansson, and Timothy E. Weaver. Processing of Pulmonary Surfactant Protein B by Napsin and Cathepsin H. *Biol. Chem.*, 2004, Vol. 279, Issue 16, 16178-16184, April 16.
 41. Kristin D. Gerson, Cherie D. Foster, Peggy Zhang, Zhenguo Zhang, Michael M. Rosenblatt, and Susan H. Guttentag. Pepsinogen C proteolytic processing of surfactant protein B. *J. Biol. Chem*, 2008, 10.1074/jbc.M707516200.
 42. Frank Brasch, Anja ten Brinke, Georg Johnen, Matthias Ochs, Nadine Kapp, Klaus M. Müller, Michael F. Beers, Heinz Fehrenbach, Joachim Richter, Joseph J. Batenburg, and Frank Bühling. Involvement of Cathepsin H in the Processing of the Hydrophobic Surfactant-Associated Protein C in Type II Pneumocytes. *Am. J. Respir. Cell Mol. Biol.*, 2002, Volume 26, Number 6, June 2002 659-670.
 43. Soll, RF. Clinical trials of surfactant therapy in the newborn. In *Surfactant Therapy for Lung Disease* Edited by Robertson B, Taeusch HW New York: Marcel Dekker, 1995, pp. 407–442.
 44. Beers MF, Hamvas A, Moxley MA, Gonzales LW, Guttentag SH, Solarin KO, Longmore WJ, Nogee LM, and Ballard PL. Pulmonary surfactant metabolism in infants lacking surfactant protein B. *Am J Respir Cell Mol Biol.*, 2000, 22: 380–391.
 45. Keisuke Tokieda, Jeffrey A. Whitsett, Jean C. Clark, Timothy E. Weaver, Kazushige Ikeda, Keith B. McConnell, Alan H. Jobe, Machiko Ikegami, and Harriet S. Iwamoto. Pulmonary dysfunction in neonatal SP-B-deficient mice. *Am J Physiol Lung Cell Mol Physiol.*, 1997, Vol. 273, Issue 4, L875-L882, October.
 46. D.K. Vorbroker, S.A. Profit, L.M. Nogee, J.A. Whitsett. *Am. J. Physiol. Lung Cell Mol. Physiol.*, 1995, 268; L647-L656.
-

-
47. Ashbaugh DG, Bigelow DB, Petty TL, Levine BE. Acute respiratory distress in adults. *Lancet*, 1967, 2: 319-323.
 48. American Thoracic Society/European Respiratory Society International Multidisciplinary Consensus Classification of the Idiopathic Interstitial Pneumonias. This joint statement of the American Thoracic Society (ATS), and the European Respiratory Society (ERS) was adopted by the ATS board of directors, June 2001 and by the ERS Executive Committee, June 2001. *Am J Respir Crit Care Med.*, 2002, 165, 277-304.
 49. Noble, P.W. & Homer, R.J. Back to the future: historical perspective on the pathogenesis of idiopathic pulmonary fibrosis. *Am J Respir Cell Mol Biol.*, 2005, 33, 113-20.
 50. Katzenstein ALA, Myers JL: Idiopathic pulmonary fibrosis – Clinical relevance of pathologic classification. *American Journal of Respiratory and Critical Care Medicine*, 1998, 157:1301-1315.
 51. Corrin, B., Dewar, A., Rodriguez-Roisin, R. & Turner-Warwick, M. Fine structural changes in cryptogenic fibrosing alveolitis and asbestosis. *J Pathol.*, 1985,147, 107-19.
 52. Myers, J.L. & Katzenstein, A.L. Epithelial necrosis and alveolar collapse in the pathogenesis of usual interstitial pneumonia. *Chest*, 1988,94, 1309-11.
 53. F. Hermansky and P.Pudlak. Albinism associated with hemorrhagic diathesis and unusual pigmented reticular cells in the bone marrow: Report of two cases with histochemical studies. *Blood*, 1959, 14: 162-169.
 54. Huizing and William A. Gahl, Mark Brantly, Nilo A. Avila, Vorasuk Shotelersuk, Cynthia Lucero, Marjan. Pulmonary Function and High-Resolution CT Findings in Patients With an Inherited Form of Pulmonary Fibrosis, Hermansky-Pudlak Syndrome, Due to Mutations in HPS-1. *Chest*, 2000, 17; 129-136.
 55. David J. Lederer, Steven M. Kawut, Joshua R. Sonett, Efsevia Vakiani, Samuel L. Seward, James G. White, Jessie S. Wilt, Charles C. Marboe, MD, William A. Gahl, and Selim M. Arcasoy. Successful Bilateral Lung Transplantation for Pulmonary Fibrosis Associated With the Hermansky-Pudlak Syndrome. , 2005, Volume 24, Issue 10,1697-1699.
 56. Pulmonary fibrosis in Hermansky Pudlak Syndrome-A case report. Diane M. Pierson, Diana Ionescu, Gefei Qing, Abdullah M. Yonan, Kent Parkinson, Thomas C. Colby, Kevin Leslie. *Respiration*, 2006, 73:382–395.
 57. Yukio Nakatani, Nobuo Nakamura Jinyu Sano, Yoshiaki Inayama Naomi Kawano Shoji Yamanaka, Yohei Miyagi Yoji, Nagashima Chiho Ohbayashi, Mutsue Mizushima Toshiaki Manabe, Makoto Kuroda Toyoharu Yokoi,
-

- Osamu Matsubara. Interstitial pneumonia in Hermansky-Pudlak syndrome: significance of florid foamy swelling/degeneration (giant lamellar body degeneration) of type II pneumocytes. *Virchows Arch.*, 2000, 437:304–313.
58. Anikster Y, Huizing M, White J, Shevchenko YO, Fitzpatrick DL, Touchman JW, Compton JG, Bale SJ, Swank RT, Gahl WA, Toro JR: Mutation of a new gene causes a unique form of Hermansky-Pudlak syndrome in a genetic isolate of central Puerto Rico. *Nat Genet.*, 2001; 28: 376–380.
59. Wildenberg SC, Oetting WS, Almodovar C, Krumwiede M, White JG, King RA: A gene causing Hermansky-Pudlak syndrome in a Puerto Rican population maps to chromosome 10q2. *Am. J. Hum Genet.*, 1995, 57: 755–765.
60. Witkop CJ, Nunez Babcock M, Rao GH, Gaudier F, Summers CG, Shanahan F, Harmon KR, Townsend D, Sedano HO, King RA, et al: Albinism and Hermansky-Pudlak syndrome in Puerto Rico. *Bol. Asoc. Med. P. R.*, 1990; 82: 333–339.
61. Bachli EB, Brack T, Eppler E, Stallmach T, Trueb RM, Huizing M, Gahl WA: Hermansky-Pudlak syndrome type 4 in a patient from Sri Lanka with pulmonary fibrosis. *Am. J. Med. Genet.*, 2004, 127A:201–207.
62. Schallreuter KU, Frenk E, Wolfe LS, Witkop CJ, Wood JM: Hermansky-Pudlak syndrome in a Swiss population. *Dermatology*, 1993, 187: 248–256.
63. Izquierdo NJ, Royuela MA, Maumenee IH: Possible origins of the gene of Hermansky-Pudlak in Puerto Rico. *P R Health Sci J.*, 1993, 12: 147–148.
64. Poddar RK, Coley S, Pavord S: Hermansky-Pudlak syndrome in a pregnant patient. *Br J Anaesth.*, 2004, 93: 740–742.
65. Poletti V, Costabel U, Casoni GL, Bigliuzzi C, Drent M, Olivieri D: Rare infiltrative lung diseases: a challenge for clinicians. *Respiration*, 2004, 71: 431–443.
66. Li W, Rusiniak ME, Chintala S, Gautam R, Novak EK, Swank RT: Murine Hermansky-Pudlak syndrome genes: regulators of lysosome-related organelles. *Bioessays.*, 2004, 26: 616–628.
67. Gwynn B, Martina JA, Bonifacino JS, Sviderskaya EV, Lamoreux ML, Bennett DC, Moriyama K, Huizing M, Helip-Wooley A, Gahl WA, Webb LS, Lambert AJ, Peters LL: Reduced pigmentation (rp), a mouse model of Hermansky-Pudlak syndrome, encodes a novel component of the BLOC-1 complex. *Blood*, 2004, 104: 3181–3189.
-

-
68. Oh J, Bailin T, Fukai K, Feng GH, Ho L, Mao JI, Frenk E, Tamura N, Spritz RA: Positional cloning of a gene for Hermansky-Pudlak syndrome, a disorder of cytoplasmic organelles. *Nat Genet.*, 1996, 14: 300–306.
 69. Oiso N, Riddle SR, Serikawa T, Kuramoto T, Spritz RA: The rat Ruby (R) locus is Rab38: identical mutations in Fawn-hooded and Tester-Moriyama rats derived from an ancestral Long Evans rat sub-strain. *Mamm Genome.*, 2004, 15: 307–314.
 70. Suzuki T, Ito S, Inagaki K, Suzuki N, Tomita Y, Yoshino M, Hashimoto T: Investigation on the IVS5 +5G] A splice site mutation of HPS1 gene found in Japanese patients with Hermansky-Pudlak syndrome. *J Dermatol Sci.*, 2004, 36: 106–108.
 71. Nguyen T, Wei ML: Characterization of melanosomes in murine Hermansky-Pudlak syndrome: mechanisms of hypopigmentation. *J Invest Dermatol.*, 2004, 122: 452–460.
 72. Feng L, Novak EK, Hartnell LM, Bonifacino JS, Collinson LM, Swank RT: The Hermansky-Pudlak syndrome 1 (HPS1) and HPS2 genes independently contribute to the production and function of platelet dense granules, melanosomes, and lysosomes. *Blood*, 2002, 99:1651–1658.
 73. Gardner JM, Wildenberg SC, Keiper NM, Novak EK, Rusiniak ME, Swank RT, Puri N, Finger JN, Hagiwara N, Lehman AL, Gales TL, Bayer ME, King RA, Brilliant MH: The mouse pale ear (ep) mutation is the homologue of human Hermansky-Pudlak syndrome. *Proc Natl Acad Sci USA*, 1997; 94: 9238–9243.
 74. Li W, Zhang Q, Oiso N, Novak EK, Gautam R, O'Brien EP, Tinsley CL, et al: Hermansky-Pudlak syndrome type 7 (HPS-7) results from mutant dysbindin, a member of the biogenesis of lysosome-related organelles complex 1 (BLOC-1). *Nat Genet.*, 2003, 35: 84–89.
 75. Wei Li, Michael E. Rusiniak, Sreenivasulu Chintala, Rashi Gautam, Edward K. Novak, and Richard T. Swank. Murine Hermansky–Pudlak syndrome genes: regulators of lysosome-related organelles. *Bio Essays*, Volume 26, (6) 616-628.
 76. Santiago M. Di Pietro, Juan M. Falco´n-Pe´rez, Danie`le Tenza, Subba R.G. Setty, Michael S. Marks, Grac¸a Raposo, and Esteban C. Dell'Angelica. BLOC-1 Interacts with BLOC-2 and the AP-3 Complex to Facilitate Protein Trafficking on Endosomes. *Molecular Biology of the Cell*, 2006, Vol. 17, 4027–4038.
 77. Subba Rao Gangi Setty, Danièle Tenza, Steven T. Truschel, Evelyn Chou, Elena V. Sviderskaya, Alexander C. Theos, M. Lynn Lamoreux, Santiago M. Di Pietro, Marta Starcevic, Dorothy C. Bennett, Esteban C. Dell'Angelica,
-

- Grac¸a Raposo, and Michael S. Marks. BLOC-1 Is Required for Cargo-specific Sorting from Vacuolar Early Endosomes toward Lysosome-related Organelles. *Molecular Biology of the Cell*, 2007, Vol. 18, 768–780.
78. Santiago M. Di Pietro, Juan M. Falco´ n-Pe´ rez and Esteban C. Dell'Angelica. Characterization of BLOC-2, a Complex Containing the Hermansky–Pudlak Syndrome Proteins HPS3, HPS5 and HPS6. *Traffic*, 2004, 5: 276–283.
79. Juan S. Bonifacino. Insights into the Biogenesis of Lysosome-Related Organelles from the Study of the Hermansky-Pudlak Syndrome. *Ann. N.Y. Acad. Sci.*, 2004, 1038: 103–114.
80. Rashi Gautam, Edward K. Novak, Jian Tan, Kazumasa Wakamatsu, Shosuke Ito and Richard T. Swank. Interaction of Hermansky-Pudlak Syndrome Genes in the Regu. of Lysosome-Related Organelles. *Traffic*, 2006, 7: 779–792.
81. Marta Starcevic, Ramin Nazarian and Esteban C. Dell'Angelica. The molecular machinery for the biogenesis of lysosome-related organelles: lessons from Hermansky–Pudlak syndrome. *Seminars in Cell & Developmental Biology*, 2002, Vol. 13, pp. 271–278.
82. Li, W. et al. Hermansky-Pudlak syndrome type 7 (HPS-7) results from mutant dysbindin, a member of the biogenesis of lysosome-related organelles complex 1 (BLOC-1). *Nat. Genet.*, 2003, 35, 84–89.
83. Gwynn, B. *et al.* (2004). Reduced pigmentation (*rp*), a mouse model of Hermansky-Pudlak syndrome, encodes a novel component of the BLOC-1 complex. *Blood*, 2004, 104, 3181–3189.
84. Moriyama, K., and Bonifacino, J. S. Pallidin is a component of a multi-protein complex involved in the biogenesis of lysosome-related organelles. *Traffic*, 2002, 3, 666–677.
85. Ciciotte, S. L., Gwynn, B., Moriyama, K., Huizing, M., Gahl, W. A., Bonifacino, J. S., and Peters, L. L. Cappuccino, a mouse model of Hermansky-Pudlak syndrome, encodes a novel protein that is part of the pallidin-muted complex (BLOC-1). *Blood*, 2003, 101, 4402–4407.
86. Gautam, R., Chintala, S., Li, W., Zhang, Q., Tan, J., Novak, E. K., Di Pietro, S. M., Dell'Angelica, E. C., and Swank, R. T. The Hermansky-Pudlak syndrome 3 (*cocoa*) protein is a component of the biogenesis of lysosomerelated organelles complex-2 (BLOC-2). *J. Biol. Chem.*, 2004, 279, 12935–12942.
87. Qing Zhang, Baohui Zhao, Wei Li, Naoki Oiso, Edward K. Novak, Michael E. Rusiniak, Rashi Gautam, Sreenivasulu Chintala, Edward P. O'Brien, Yuke
-

- Zhang, Bruce A. Roe, Rosemary W. Elliott, Eva M. Eicher, Ping Liang, Christian Kratz, Eric Legius, Richard A. Spritz, T. Norene O'Sullivan, Neal G. Copeland, Nancy A. Jenkins & Richard T. Swank. Ru2 and Ru encode mouse orthologs of the genes mutated in human Hermansky-Pudlak syndrome types 5 and 6. *Nature Genetics*, 2003, 33, 145 – 153.
88. GH Feng, T Bailin, J Oh and RA Spritz . Mouse pale ear (ep) is homologous to human Hermansky-Pudlak syndrome and contains a rare 'AT-AC' intron. *Human Molecular Genetics*, Vol 6, 793-797.
89. Tamio Suzuki, Wei Li, Qing Zhang, Amna Karim, Edward K. Novak, Elena V. Sviderskaya, Simon P. Hill, Dorothy C. Bennett, Alex V. Levin, H. Karel Nieuwenhuis, Chin-To Fong, Claudio Castellan, Bianca Mitterski, Richard T. Swank & Richard A. Spritz. Hermansky-Pudlak syndrome is caused by mutations in HPS4, the human homolog of the mouse light-ear gene. *Nature Genetics*, 2002, 30, 321-324.
90. Juan M. Falcón-Pérez, Marta Starcevic, Rashi Gautam, and Esteban C. Dell'Angelica. BLOC-1, a Novel Complex Containing the Pallidin and Muted Proteins Involved in the Biogenesis of Melanosomes and Platelet-dense Granules. *J. Biol. Chem.*, 2002, Vol. 277, Issue 31, 28191-28199..
91. Juan M. Falcón-Pérez, Ramin Nazarian, Chiara Sabatti, and Esteban C. Dell'Angelica. Distribution and dynamics of Lamp1-containing endocytic organelles in fibroblasts deficient in BLOC-3. *Journal of Cell Science*, 2005, 118, 5243-5255.
92. Esteban C Dell'Angelica. The building BLOC(k)s of lysosomes and related organelles. *Current Opinion in Cell Biology*, 2004, 16:458–464.
93. Greg Odorizzi, Christopher R. Cowles and Scott D. Emr The AP-3 complex: a coat of many colours. *Trends in cell biology*, 1998, Volume 8, Issue 7, 282-288.
94. Fiona Simpson, Andrew A. Peden, Lina Christopoulou, Margaret S. Robinson. Characterization of the Adaptor-related protein complex, AP-3. *The Journal of Cell Biology*, 1997, Volume 137, 835-845.
95. Kantheti P, Qiao X, Diaz ME, Peden AA, Meyer GE, Carskadon SL, Kapfhamer D, Sufalko D, Robinson MS, Noebels JL, and Burmeister M. Mutation in AP-3 delta in the mocha mouse links endosomal transport to storage deficiency in platelets, melanosomes and synaptic vesicles. *Neuron*, 1998, 21: 111-122.
96. Timothy A. Lyerla, Michael E. Rusiniak, Michael Borchers, Gerald Jahreis, Jian Tan, Patricia Ohtake, Edward K. Novak, and Richard T. Swank. Aberrant lung structure, composition, and function in a murine model of Hermansky-
-

- Pudlak syndrome. *Am J Physiol Lung Cell Mol Physiol.*, 2003, 285: L643-L653.
97. Santiago M. Di Pietro, Juan M. Falcón-Pérez, Danièle Tenza[†], Subba R.G. Setty, Michael S. Marks, Graça Raposo, and Esteban C. Dell'Angelica. BLOC-1 interacts with BLOC-2 and the AP-3 complex to facilitate protein trafficking on endosomes. *Molecular Biology of the Cell*, 2006, Vol. 17, Issue 9, 4027-4038.
98. Gahl WA, Brantly M, Troendle J, Avila NA, Padua A, Montalvo C, Cardona H, Calis KA, Gochuico B: Effect of pirfenidone on the pulmonary fibrosis of Hermansky-Pudlak syndrome. *Mol Genet Metab.*, 2002, 76: 234–242.
99. Huizing M, Gahl WA: Disorders of vesicles of lysosomal lineage: the Hermansky-Pudlak syndromes. *Curr Mol Med.*, 2002, 2: 451–467.
100. Anderson PD, Huizing M, Claassen DA, White J, Gahl WA: Hermansky-Pudlak syndrome type 4 (HPS-4): clinical and molecular characteristics. *Hum Genet.*, 2003, 113: 10–17.
101. Maria L. Wei. Hermansky-Pudlak syndrome: a disease of protein trafficking and organelle function. *Pigment Cell Res.*, 2006, 19:19-42.
102. Lijun Feng, Brian W. Rigatti, Edward K. Novak, Michael B. Gorin and Richard T. Swank. Genomic Structure of the Mouse *Ap3b1* Gene in Normal and Pearl Mice. *Genomics*, 2000, Volume 69, Issue 3, 370-379.
103. Andrew A. Peden, Rachel E. Rudge, Winnie W.Y. Lui and Margaret S. Robinson. Assembly and function of AP-3 complexes in cells expressing mutant subunits. *The Journal of Cell Biology*, 2002, Volume 156, Number 2, 327-336.
104. MP McGarry, M Reddington, EK Novak and RT Swank. Survival and lung pathology of mouse models of Hermansky-Pudlak syndrome and Chediak-Higashi syndrome. *Proceedings of the Society for Experimental Biology and Medicine*, 2003, Vol 220, 162-168.
105. Wixler V., Laplantine E., Geerts D., Sonnenberg A., Petersohn D., Eckes B., Paulsson M., Aumailley M. Identification of novel interaction partners for the conserved membrane proximal region of α -integrin cytoplasmic domains. *FEBS Letters*, 1999, Volume 445, Number 2, 351-355(5).
106. Susan H. Guttentag, Amana Akhtar, Jian-Qin Tao, Elena Atochina, Michael E. Rusiniak, Richard T. Swank, and Sandra R. Bates. Defective Surfactant Secretion in a Mouse Model of Hermansky-Pudlak Syndrome. *Am J Respir Cell Mol Biol.*, 2005, Vol 33; 14–21.
-

-
107. Cheng-Lun Na, ChenXia Duan, Karen S. Apsley and Timothy E. Weaver. Abnormal alveolar type 2 cell phenotype in AP-3 Mutant Mocha and Pearl mice: an electron microscopy study. *Microsc Microanal.*, 2003, 9:1426–1427.
 108. Dell'Angelica EC, Augilar RC, Wolins N, Hazelwood S, Gahl WA, Bonifacino JS. Molecular characterization of the protein encoded by the Hermansky-Pudlak syndrome type 1 gene. *J Biol Chem.*, 2000, 275:1300-1306.
 109. Karen Newell-Litwa, Eunju Seong, Margit Burmeister and Victor Faundez. Neuronal and non-neuronal functions of the AP-3 sorting machinery. *Journal of Cell Science*, 2007, 120; 531-541.
 110. Chean Eng Ooi, Esteban C.Dell' Angelica and Juan S.Bonifacino. ADP-Ribosylation Factor 1 (ARF1) regulates recruitment of the AP-3 adaptor complex to membranes. *The Journal of Cell Biology*, 1998, Vol 142; 391-402.
 111. Bjoern Chapuy, Ritva Tikkanen, Chris Muehlhausen, Dirk Wenzel, Kurt von Figura and Stefan Hoening. AP-1 and AP-3 Mediate Sorting of Melanosomal and Lysosomal Membrane Proteins into Distinct Post-Golgi Trafficking Pathways. *Traffic*, 2008; 9: 1157–1172.
 112. Harrison-Lavoie KJ, Michaux G, Hewlett L, Kaur J, Hannah MJ, Lui-Roberts WW, Norman KE, Cutler DF. P-selectin and CD63 use different mechanisms for delivery to Weibel-Palade bodies. *Traffic*, 2006 Jun;7(6):647-62.
 113. Daugherty BL, Straley KS, Sanders JM, Phillips JW, Disdier M, McEver RP, Green SA. AP-3 adaptor functions in targeting P-selectin to secretory granules in endothelial cells. *Traffic*, 2001 Jun;2(6):406-13.
 114. Gundrun Ihrke, Aija Kyttaala, Matthew R.G. Russell, Brian A. Rous and J. Paul Luzio. Differential use of two AP-3 mediated pathways by lysosomal membrane proteins. *Traffic*, 2004, 5; 946-962.
 115. Brian A. Rous, Barbara J. Reaves, Gudrun Ihrke, John A.G. Briggs, Sally R.Gray, David J. Stephens, George Banting, and J. Paul Luzio. Role of Adaptor Complex AP-3 in Targeting Wild-Type and Mutated CD63 to Lysosomes. *Molecular Biology of the Cell*, 2002, Vol. 13, 1071–1082, March.
 116. Dell'Angelica EC, Augilar RC, Wolins N, Hazelwood S, Gahl WA, Bonifacino JS. Molecular characterization of the protein encoded by the Hermansky-Pudlak syndrome type 1 gene. *J Biol Chem.*, 2000, 275:1300-1306.
 117. Clark, R.H. and Stinchcombe, J.C. and Day, A. and Blott, E. and Booth, S. and Bossi, G. and Hamblin, T. and Davies, E.G. and Griffiths, G.M. Adaptor protein 3–dependent microtubule-mediated movement of lytic granules to the
-

- immunological synapse. *Nature Immunology*, 2003, 4 (11). pp. 1111-1120. ISSN 15292908.
118. John L. Prueitt, Emil Y. Chi, and David Lagunoff. Pulmonary surface-active materials in the Chediak-Higashi syndrome. *Journal of Lipid Research*, 1978, Volume 19.
119. Kazuhiro Osanai, Rieko Oikawa, Junko Higuchi, Makoto Kobayashi, Katsuma Tsuchihara, Masaharu Iguchi, Huang Jongsu, Hirohisa Toga and Dennis R. Voelker. A Mutation in Rab38 Small GTPase Causes Abnormal Lung Surfactant Homeostasis and Aberrant Alveolar Structure in Mice. *American Journal of Pathology*, 2008, 173:1265-1274.
120. S. Palmeri, P. Tarugi, F. Sicurelli, R. Buccoliero, A. Malandrini, M.M. De Santi, G. Marciànò C. Battisti, M.T. Dotti, S. Calandra, A. Federico. Lung involvement in Niemann-Pick disease type C1: improvement with bronchoalveolar lavage. *Neurol Sci.*, 2005, 26:171–173.
121. Margaret M. McGovern, Melissa P. Wasserstein, Roberto Giugliani, Bruno Bembi, Marie T. Vanier, Eugen Mengel, Scott E. Brodie, David Mendelson, Gwen Skloot, Robert J. Desnick, Noriko Kuriyama, MAJ, Gerald F. Cox. A Prospective, Cross-sectional Survey Study of the Natural History of Niemann-Pick Disease Type B. *Pediatrics*, 2008, 122:e341–e349.
122. Björn Bjurulf, Signe Spetalen, Aage Erichsen, Marie T. Vanier, Erik H. Strom, Petter Stromme. Niemann-Pick disease type C2 presenting as fatal pulmonary alveolar lipoproteinosis: Morphological findings in lung and nervous tissue. *Med Sci Monit.*, 2008, 14(8): CS71-75.
123. Buccoliero R, Ginzburg L, Futerman AH. Elevation of lung surfactant phosphatidylcholine in mouse models of Sandhoff and Niemann-Pick disease. *J Inher Metab Dis.*, 2004, 27:641–648.
124. Rajwinder Dhani, Xingxuan He, Ronald E Gordon and Edward H Schuchman. Analysis of the Lung Pathology and Alveolar Macrophage Function in the Acid Sphingomyelinase–Deficient Mouse Model of Niemann-Pick Disease. *Lab Invest.*, 2001, 81:987–999.
125. Amin RS, Wert SE, Baughman RP, Tomashefski JF, Nogee LM, Brody AS. Surfactant protein deficiency in familial interstitial lung disease. *Journal of Pediatrics*, 2001, 139:85-92.
126. Nogee LM, Dunbar AE, Wert SE, Askin F, Hamvas A, Whitsett JA: A mutation in the surfactant protein C gene associated with familial interstitial lung disease. *New England Journal of Medicine* 2001, 344:573-579.
-

-
127. Stillwell PC, Norris DG, Oconnell EJ, Rosenow EC, Weiland LH, Harrison EG: Desquamative Interstitial Pneumonitis in Children. *Chest*, 1980, 77:165-171.
 128. King TE: Diagnostic Advances in Idiopathic Pulmonary Fibrosis. *Chest* 1991, 100:238-241.
 129. Surafel Mulugeta, Vu Nguyen, Scott J. Russo, Madesh Muniswamy and Michael F. Beers. A Surfactant Protein C Precursor Protein BRICHOS Domain Mutation Causes Endoplasmic Reticulum Stress, Proteasome Dysfunction, and Caspase 3 Activation. *American Journal of Respiratory Cell and Molecular Biology*, 2005, Vol. 32, pp. 521-530.
 130. Glasser SW, Detmer EA, Ikegami M, Na CL, Stahlman MT, Whitsett JA: Pneumonitis and emphysema in SP-C gene targeted mice. *J Biol Chem.*, 2003, 278:14291-14298.
 131. Sergey Shulenin, Ph.D., Lawrence M. Noguee, M.D., Tarmo Annilo, Ph.D., Susan E. Wert, Jeffrey A. Whitsett, and Michael Dean. ABCA3 Gene Mutations in Newborns with Fatal Surfactant Deficiency. *N Engl J Med.*, 2004, 350; 1296-303.
 132. Janine E. Bullard, Susan E. Wert, Jeffrey A. Whitsett, Michael Dean, and Lawrence M. Noguee. ABCA3 Mutations Associated with Pediatric Interstitial Lung. *Am J Respir Crit Care Med.*, 2005, October 15; 172(8): 1026–1031.
 133. Christiane Albrecht, Enrique Viturro. The ABCA subfamily—gene and protein structures, functions and associated hereditary diseases. *Pflugers Arch - Eur J Physiol.*, 2007, 453: 581–589.
 134. Lisa R. Young, Lawrence M. Noguee, Bruce Barnett, Ralph J. Panos, Thomas V. Colby, and Gail H. Deutsch. Usual Interstitial Pneumonia in an Adolescent with ABCA3 Mutations. *Chest*, 2008; 134:192-195.
 135. Esteban C. Dell’Angelica, Chris Mullins, Steve Caplan, and Juan S. Bonifacino. Lysosome related organelles. *The FASEB Journal*, 2000, 14:1265-1278.
 136. Lijun Feng, Edward K. Novak, Lisa M. Hartnell, Juan S. Bonifacino, Lucy M. Collinson and Richard T. Swank. The Hermansky-Pudlak syndrome 1 (HPS1) and HPS2 genes independently contribute to the production and function of platelet dense granules. *Blood*, 2002, 99: 1651-1658.
 137. Katarina Kaedgal, Uno Johansson and Karin Oellinger. The lysosomal protease cathepsin D mediates apoptosis induced by oxidative stress. *FASEB*, 2001, Vol. 15, 1592-1594.
-

-
138. Heidi K. Baumgartner, Julia V. Gerasimenko, Christopher Thorne, Louise H. Ashurst, Stephanie L. Barrow, Michael A. Chvanov, Stuart Gillies, David N. Criddle, Alexei V. Tepikin, Ole H. Petersen, Robert Sutton, Alastair J. M. Watson, and Oleg V. Gerasimenko. Caspase-8-mediated apoptosis induced by oxidative stress is independent of the intrinsic pathway and dependent on cathepsins. *Am J Physiol.*, 2007, 293: G296.
 139. Xiaopeng Li, Heather Rayford, Ruijie Shu, Jiaju Zhuang, and Bruce D. Uhal. Essential role for cathepsin D in bleomycin-induced apoptosis of alveolar epithelial cells. *Am J Physiol Lung Cell Mol Physiol*, 2004, 287: L46–L51.
 140. B.D. Uhal. Epithelial apoptosis in the initiation of lung fibrosis. *Eur Respir J*, 2003, 22:7s-9s.
 141. Alina Minarowska, Lukasz Miarowski, Alicja Karwowska, Marek Gacko. Regulatory role of cathepsin D in apoptosis. *Folia Histochemica ET Cytobiologica*, 2007, Vol. 45, No. 3, 2007 pp. 159-163.
 142. Roberta Castino, Natascia Bellio, Giuseppina Nicotra, Carlo Follo, Nicol F. Trincheri, Ciro Isidoro Cathepsin D–Bax death pathway in oxidative stressed neuroblastoma cells. *Free Radical Biology & Medicine* 42, 2007, 1305–1316.
 143. Robert Blomgran, Limin Zheng, and Olle Stendahl. Cathepsin-cleaved Bid promotes apoptosis in human neutrophils via oxidative stress-induced lysosomal membrane permeabilization *J Leukoc Biol.*, 2007, 81: 1213–1223.
 144. ALberts, Johnson, Lewis, Raff, Roberts, Walter. *Molecular biology of the cell*. ISBN 0-8153-3218-1.
 145. Stefan J. Marciniak and David Ron. Endoplasmic Reticulum Stress Signaling in Disease. *Physiol.*, 2006, Rev. 86: 1133-1149, doi: 10.1152 / physrev.00015.2006.
 146. Yoshida H. ER stress and diseases. *Febs J.*, 2007, 274: 630-658.
 147. Jianze Li, Brenda Lee, and Amy S. Lee. Endoplasmic reticulum-stress induced apoptosis: Multiple pathways and activation of PUMA and NOXA by p53. *J. Biol. Chem.*, 2006, 281(11):7260-70.
 148. S.Oyadomari, and M Mori. Roles of CHOP/GADD153 in endoplasmic reticulum Stress. *Cell Death and Differentiation*, 2004, 11, 381–389.
 149. Remotti, James L. Stevens and David Ron Helene Zinszner, Masahiko Kuroda, XiaoZhong Wang, Nikoleta Batchvarova, Richard T. Lightfoot, Helen. CHOP is implicated in programmed cell death in response to impaired function of the endoplasmic reticulum. *Genes & Dev*, 1998, 12: 982-995.
-

-
150. Wang XZ, Lawson B, Brewer JW, Zinszner H, Sanjay A, Mi LJ, Boorstein R, Kreibich G, Hendershot LM and Ron D. Signals from the stressed endoplasmic reticulum induce C/EBP-homologous protein (CHOP/GADD153). *Mol. Cell. Biol.*, 1996, 16: 4273–4280.
 151. Oyadomari S, Takeda K, Takiguchi M, Gotoh T, Matsumoto M, Wada I, Akira S, Araki E and Mori M. Nitric oxide-induced apoptosis in pancreatic beta cells is mediated by the endoplasmic reticulum stress pathway. *Proc. Natl. Acad. Sci.*, 2001, 98: 10845–10850.
 152. Endo M, Oyadomari S, Suga M, Mori M, and Gotoh T. The ER stress pathway involving CHOP is activated in the lungs of LPS-treated mice. *J Biochem (Tokyo)*, 2005, 138: 501-507.
 153. Yoshida H. ER stress and diseases. *Febs J.*, 2007, 274: 630-658.
 154. Surafel Mulugeta, Vu Nguyen, Scott J. Russo, Madesh Muniswamy and Michael F. Beers. A Surfactant Protein C Precursor Protein BRICHOS Domain Mutation Causes Endoplasmic Reticulum Stress, Proteasome Dysfunction, and Caspase 3 Activation. *American Journal of Respiratory Cell and Molecular Biology*, 2005, Vol. 32, pp. 521-530.
 155. Martina Korfei, Clemens Ruppert, Poornima Mahavadi, Ingrid Henneke, Philipp Markart, Miriam Koch, Gyoergy Lang, Ludger Fink, Rainer-Maria Bohle, Werner Seeger, Timothy E. Weaver and Andreas Guenther. Epithelial endoplasmic reticulum stress and apoptosis in sporadic idiopathic pulmonary fibrosis. *Am. J. Respir. Crit.Care. Med.*, 2008, Vol.178; 00838-846.
 156. Alexander C. Theos, Joanne F. Berson, Sarah C. Theos, Kathryn E. Herman, Dawn C. Harper, Danie`le Tenza, Elena V. Sviderskaya, M. Lynn Lamoreux, Dorothy C. Bennett, Grac_a Raposo, and Michael S. Marks. Dual Loss of ER Export and Endocytic Signals with Altered Melanosome Morphology in the *silver* Mutation of Pmel17. *Molecular Biology of the Cell*, 2006, Vol. 17, 3598–3612.
 157. A d'Azzo, A Tessitore and R Sano. Gangliosides as apoptotic signals in ER stress response *Cell Death and Differentiation*, 2006, 13, 404–414.
 158. Alessandra Tessitore, Maria Del.P.Martin, Renata Sano, Yanjun Ma, Linda Mann, Angela Ingrassia, Eric D.Laywell, Dennis A.Steindler, Linda M.Hendershot and Alessendara d'Azzo. GM₁-Ganglioside-mediated activation of the unfolded protein response causes neuronal death in a neurodegenerative Gangliosidosis. *Molecular Cell*, 2004, Vol.15, 753-766.
 159. Sophie Degroote, Jasja Wolthoorn, Gerrit van Meer. The cell biology of glycosphingolipids. *Seminars in Cell and Developmental Biology*, 2004, 15: 375-387.
-

-
160. M. Elleder. Glucosylceramide transfer from lysosomes—the missing link in molecular pathology of glucosylceramidase deficiency: A hypothesis based on existing data. *J Inherit Metab Dis.*, 2006, 29:707–715.
161. Lisa R. Young, Michael T. Borchers, Holly L. Allen, Reta S. Gibbons, and Francis X. McCormack. Lung-Restricted Macrophage Activation in the Pearl Mouse Model of Hermansky-Pudlak Syndrome. *The Journal of Immunology*, 2006, 176: 4361–4368.
162. Lisa R. Young, Rajamouli Pasula, Peter M. Gulleman, Gail H. Deutsch and Francis X. McCormack. Susceptibility of Hermansky-Pudlak Mice to Bleomycin-Induced Type II Cell Apoptosis and Fibrosis. *American Journal of Respiratory Cell and Molecular Biology*, 2007, Vol. 37, pp. 67-74.
163. Judit E Pongracz and Robert A Stockley. Wnt signalling in lung development and diseases. *Respiratory Research*, 2006, 7:15.
164. Melanie Koenigshoff, Nisha Balsara, Eva-Maria Pfaff, Monika Kramer, Izabella Chrobak, Werner Seeger, Oliver Eickelberg. Functional Wnt Signaling Is Increased in Idiopathic Pulmonary Fibrosis. *PLoS ONE*, 2008, Volume 3, Issue 5, e2142.
165. Minhong Yan and Greg D. Plowman. Delta-like 4/Notch Signaling and Its Therapeutic Implications. *Clin Cancer Res.*, 2007, 13(7243 24).
166. Biao Hu, Tianju Liu, Zhe Wu, and Sem H. Phan. Notch regulation of telomerase induction in pulmonary fibrosis. *FASEB J.*, 2008, 22:596.1 [Meeting Abstract]
167. Anna Serrano-Mollar, Maria Nacher, Gemma Gay-Jordi, Daniel Closa, Antoni Xaubet, and Oriol Bulbena. Intratracheal Transplantation of Alveolar Type II Cells Reverses Bleomycin-induced Lung Fibrosis. *Am J Respir Crit Care Med.*, 2007, Vol 176. pp 1261–1268.
168. James P. Bridges,¹ Yan Xu,¹ Cheng-Lun Na,¹ Hector R. Wong,² and Timothy E. Weaver. Adaptation and increased susceptibility to infection associated with constitutive expression of misfolded SP-C. *The Journal of Cell Biology*, Vol. 172, No. 3, January 30, 2006 395–407.
169. Apoptosis and necrosis induced by cyclic mechanical stretching in alveolar type-II-cells--influence of captopril and L-Arginine. Hammerschmidt S, Kuhn H, Grasenack T, Gessner C, Wirtz H. *Pneumologie*, 2004, 58(4): 222-9.
170. Immunolocalization of cathepsin D in pneumocytes of normal human lung and in pulmonary fibrosis. M. Kasper, M. Haase, D. Schuh, M. Müller and P. Lackie. *Virchows archives*, 1996, Volume 428, Numbers 4-5.
-

Acknowledgements

My first and foremost acknowledgement goes to my principle investigator, Prof. Dr. Andreas Guenther. I am greatly indebted to him for his immense belief in me and his all time support and encouragement during the bad and good times of my PhD career. I have started my research career in his lab and it is only because of his able guidance, that I have reached this phase of my PhD career. "Thank you" is a very small word to extend my gratitude to Andreas.

I extend my sincere gratitude to Prof. Dr. Michael Martin who readily agreed to be my co-principle investigator and who guided me through the process of obtaining my PhD.

I sincerely thank Prof. Dr. Gerd Schmitz and Dr. Gerhard Liebisch, without whose co-operation, the lipidomics study would not have been possible.

I would like to extend my sincere thanks to the "Molecular Biology Medicine of the Lung" International Graduate Program, where I have learnt the essence of science. I would like to extend my sincere gratitude to Prof. Dr. Werner Seeger for giving me the opportunity of learning science in an international atmosphere.

I would like to thank Dr. Martina Korfei, who is more a friend than my post-Doc and from whom I have learnt the fine aspects of research. I always appreciate her immense guidance during my PhD work. I sincerely thank Dr. Clemens Ruppert, for excellently handling and managing all the HPS mice and for all his patience to answer all my questions. His technical guidance has always been immensely useful.

I would like to thank Ingrid Henneke for extending all her help in my animal experiments. I thank my lab technicians, Silke Haendel and Juliane Mest for their all time help. My sincere thanks to Dr. Karin Endris, from whom I received unforgettable help in administrative issues.

My husband always stood by me with a lot of patience, understanding and caring. He is my twin soul and his constant support and encouragement have helped me althrough my career. Mummy and nana (my parents) have always been my pillars of support. I dedicate my thesis to my parents and it goes without saying that my mom, dad and my brother, ever deserve my deepest gratitude.

Anhang

Publications

1. Markart. P, Luboeinski. T, Korfei. M, Schmidt. R, Wygrecka. M, Mahavadi. P, Mayer K, Wilhelm J, Seeger. W, Guenther. A, Ruppert. C. Alveolar oxidative stress is associated with elevated levels of non-enzymatic low-molecular-weight antioxidants in patients with different forms of chronic fibrosing interstitial lung diseases. *Antioxid Redox Signal* (2009)11(2):227-40
2. Korfei. M, Ruppert. C, Mahavadi. P, Henneke. I, Markart. P, Koch. M, Lang. G, Fink. L, Bohle. RM, Seeger. W, Weaver. TE, Guenther. A. Epithelial endoplasmic reticulum stress and apoptosis in sporadic idiopathic pulmonary fibrosis. *Am J Respir Crit Care Med.*, (2008) 15;178(8):838-46.
3. Ruppert C, Mahavadi P, Wygrecka M, Magdolen V, Idell S, Preissner K.T, Seeger.W, Guenther.A, Markart.P. Recombinant production of a hybrid plasminogen activator composed of surfactant protein B and low-molecular weight urokinase. *Thrombosis and Haemostasis* (2008)100(6):1185-92.

Oral presentations

1. Mahavadi. P, Korfei. M, Ruppert. C Henneke. I, Liebisch. G, Schmitz. G, Bernadette. G, Seeger. W., and Guenther. A. Evidence of Surfactant Accumulation and Type II Pneumocyte Apoptosis in Hermansky Pudlak Syndrome Associated Lung Fibrosis. *American Thoracic Society, Toronto, Canada, 16-21 May, 2008.*
 2. Mahavadi P, Schwertner. L., Mokry. T, Henneke. I, Korfei. M, Seeger. W, Guenther. W, Ruppert C. Surfactant Alterations and Lung Fibrosis in a Murine Model of Amiodarone-Induced Pulmonary Fibrosis. *Herbst treffen, Section Zell Biologie - Deutsche Gessellschaft fur Pneumologie, Munchen, Germany, November, 2007.*
 3. Mahavadi. P, Korfei. M, Ruppert. C Henneke. I, Seeger. W, and Guenther. A. Impaired lysosomal trafficking and epithelial apoptosis in a murine model of Hermansky-Pudlak-Syndrome. *MBML annual retreat, Rauischholzhausen, Germany, 31 July- 2 August 2006.*
 4. Mahavadi. P, Korfei. M, Ruppert. C Henneke. I, Seeger. W, and Guenther. A. Impaired lysosomal trafficking in a murine model of Hermansky-Pudlak-Syndrome. *Kongress der Deutsche Gessellschaft fur Pneumologie und Beatmungsmedizin, Nurnberg, Germany, 29 March – 1 April, 2006.*
 5. Mahavadi. P, Korfei. M, Ruppert. C Henneke. I, Seeger. W, and Guenther. A. Altered surfactant metabolism in a murine model of Hermansky-Pudlak syndrome. *Herbst treffen, Section Zell Biologie - Deutsche Gessellschaft fur Pneumologie, Bonn, Germany, October, 2005.*
-

6. Mahavadi. P, Korfei. M, Ruppert. C Henneke. I, Seeger. W, and Guenther. A. Surfactant alterations trafficking in a murine model of Hermansky-Pudlak-Syndrome. *MBML annual retreat, Rauischholzhausen, Germany, 1- 3 August 2005.*

Poster presentations

1. Mahavadi. P, Korfei. M, Ruppert. C Henneke. I, Liebisch. G, Schmitz. G, Bernadette. G, Seeger. W., and Guenther. A. Role of impaired lysosomal trafficking in a murine model of Hermansky-Pudlak-syndrome associated interstitial pneumonia (HPSIP). *Herbst treffen, Section Zell Biologie - Deutsche Gessellschaft fur Pneumologie, Freiburg, Germany, 08-08 November, 2008*
2. Mahavadi. P, Korfei. M, Ruppert. C Henneke. I, Liebisch. G, Schmitz. G, Bernadette. G, Weaver. T, Seeger. W., and Guenther. A. Evidence of type II pneumocyte apoptosis and lung fibrosis in murine Hermansky-Pudlak-Syndrome associated interstitial pneumonia (HPSIP). *European Respiratory Society, Berlin, Germany, 4-8 October, 2008.*
3. Mahavadi. P, Korfei. M, Ruppert. C Henneke. I, Liebisch. G, Schmitz. G, Bernadette. G, Weaver. T, Seeger. W., and Guenther. A. Role of impaired lysosomal trafficking and epithelial apoptosis in a murine model of Hermansky-Pudlak-Syndrome associated Interstitial Pneumonia (HPSIP). *International colloquium for airway and lung fibrosis, North Carolina, USA, 28 September to 01 October, 2008.*
4. Mahavadi. P, Korfei. M, Ruppert. C Henneke. I, Liebisch. G, Schmitz. G, Bernadette. G, Weaver. T, Seeger. W., and Guenther. A. Extensive intracellular accumulation of surfactant phospholipids and proteins underlies development of epithelial stress, apoptosis and lung fibrosis in murine Hermansky Pudlak Syndrome 1/2. *Leopoldina Symposium on Lipid Signalling, Frankfurt, Germany, 4-7 September, 2008.*
5. Mahavadi P, Schwertner. L., Mokry. T, Henneke. I, Korfei. M, Seeger. W, Guenther. W, Ruppert C. Surfactant Alterations and Lung Fibrosis in a Murine Model of Amiodarone-Induced Pulmonary Fibrosis. *American Thoracic Society, Toronto, Canada, 16-21 May, 2008.*
6. Mahavadi P, Schwertner. L., Mokry. T, Henneke. I, Korfei. M, Seeger. W, Guenther. W, Ruppert C. Surfactant Alterations and Lung Fibrosis in a Murine Model of Amiodarone-Induced Pulmonary Fibrosis. *Kongress der Deutsche Gessellschaft fur Pneumologie und Beatmungsmedizin, Luebeck, Germany. 9-12 April, 2008.*
7. Mahavadi. P, Korfei. M, Ruppert. C Henneke. I, Seeger. W, and Guenther. A. Role of impaired lysosomal trafficking and epithelial apoptosis in a murine model of Hermansky-Pudlak-Syndrome associated Interstitial Pneumonia (HPSIP). *International Colloquium on Lung Fibrosis, Reinhartshausen, Germany, 7-10 September 2006.*

8. Mahavadi. P, Korfei. M, Ruppert. C Henneke. I, Seeger.W, and Guenther. A. Role of impaired lysosomal trafficking and epithelial apoptosis in a murine model of Hermansky-Pudlak-Syndrome associated Interstitial Pneumonia (HPSIP). *American Thoracic Society, San Diego, USA, 18-23 May 2006.*
-